



VCU

Virginia Commonwealth University
VCU Scholars Compass

Theses and Dissertations

Graduate School

2020

ROLE OF CLIC4 AND THE SYNAPTIC TRANSCRIPTOME IN THE BEHAVIORAL AND MOLECULAR NEUROBIOLOGY OF ETHANOL

Rory M. Weston
Virginia Commonwealth University

Follow this and additional works at: <https://scholarscompass.vcu.edu/etd>



Part of the [Behavioral Neurobiology Commons](#), and the [Genomics Commons](#)

© The Author

Downloaded from

<https://scholarscompass.vcu.edu/etd/6353>

This Dissertation is brought to you for free and open access by the Graduate School at VCU Scholars Compass. It has been accepted for inclusion in Theses and Dissertations by an authorized administrator of VCU Scholars Compass. For more information, please contact libcompass@vcu.edu.

Copyright © 2020

Rory M. Weston

All rights reserved

ROLE OF CLIC4 AND THE SYNAPTIC TRANSCRIPTOME
IN THE BEHAVIORAL AND MOLECULAR
NEUROBIOLOGY OF ETHANOL

A dissertation submitted in partial fulfillment of the requirements for the degree
of Doctor of Philosophy at Virginia Commonwealth University.

by

Rory M. Weston

Bachelor of Science, Florida State University, 2007

Bachelor of Arts, Western Washington University, 2013

Director: Michael F. Miles, M.D., Ph.D.

Professor, Department of Pharmacology and Toxicology

Virginia Commonwealth University

Richmond, VA

March 9, 2020

Acknowledgements

Foremost, I would like to thank my advisor, Dr. Michael Miles, not only for his guidance, wisdom, and expertise, but also for his creative out-of-the-box thinking which inspires me to approach complex problems from new angles. Under his advisement, I have learned a great deal about interpreting, conducting, and speaking about research.

I thank my committee members, Dr. Darlene Brunzell, Dr. Babette Fuss, Dr. Mike Grotewiel, and Dr. Jolene Windle. Their unique perspectives and critical analysis of my work helped shape this project and the way I approach scientific research. Similarly, Dr. Jennifer Wolstenholme has been a constant positive influence on my training, offering her technical expertise, life advice, and encouragement.

I would also like to thank my wife, Nicole Weston, who as a fellow graduate student acted both as a second opinion on technical matters and a sympathetic ear during the more difficult times of my training. Thank you to my parents, Teresa and Wes, for encouraging me to “ask why” when I was a child and supporting my

meandering endeavors. Also, for the support of my siblings, especially my sister Ashleen.

To my friends and labmates, Guy Harris and Andrew van der Vaart, I have appreciated our long discussions inside and outside of lab. It has been a true pleasure going through this experience alongside you.

I would like to express my gratitude to the VCU MD-PhD program and especially Dr. Gordon Archer, for taking a chance and investing in me. I also thank Dr. Donnenberg for his dedication to improving the program and increasing the wellbeing of its students. Also, to Sandra Sorrell, thank you for all of your help, support, and positivity along the way.

Last but not least, I would like thank Dr. Jeff Carroll and Dr. Janet Finlay for sparking a passion in me for neuroscience when I was a naïve premed and providing so many opportunities for me to grow.

Table of Contents

List of Tables	i
List of Figures	iii
List of Abbreviations	v
Clarification of Contributions	vii
Abstract	xi
CHAPTER 1	
Introduction	1
1.1 Alcohol Use Disorder	1
1.2 Risk Factors	3
1.3 Chloride Intracellular Channel 4	6
1.4 Improving Our Understanding of AUD	7
CHAPTER 2	
Background	9
2.1 Introduction	9
2.2 Medial Prefrontal Cortex	10
2.2.1 Anatomy and Composition	10

2.2.2 Medial Prefrontal Cortex Networks and Connectivity	11
2.3 Medial Prefrontal Cortex in Alcohol Use Disorder	20
2.3.1 Associations with Alcohol Use Disorder	20
2.3.2 Dopamine and the Mesolimbic Reward Pathway	21
2.3.3 Altered Pyramidal Neurons	25
2.3.4 Opioid Peptide Signaling in Withdrawal	26
2.3.5 CRF Receptors and Amygdala Overactivation	27
2.3.6 Dichotomous Projections to Nucleus Accumbens	28
2.4 White Matter in Alcohol Use Disorder	30
2.5 Characteristics of Chloride Intracellular Channel 4	32
2.6 Alcohol Use Disorder Studies in Model Organisms	35
CHAPTER 3	
Ethanol Sensitization and the Synaptic Transcriptome	39
3.1 Introduction	39
3.3 Materials and Methods	43
3.4 Results	56
3.4.1 Synaptoneurosome Fraction Characterization	56
3.4.2 Sensitization Alters the Synaptic Transcriptome	61
3.4.3 Sensitization is Accompanied by Differential Splicing	64
3.4.4 Enrichment of RNA Binding Protein Targets	66

3.5 Discussion	70
CHAPTER 4	
<i>Drosophila Clic</i> Knockdown Alters the Transcriptome	79
4.1 Introduction	79
4.2 Methods	83
4.3 Results	86
4.3.1 Differential Gene Expression Following <i>Clic</i> Knockdown	86
4.3.2 Perturbed Oxidation-Reduction and Cytoplasmic Translation	92
4.3.3 Overlap with Ethanol Regulated Genes	94
4.3.4 Ethanol Sensitivity Altered by Knockdown and Hyperoxia	97
4.4 Discussion	100
CHAPTER 5	
<i>Clic4</i> Modulates Ethanol and Anxiety-like Behaviors	108
5.1 Introduction	108
5.2 Methods	111
5.3 Results	119
5.3.1 Global Oligodendrocyte-specific <i>Clic4</i> Deletion	119
5.3.2 Ethanol Consumption Altered by <i>Clic4</i> Deletion	122
5.3.3 Anxiety-like Behavior Altered by <i>Clic4</i> Deletion	124

5.3.4 Ethanol Consumption Altered by mPFC <i>Clic4</i> Deletion	127
5.4 Discussion	131
CHAPTER 6	
<i>Clic4</i> Gene Expression Characteristics	138
6.1 Introduction	138
6.2 Methods	141
6.3 Results	148
6.3.1 Expression Profile of CLIC4 in mPFC	148
6.3.2 PFC <i>Clic4</i> Expression Following Ethanol Exposure	154
6.3.3 Transcriptomic Response to Acute Ethanol and <i>Clic4</i> Deletion	156
6.4 Discussion	165
CHAPTER 7	
Conclusions, Discussion, and Future Directions	171
7.1 Ethanol and the Synaptic Transcriptome	171
7.2 <i>Clic4</i> in Ethanol and Anxiety-related Behavior	173
7.3 CLIC4 Protein Expression in PFC	176
7.4 <i>Clic4</i> , Acute Ethanol, and the Transcriptome	180
7.5 Concluding Remarks	181
REFERENCES	183

List of Tables

TABLE 2.1: CHLORIDE INTRACELLULAR CHANNEL GENE FAMILY HOMOLOGY.	31
TABLE 3.1. SEQUENCE MOTIF DISCOVERY.	69
TABLE 6.1. SUMMARY OF DIFFERENTIAL GENE REGULATION.	158
TABLE 6.2. ETHANOL DIFFERENTIALLY REGULATED GENES BETWEEN SEXES.	158
TABLE 7.1: SUMMARY OF BEHAVIORAL CHANGES FOLLOWING <i>CLIC4</i> -DELETION.	174
TABLE 7.2: SUMMARY OF <i>CLIC4</i> PROTEIN EXPRESSION IN PFC.	177

List of Figures

FIGURE 2.1: SUBDIVISIONS OF MPFC.	12
FIGURE 2.2: NUCLEI OF THE AMYGDALA.	15
FIGURE 2.3: MESOLIMBIC REWARD PATHWAY.	23
FIGURE 3.1. ETHANOL BEHAVIORAL SENSITIZATION IN MALE D2 MICE.	57
FIGURE 3.2. CHARACTERIZATION OF SYNAPTONEUROSOME PREPARATIONS.	58
FIGURE 3.3. SYNAPTONEUROSOMES DISPLAY DISTINCT RNA POPULATIONS.	59
FIGURE 3.4. DGE FOLLOWING ACUTE ETHANOL EXPOSURE OR SENSITIZATION.	62
FIGURE 3.5. DEU FOLLOWING ACUTE ETHANOL EXPOSURE OR SENSITIZATION.	65
FIGURE 3.6. SYNAPSE-SPECIFIC DEU IS ENRICHED IN RNABP TARGETS.	68
FIGURE 4.1. OVERVIEW OF <i>CLIC</i> KNOCKDOWN APPROACH.	88
FIGURE 4.2. <i>CLIC</i> KNOCKDOWN-RESPONSIVE GENE EXPRESSION.	89
FIGURE 4.3: DIFFERENTIAL GENE EXPRESSION BY STRAIN.	91
FIGURE 4.4. GO TERMS ENRICHED BY <i>CLIC</i> KNOCKDOWN.	93
FIGURE 4.5. GENE SETS OVERLAPPING WITH <i>CLIC</i> KNOCKDOWN.	95
FIGURE 4.6: HYPEROXIA SURVIVAL.	98
FIGURE 4.7. ETHANOL SENSITIVITY UNDER HYPEROXIA.	99
FIGURE 5.1. VALIDATION OF <i>CLIC4</i> DELETION.	120
FIGURE 5.2. WESTERN BLOT ASSESSMENT OF <i>CLIC4</i> DELETION.	121

FIGURE 5.3. ETHANOL CONSUMPTION IS ALTERED BY <i>CLIC4</i> DELETION.	123
FIGURE 5.4. DELETION OF <i>CLIC4</i> ALTERS ANXIETY-LIKE BEHAVIOR.	125
FIGURE 5.5. VALIDATION OF MPFC DELETION OF <i>CLIC4</i> IN OLIGODENDROCYTES.	128
FIGURE 5.6. CHARACTERIZATION OF MPFC OLIGODENDROCYTE <i>CLIC4</i> DELETION.	129
FIGURE 5.7. MPFC EXPRESSION OF <i>CLIC4</i> .	137
FIGURE 5.8. BRAIN REGION-SPECIFIC <i>CLIC4</i> EXPRESSION.	137
FIGURE 6.1. CLIC PROTEIN EXPRESSION IN OLIGODENDROCYTES.	149
FIGURE 6.2. CLIC PROTEIN EXPRESSION IN NEURONS.	151
FIGURE 6.3. CLIC PROTEIN EXPRESSION IN MICROGLIA.	152
FIGURE 6.4. CLIC PROTEIN EXPRESSION IN ASTROCYTES.	153
FIGURE 6.5. <i>CLIC4</i> MRNA EXPRESSION AFTER ETHANOL EXPOSURE.	155
FIGURE 6.6. SUMMARY OF DIFFERENTIAL GENE EXPRESSION.	159
FIGURE 6.7. GO TERMS: ETHANOL TREATMENT IN MALE MICE.	161
FIGURE 6.8. GO TERMS: <i>CLIC4</i> DELETION IN SALINE-TREATED MALE MICE.	162
FIGURE 6.9. GO TERMS: <i>CLIC4</i> DELETION IN ETHANOL-TREATED MALE MICE.	163
FIGURE 6.10. OVERLAP OF ETHANOL-RESPONSIVE GENE SETS.	164

List of Abbreviations

3BC	Three-bottle-choice
AAV	Adeno-associated virus
AUD	Alcohol use disorder
B6	C57BL/6J mice
CIE	Chronic intermittent ethanol vapor exposure
CLIC4	Chloride intracellular channel 4
Cre	Cre recombinase
CRF	Corticotropin-releasing factor
Cyp	Cytochrome p450
D2	DBA/2J mice
DEU	Differential exon usage
DGE	Differential gene expression
ER ^T	Tamoxifen-sensitive recombinant estrogen receptor
FDR	False discovery rate
GABA	Gamma aminobutyric acid
GO	Gene Ontology
GST	Glutathione S-transferase
i.p.	Intraperitoneal injection
IEA	Intermittent ethanol access

KEGG	Kyoto Encyclopedia of Genes and Genomes
MBP	Myelin basic protein
mPFC	Medial prefrontal cortex
NAc	Nucleus accumbens
NMDA	N-methyl-D-aspartate
P2	Synaptic fraction of synaptoneurosome preparation
PFC	Prefrontal cortex
PLP	Proteolipid protein
qRT-PCR	Quantitative reverse-transcriptase polymerase chain reaction
QTL	Quantitative trait loci
RNABP	RNA-binding protein
S2	Somatic fraction of synaptoneurosome preparation
VTA	Ventral tegmental area

Clarification of Contributions

Invaluable assistance, collaboration, and data sharing was provided during the below listed studies. All other work described in this dissertation was performed exclusively by the author.

Chapter 3

This chapter was recently published as a co-first author manuscript (O'Brien et al., 2018) and was a combined effort between Dr. Megan O'Brien and myself. Under the advising of Dr. Michael Miles, Dr. O'Brien conceived of and began this study during her own Ph.D. dissertation project, carrying out the behavioral studies, synaptoneurosome isolations, and initial molecular studies. Dr. John Bigbee provided the electron microscopy work to validate the synaptoneurosome preparations. Nihar Sheth and Sean Bradley provided initial low-level analysis for the differential gene expression work.

Chapter 4

This work was conceived of by Dr. Michael Grotewiel and Dr. Michael Miles. Functional work for this chapter was performed by the lab of Dr. Mike Grotewiel, including *Drosophila* husbandry, hyperoxia and ethanol sedation experiments, and RNA isolation by Rebecca Schmitt. Microarray preparation was performed by Lorna Mcleod of the Miles lab. Microarray hybridization, washing, staining, and scanning were performed by VCU Massey Cancer Center Tissue and Data Acquisition and Analysis Core.

Chapter 5

Dalton Huey was instrumental in the Western blot analyses involving CLIC4, MBP, and PLP following *Clic4* deletion. Dr. Jennifer Wolstenholme provided retro-orbital blood draws for the ethanol metabolism study. Pam Waters provided invaluable support in maintaining the various transgenic mouse lines used in the studies reported in Chapters 5 and 6.

Chapter 6

Dr. Bernas and Frances White with the VCU Microscopy Facility provided invaluable advising and troubleshooting on confocal and super resolution

microscopy technique. Guy Harris and Dr. Andrew van der Vaart provided the behavioral work and tissue samples for the acute and chronic ethanol exposure qRT-PCR studies and Morgan Driver provided assistance in running the qRT-PCR analyses. Assistance with tissue dissection for the microarray study was provided by Guy Harris. Microarray hybridization, washing, staining, and scanning were performed by VCU Massey Cancer Center Tissue and Data Acquisition and Analysis Core.

Core resources

Microscopy was performed at the VCU Microscopy Facility, supported, in part, by funding from NIH-NCI Cancer Center Support Grant P30 CA016059.

Services and products in support of the research project were generated by the Virginia Commonwealth University Cancer Mouse Models Core Laboratory, supported, in part, with funding from NIH-NCI Cancer Center Support Grant P30 CA016059.

Services in support of the research project were provided by the VCU Massey Cancer Center Tissue and Data Acquisition and Analysis Core, supported, in part, with funding from NIH-NCI Cancer Center Support Grant P30 CA016059.

Abstract

Alcohol use disorder (AUD) is a prevalent neuropsychiatric disease with profound health, social, and economic consequences. With an estimated 50% heritability, identifying genes that engender risk and contribute to the underlying neurobiological mechanisms represents an important first step in developing effective treatments. Gene expression studies are an important source of candidate genes for studying AUD, providing windows into the molecular machinery engaged by the brain in response to ethanol. Published studies have identified chloride intracellular channel 4 (*Clic4*) as an ethanol-regulated gene in brain capable of modulating sensitivity to sedation in multiple species. The functions of *Clic4* are not well understood but have been associated with diverse biological processes including ion channel activity, cellular stress, cytoskeleton remodeling, intracellular trafficking, and oxidoreductase reactions. In this series of studies, we have characterized gene expression changes specific to frontal cortex synapses after acute and repeated ethanol exposures. We additionally identified genes differentially regulated in response to knockdown of *Drosophila* ortholog *Clic* and

deletion of *Clic4* in mice, both implicating oxidation-reduction-related processes as potentially mechanistic to their involvement in ethanol sedation sensitivity. Lastly, we show that CLIC4 is robustly expressed in oligodendrocytes where deletion of *Clic4* produces altered ethanol consumption and anxiety-like behaviors in mice. Considering its abundant expression in oligodendrocytes, induction by acute ethanol, and function in modulating ethanol consumption, our work here suggests that *Clic4* has an important role in the molecular response to ethanol in brain and development of maladaptive ethanol-related behaviors.

Chapter 1

Introduction

1.1 Alcohol Use Disorder

AUD is a neuropsychiatric disease characterized by the American Psychiatric Association's Diagnostic and Statistical Manual of Mental Disorders 5 as a spectrum of chronic ethanol abuse and dependence (American Psychiatric Association, 2013). Individuals with AUD exhibit ethanol craving, poor self-regulation, and damaging behaviors that lead to significant social, emotional, and physical harm. AUD is common in the United States, having an overall lifetime prevalence of 36% in males and 23% in females (Grant et al., 2015). AUD is the third leading cause of preventable death, following tobacco usage and poor diet and exercise (Mokdad, 2004). Associated damages to property and loss of productivity are estimated to cost the United States an excess of \$249 billion dollars per year (Sacks et al., 2015).

Relapse rates for AUD are similar to opiate dependence, being reported as

high as 90% (Hodgson, 1980), rendering the disease challenging to treat. While behavioral and pharmacological therapies exist for AUD, treatment efficacies are modest and, in many cases, ineffective. Naltrexone and Acamprosate, the current first line medications for treating AUD, have only been shown to reduce the number of individuals returning to heavy drinking by 10% over placebo (Jonas et al., 2014). Similarly, in a 16-week study employing cognitive behavioral therapy, individuals receiving treatment achieved only 6% more abstinent days than those without therapy (Anton et al., 2006). Since AUD has proven to be largely refractory to conventional treatments, further exploration into the etiology and pathophysiology of the disorder is necessary to better understand and successfully treat it.

AUD, similar to other addictive disorders, develops as a progression from impulsivity to compulsivity where drug-seeking motivation is sustained by a balance between positive and negative reinforcement (George F. Koob, 2013). By lowering hedonic reward thresholds, alcohol exposure produces positive reinforcement that can lead to impulsive binge-like behaviors and loss of control over intake. Conversely, alcohol withdrawal produces an increased threshold for hedonic reward and a combination of negative physical and affective symptoms. Further alcohol consumption may relieve these symptoms, but in doing so, produces negative reinforcement. Following repeated bouts of heavy drinking,

hedonic reward becomes more and more difficult to achieve and positive reinforcement is diminished (George F. Koob, 2013). Simultaneously, a positive feedback loop known as kindling occurs whereby functional changes in the brain due to repeated alcohol withdrawal begin to drive progressively worse withdrawal states (Ballenger & Post, 1978). As severity of withdrawal increases, so does the value of negative reinforcement provided by compensatory alcohol consumption. As the cycle continues and motivation for alcohol consumption shifts from positive to negative reinforcement, hedonic reward-based impulsivity gives way to compulsivity and alcohol dependence is established.

1.2 Risk Factors

Most individuals that consume alcohol will not develop AUD, despite the cycle of positive and negative reinforcement even a single binge event can produce. It has been estimated that 48-58% of the risk for developing AUD is due to genetic factors, with the remainder resulting from environmental influences (Prescott & Kendler, 1999). As a consequence, a major priority in AUD research has been to identify genes influential in conferring this risk in order to better understand the etiology of the disorder and to develop more targeted pharmacological therapies. Human genetic studies originally sought to identify an “alcoholism gene” or limited set of alleles responsible for the majority of the

disorder's heritability. The findings have been much less straightforward, identifying a large number of genetic variants each contributing only minor components of the overall risk. This characteristic defines complex genetic disorders and makes identification of therapeutically meaningful candidate genes difficult. Linkage and genome-wide association studies have identified tens to hundreds of genetic variants (Deak et al., 2019), with the most reproducible being alcohol metabolism genes in the aldehyde and alcohol dehydrogenase gene families (Clarke et al., 2017; Tawa et al., 2016). Neurotransmitter receptor genes such as dopamine receptor D2 have also been identified by these approaches, however with less consistent reproducibility (Clarke et al., 2017; Tawa et al., 2016). One possible translational example is the drug disulfiram, which selectively inhibits aldehyde dehydrogenase producing severe alcohol withdrawal symptoms. Unfortunately positive treatment outcomes for disulfiram are less than first line drugs naltrexone and acamprosate (Jonas et al., 2014).

Large scale human genetic studies have identified many promising candidate genes, some of which are currently undergoing further characterization. However, these studies have thus far failed to produce new pharmacological therapies more effective than current standard of care. One possible explanation is that selectively targeting heritable candidate genes only addresses a minor component of the combinatorial effects of multiple risk alleles in AUD. A different

perspective can be gained through transcriptomic approaches, which instead focus on the unique transcriptional landscape of AUD and complex web of biological processes and gene networks that underlie it. Here the goal is to target a gene “hub” whose expression is influential on networks of interacting genes related to the pathophysiology of AUD. Identifying candidate genes with this approach and evaluating them in transgenic animal models is an area of research active research, with many promising genes having already been identified (Liu et al., 2006). Animal models of AUD have also contributed candidate genes in this manner, while permitting a more direct and controlled evaluation of relationships between genes and behaviors(Kerns et al., 2005)(Kerns et al., 2005)(Kerns et al., 2005)(Kerns et al., 2005)(Kerns et al., 2005). While animal models cannot perfectly recapitulate the human AUD disease process, they can be useful in studying the genetics underlying discrete behaviors such as ethanol sedation sensitivity and voluntary ethanol consumption.

Ethanol-related behaviors can vary greatly between mouse strains and transcriptomic analysis of these differences can provide insight into which genes and networks of genes contribute to the expression of these behaviors. Using this approach, Kerns et al. performed gene expression analysis of two mouse strains with contrasting acute behavioral responses to ethanol and were able to identify genes differentially regulated in brain between strains (Kerns et al., 2005). Within

the more ethanol-sensitive strain, a cluster of myelin-related genes was found to be upregulated in response to acute ethanol. One of these genes, *Clic4*, is particularly interesting due to appearing in several other publications either reproducing its regulation by ethanol or showing broader involvement in the brain's molecular response to ethanol.

1.3 Chloride Intracellular Channel 4

A growing body of literature has connected *Clic4* to the brain's molecular response to ethanol, making it a strong candidate for further investigation. *Clic4* expression is regulated by ethanol in the medial prefrontal cortex (mPFC) of mouse brain (Bhandari et al., 2012; Kerns et al., 2005; Marballi et al., 2016) and dysregulated in postmortem frontal cortex tissue of human alcoholics (Liu et al., 2006). *Clic4* is also part of an ethanol-responsive gene network in hippocampus (Farris & Miles, 2013) and is located in known quantitative trait loci (QTLs) for ethanol consumption (Tarantino et al., 1998) and anxiety (Kazuhiro Nakamura et al., 2003; Thifault et al., 2008) in mice. This is notable because anxiety is an important risk factor for AUD and a frequent co-morbidity (Morris et al., 2005). This collection of genomic evidence is strongly substantiated through Bhandari et al. (Bhandari et al., 2012), where ethanol sedation sensitivity was shown to be altered by disrupting chloride intracellular channel orthologs in invertebrates and

by overexpressing *Clic4* in mouse mPFC. This study is particularly significant in light of the fact that sensitivity to ethanol is a strong risk factor in humans (Schuckit, 1994; Schuckit & Smith, 1996). Together, these findings highlight the potential importance *Clic4* in the behavioral and molecular response to ethanol in brain.

1.4 Improving Our Understanding of AUD

There are many knowledge gaps in our current understanding of AUD. This is especially true of molecular events surrounding acute exposure to ethanol, which provide a glimpse into the first step of a chain of events leading to maladaptive changes in the brain and ethanol behaviors. There is a need for further research into identifying and characterizing genes responsive to acute ethanol and the functional brain regions, cell types, and subcellular compartments they are regulated in. This information will enrich our understanding of biological processes underlying acute ethanol exposure in brain and their potential contributions to the pathophysiology of AUD. In particular, the role of the acute ethanol-regulated gene *Clic4* in ethanol consumption and sedation sensitivity, including its cellular type of action, needs to be characterized. Additionally, the scope of *Clic4* function and genomic interaction needs to be defined in order to begin investigating the mechanisms by which it regulates ethanol-related

behavior. We hypothesize that *Clic4* will have an important role in modulating ethanol consumption behaviors in mice, possibly related to its activity in responding to cellular stress or performing oxidoreductase activities. The following body of work addresses many of the knowledge gaps that have been mentioned, characterizing the synaptic transcriptome following ethanol sensitization, profiling transcriptomic responses to deletion of mouse *Clic4* and knockdown of *Drosophila* ortholog *Clic*, and evaluating the contributions of *Clic4* to ethanol and anxiety-related behaviors in mice. Our findings offer novel insight into behavioral and molecular responses to ethanol in brain and the unique role of *Clic4*.

Chapter 2

Background

2.1 Introduction

The overall goal of this dissertation is to shed light on the molecular mechanisms leading to development of AUD. This is accomplished by examining gene expression changes in brain that follow acute ethanol exposure and by characterizing the role of *Clic4* in influencing ethanol-related behaviors. Multiple brain areas are associated with the behavioral adaptations undergone during development of AUD and the pathology that follows chronic alcohol abuse. This chapter will review the relevant neuroanatomy and functional connectivity within this context, with a focus on medial mPFC, where *Clic4* has shown ethanol regulation and an ability to modulate ethanol sedation sensitivity in mice (Bhandari et al., 2012). Discussed later in this dissertation, mPFC was targeted for specific genetic manipulations of *Clic4* and gene expression profiling of acute responses to ethanol. This chapter will also provide a deeper review of *Clic4* and

what is known about its biological functions. Lastly, a discussion on the use of model organisms for researching AUD will be provided, with an emphasis on the mouse strains and ethanol self-administration paradigms employed later in this dissertation.

2.2 Medial Prefrontal Cortex

2.2.1 Anatomy and Composition

Prefrontal cortex (PFC), and especially mPFC, has been associated with decision making, impulsivity and compulsivity, motivation, learning, reactivity to stress, and salience attribution (Goldstein & Volkow, 2011). Because of these cognitive roles, PFC is thought to be a contributor to both the impulsive self-administration seen in early stages of addiction, as well as the compulsive drug-seeking seen in late stages (Crews & Boettiger, 2009; Volkow & Fowler, 2000). The mPFC is a cytoarchitecturally distinct region within the PFC, possessing unique network connectivity and functional roles setting it apart from other prefrontal cortical areas. mPFC is largely comprised of excitatory glutamatergic pyramidal neurons synapsing on distant brain regions as well as gamma aminobutyric acid (GABA) interneurons providing local inhibition to the same pyramidal neurons (George et al., 2012; A. Peters & Jones, 1984). There is also a sparse population of

corticotropin-releasing factor (CRF) interneurons that appear to serve roles in producing negative emotional states and responding to stressful stimuli (George et al., 2012; Swanson et al., 1983; Zorrilla et al., 2014).

The layout and connectivity of the mPFC is relatively conserved among species, but varies greatly in the content of granular tissue (Ongür & Price, 2000; Petrides & Pandya, 1994). Rodents, unlike humans and monkeys, do not possess granular tissue in the PFC and were not initially considered to have a comparable frontal cortex region when originally mapped by Brodmann (Brodmann, 1910; Ongür & Price, 2000). In humans, mPFC conservatively includes Brodmann areas 10, 24, 25, and 32, which other than non-homologous area 32, is similar in monkeys (**Figure 2.1**). Areas 24 and 32 form the anatomically distinct anterior cingulate cortex, which wraps the rostral face of the corpus callosum. Brodmann area 10, frontopolar PFC, and Brodmann area 25, subgenual area, constitute the rest of mPFC and are equivalent to prelimbic and infralimbic regions of rodent mPFC, respectively (Ongür & Price, 2000).

2.2.2 Medial Prefrontal Cortex Networks and Connectivity

Activity in mPFC is associated with complex behaviors such as decision making and expression of emotion, which requires extensive connectivity to different brain areas. This includes cortico-cortical, limbic, thalamic, striatal,

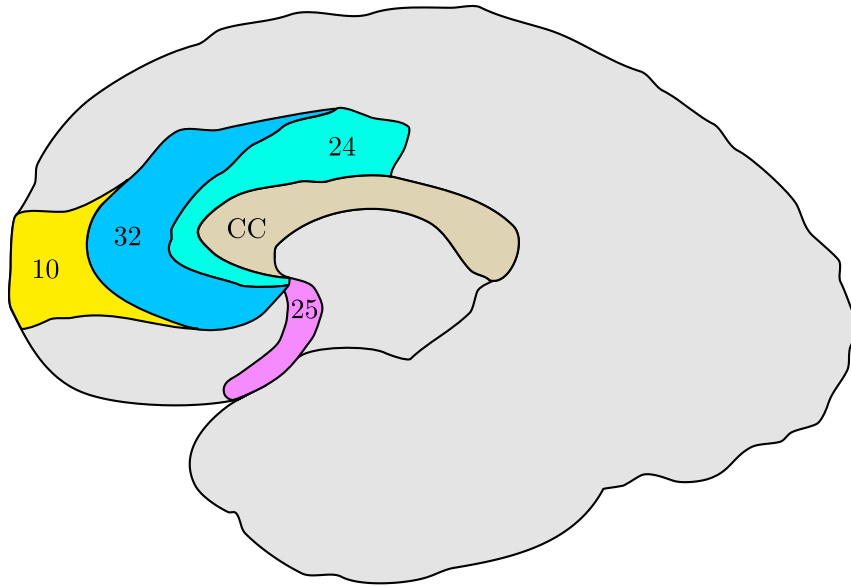


Figure 2.1: Subdivisions of mPFC. Mid-sagittal illustration of mPFC subdivisions according to Brodmann classification. Major regions include the anterior cingulate cortex (32), subgenual area (25) and frontopolar prefrontal cortex (10).

hypothalamic, and midbrain connections (Ongür & Price, 2000). Among cortico-cortical connections, mPFC networks synapse bi-directionally with the sensory-receptive orbitofrontal cortex (OFC) network (Carmichael & Price, 1995; Ongür & Price, 2000). Unlike mPFC, which has minimal direct sensory input, OFC receives and integrates multiple sensory modalities and is therefore able to involve mPFC in the sensorimotor information stream (Ongür & Price, 2000). Anterior cingulate cortex also contains reciprocal cortico-cortical connections, bridging Brodmann areas 24a and 24b with caudal cingulate areas 23a and 23b (Carmichael & Price, 1995). Both of these areas have extensive connectivity with other limbic structures including amygdala, hippocampus, and parahippocampal cortex (Rosene & Van Hoesen, 1977; Vogt & Pandya, 1987).

The mesolimbic reward pathway of the brain is integral to the addiction process, interconnecting the dopamine-producing ventral tegmental area (VTA) of the midbrain with the basal forebrain by way of the medial forebrain bundle. Excitatory activity along this pathway is associated with the rewarding properties of alcohol use, whereas withdrawal from alcohol is associated with depression of the pathway (Weiss et al., 1996). The principle basal forebrain structures along this pathway include the nucleus accumbens (NAc), amygdala, and PFC (George F. Koob et al., 2012).

Amygdala

The mPFC possesses extensive interconnectivity with structures of the limbic system (Carmichael & Price, 1995). This includes the amygdala, an almond-shaped structure located deep within the temporal lobes that has been linked to emotional learning and memory. The amygdala can be subdivided into distinct nuclei (**Figure 2.2**) including the basolateral amygdala (BLA), central nucleus of the amygdala (CeA), and intercalated cell masses (Lee et al., 2013). BLA is cortex-like cytoarchitecturally and consists predominately of glutamatergic projection neurons (Carlsen, 1988; Lee et al., 2013). The CeA has a more striatum-like appearance and consists largely of GABAergic interneurons (Lee et al., 2013; McDonald, 1982). The BLA can be further subdivided into lateral amygdala (LA) and basal amygdala (BA), which in turn is subdivided into basolateral (BL) and basomedial nuclei (BM). The majority of amygdalar projections to mPFC originate within the BA, with far fewer projections originating in LA and CeA (Barbas & de Olmos, 1990; Carmichael & Price, 1995; Ongür & Price, 2000). BL and BM project to every area of mPFC. Unique to BL, there are OFC and mPFC projections originating in the same portion of the nucleus that subsequently share cortico-cortical interconnections in the PFC (Carmichael & Price, 1995).

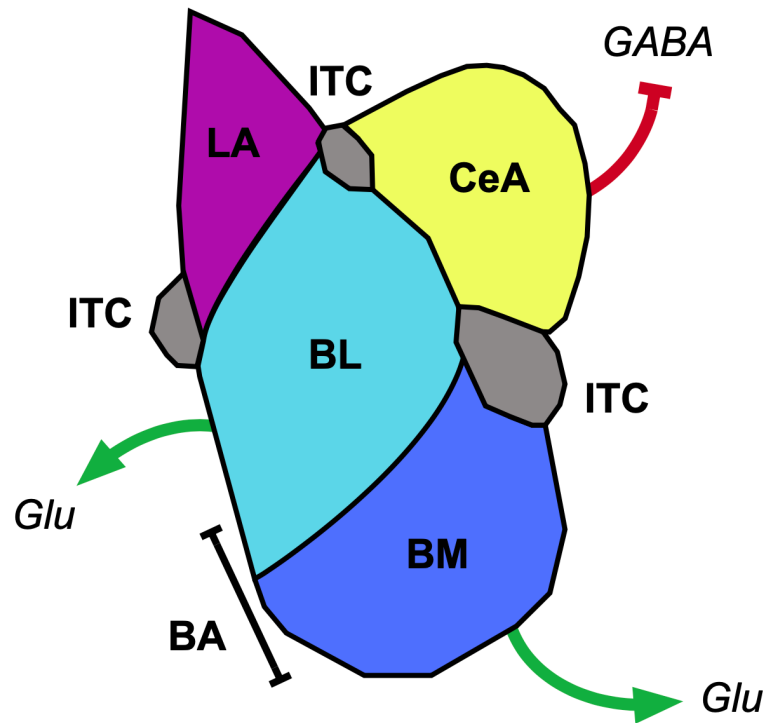


Figure 2.2: Nuclei of the amygdala. Cortex-like basal lateral amygdala (BLA) includes lateral (LA) and basal (BA) amygdala with predominately glutamatergic projections. BA can be subdivided into basolateral (BL) and basomedial (BM) nuclei. Striatum-like central nucleus of the amygdala (CeA) is largely GABAergic. Intercalated cell masses (ITC) comprise the remaining amygdalar nuclei.

The majority of afferent fibers projecting to the amygdala originate in OFC and mPFC. These both receive reciprocal connectivity, largely returning projections to the originating BLA nuclei, but also non-reciprocal projections synapsing on additional amygdalar areas, including CeA (Aggleton et al., 1980; Carmichael & Price, 1995; M. J. Kim et al., 2011). Amygdala also receives projections from multiple sensory modalities, including projections from auditory and visual cortex (Barbas & de Olmos, 1990), and projects to hippocampus, basal ganglia, thalamus, and brainstem (Kandel et al., 2012). This unique array of connectivity is key for the amygdala to generate affective associations to sensory stimuli and drive motivational and somatic responses.

Hippocampal Formation

The hippocampal formation is another deep temporal lobe structure, lying caudal to the amygdala and also receiving projections from mPFC. Anatomically, it includes the hippocampus, subiculum, and dentate gyrus. The hippocampal formation is involved in the consolidation of episodic memory and the dentate gyrus

is a major site of neurogenesis in adult brain (Kandel et al., 2012). Of these regions, only subiculum contains significant projections to mPFC (Carmichael & Price, 1995). Subiculum acts as the major output pathway for pyramidal neurons of the

hippocampal formation, sending efferents to a multitude of structures including mPFC, parahippocampal area, amygdala, septum, thalamus, and hypothalamus (Rosene & Van Hoesen, 1977). Connectivity between subiculum and mPFC appears to be unidirectional and largely targeted to Brodmann areas 10, 25, and 32 (Carmichael & Price, 1995; Ongür & Price, 2000; Rosene & Van Hoesen, 1977; Vogt & Pandya, 1987).

Parahippocampal Cortex

The parahippocampal cortex, which includes the entorhinal and perirhinal cortices, is another component of the limbic circuit and has reciprocal connections with the hippocampal formation (Kandel et al., 2012). Like the hippocampal formation, parahippocampal cortex is involved in formation of memory. Reciprocal connections exist between anterior cingulate and entorhinal cortex as well as areas of posterior parahippocampal cortex (Carmichael & Price, 1995). Although not part of parahippocampal cortex, the adjacent temporal polar region is also reciprocally connected to mPFC and is considered a component of the extended limbic system (Carmichael & Price, 1995; Olson et al., 2007). Temporal pole is an anatomically complex region where multiple cortical areas intersect. While not currently well understood, the temporal pole integrates multiple

sensory modalities and is believed to be involved in higher order social and emotional processing (Olson et al., 2007).

Basal Ganglia

mPFC also projects to basal ganglia, including components of ventral striatum (Haber et al., 1995). This encompasses substantial projections to medial ventral striatum and NAc, with more sparse efferents traveling to central ventral striatum (Haber et al., 1995). Projections from mPFC to NAc are partitioned into prelimbic efferents to NAc core and infralimbic efferents to NAc shell (Brog et al., 1993). Ventral striatum, including NAc, is extensively interconnected with other limbic structures such as amygdala (Ongür & Price, 2000). As part of a striato-pallido-thalamo-cortico circuit, regions of ventral striatum receiving mPFC efferents project onto globus pallidus, which in turn projects to the medial dorsal thalamic nucleus, which in turn has reciprocal projections to and from the mPFC (Ongür & Price, 2000; Ray & Price, 1993). The NAc has been implicated in encoding and anticipating rewarding and aversive states (Carlezon & Thomas, 2009; Wolfram Schultz et al., 1992) and its involvement in the striato-pallido-thalamo-cortico circuitry is thought to contribute to a synthesis of multiple brain region reward representations (Wolfram Schultz et al., 1998).

Autonomic and Neuroendocrine Structures

Extensive connectivity exists between mPFC and autonomic and neuroendocrine regions of the brain, including midbrain periaqueductal gray (PAG) and hypothalamus (Hurley et al., 1991; Ongür & Price, 2000). The PAG receives substantial projections from virtually all areas of mPFC (An et al., 1998). In addition to its well-established role in providing endogenous analgesia, PAG is also involved in coordinating autonomic and behavioral reactions to threatening stimuli (Depaulis et al., 1992).

Projections from mPFC make up the majority of all cortical afferents in the hypothalamus (Ongür et al., 1998). Brodmann areas 25, 32, and to a lesser extent 10, project all throughout the hypothalamus, but especially to the anterior and ventromedial regions. Through its extensive innervation of brain regions associated with the autonomic nervous system, mPFC is able to modulate visceral responses to stress and emotional stimuli (Hardy & Holmes, 1988; Hurley et al., 1991; Resstel & Corrêa, 2006).

Ventral tegmental area

VTA is one of two major sources of dopamine in the brain and is an integral component of the mesolimbic reward pathway. Excited by unpredicted rewards and cues associated with predicted rewards, VTA neurons release dopamine into

the mesolimbic reward pathway and mediate positive reinforcement (Wolfram Schultz, 2002). The majority of VTA dopaminergic neuron efferents terminate on amygdala, NAc, and mPFC (Beier et al., 2015). VTA receives afferent input from various brain regions including NAc, lateral hypothalamus, CeA, pallidum, lateral dorsal tegmental area, and nearly all areas of mPFC (Watabe-Uchida et al., 2012). In an apparent top-down feedback loop, excitatory anterior cortical neurons, including mPFC, terminate on NAc projecting VTA dopaminergic neurons and drive positive reinforcement (Beier et al., 2015). This suggests the existence of an alternative reward circuit that is under higher order cortical control, which would not require excitatory inputs from hindbrain regions such as the pedunclopontine or lateral dorsal tegmental areas.

2.3 Medial Prefrontal Cortex in Alcohol Use Disorder

2.3.1 Associations with Alcohol Use Disorder

The mPFC has been implicated in AUD through a combination of imaging, gene expression, and anatomical studies. For instance, functional magnetic resonance imaging studies in abstinent human alcoholics have shown increased activation of mPFC in response to alcohol-related visual cues (Grüsser et al., 2004; Heinz et al., 2007). Functional imaging studies of alcohol dependent individuals

have revealed losses in volume of grey and white matter in multiple brain areas, including mPFC, and these losses correlate with degree of cognitive impairment (Chanraud et al., 2007, 2010; Demirakca et al., 2011; Fein et al., 2002; Wobrock et al., 2009). These cognitive deficits, including decision making and working memory impairment, mirror those seen in individuals who have suffered injuries to the ventromedial PFC (Bechara, 2005; Bechara et al., 1994).

On a molecular level, gene expression and proteomic studies of post mortem frontal cortex tissue from human alcoholics have revealed decreases in the expression of myelin proteins and N-Methyl-D-aspartic acid (NMDA) receptor subunits as well as genes associated with synaptic function, cell adhesion, and neurogenesis (Lewohl et al., 2005; Liu et al., 2006; Ridge et al., 2008). From the preponderance of anatomical, behavioral, gene expression evidence, it is clear that the PFC, and mPFC in particular, is intricately involved in the development and pathology of AUD. Additionally, white matter losses and gene expression changes may underlie some of the dysfunctional changes observed in cortex and contribute to cognitive deficits.

2.3.2 Dopamine and the Mesolimbic Reward Pathway

The reinforcing effects of alcohol have been associated with both dopamine-dependent and dopamine-independent signaling pathways involving the mPFC.

The dopamine-dependent component involves the classical mesolimbic reward pathway, whereas the dopamine-independent routes are comprised of glucocorticoid and opioid peptide signaling (George F. Koob, 2013). Dopamine signaling through mesolimbic circuitry is associated with regulation of emotion, reinforcement, motivation, and learning (Gonzales et al., 2004). Within the mesolimbic reward system (**Figure 2.3**), the VTA of the midbrain provides dopaminergic projections to mPFC, NAc, and amygdala. These dopaminergic projections are tonically active but at low frequencies (W. Schultz et al., 1997). During presentation of a reward or reward-associated cue, dopaminergic neuronal firing rates are increased. However, if predicted rewards fail to be obtained, dopaminergic firing rates decrease (W. Schultz et al., 1997). It is therefore hypothesized that the VTA encodes a reward error predictor system, informing downstream targets of which stimuli encode actual rewards.

With chronic exposure to ethanol, cellular and molecular changes occur within the mesolimbic reward pathway and contribute to dependence and ethanol-seeking behavior (Gonzales et al., 2004). During the early binge/intoxication stage of AUD, activity in the mesolimbic reward pathway is

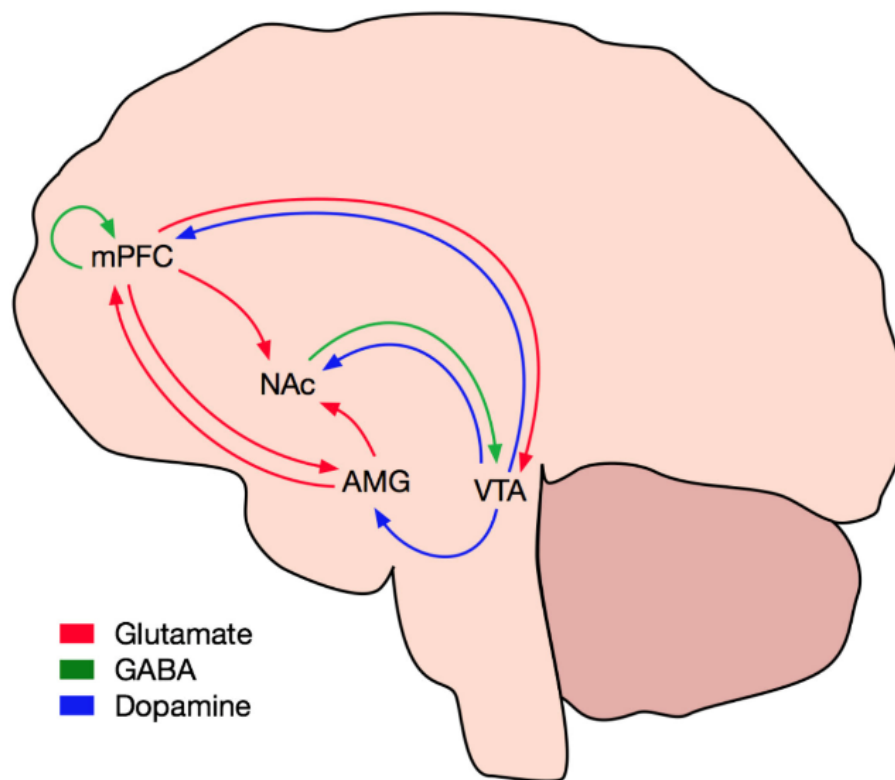


Figure 2.3: Mesolimbic reward pathway. Principal components of the mesolimbic reward pathway and their primary neurotransmitter systems. Abbreviations: Nucleus accumbens (NAc), medial prefrontal cortex (mPFC), amygdala (AMG), ventral tegmental area (VTA).

enhanced by ethanol exposure and extracellular dopamine concentrations are elevated downstream of VTA projections (Schier et al., 2013; Weiss et al., 1993). Validity for the dopamine-dependent positive reinforcement of ethanol has been demonstrated with co-administration of D1 agonists in rats (D'Souza et al., 2003).

Acute withdrawal from chronic ethanol increases refractory periods and reduces firing rates of dopaminergic VTA neurons projecting to mesolimbic structures (Diana et al., 1993). This depression of VTA output coincides with the dysphoric behavioral state of withdrawal and its effects are reversible with renewed ethanol administration. Similarly, positron emission tomography studies have revealed decreased dopaminergic signaling and responding in mPFC of recently abstained human alcoholics (Narendran et al., 2014; Volkow et al., 2007). Considering the importance of dopamine in executive functions such as decision making (Bickel et al., 2012; Floresco & Magyar, 2006), withdrawal-induced decrement of cortical dopaminergic activity may itself be a factor in relapsing behavior (Narendran et al., 2014). This is also true of long abstained alcoholics who display cognitive deficits years later (Bergman et al., 1998; O'Leary et al., 1977), which impair decision making and increase risk for relapse. Although it is unclear which pathological changes associated with chronic ethanol use are responsible

for these sustained deficits, evidence from animal models of AUD point to involvement of the dopamine system. Rats given chronic intermittent ethanol vapor exposure (CIE) show deficits in mPFC dopamine-dependent tests of cognitive flexibility and impaired mPFC dopamine receptor D2 and D4 signaling at least four weeks after discontinuing access (Trantham-Davidson et al., 2014).

2.3.3 Altered Pyramidal Neurons

Short and long-term exposures to ethanol have different effects on mPFC pyramidal neurons. Acute exposure to ethanol significantly inhibits mPFC pyramidal neuron NMDA receptor-mediated excitatory postsynaptic potentials (Weitlauf & Woodward, 2008). In contrast, chronic intermittent ethanol vapor exposure enhances NMDA receptor-mediated excitatory postsynaptic potentials (Klenowski et al., 2016; Kroener et al., 2012) and produces extensive synaptic remodeling including increased apical and basal dendritic arborization, spine density, and NMDA receptor subunit NR2B expression (Holmes et al., 2012; A. Kim et al., 2015; Klenowski et al., 2016; Kroener et al., 2012). The exact mechanism driving mPFC synaptic remodeling is not known, but is thought to be a result of inputs from overactive basolateral amygdala (Bechara, 2005; Pfarr et al., 2015), which project to the apical dendrites of mPFC pyramidal neurons (Navarro & Mandyam, 2015). Glutamatergic hyperexcitability may lead to excitotoxicity in

mPFC and is a potential cause of alcohol-induced neurodegeneration in heavy drinkers (A. Kim et al., 2015). After 3 weeks of abstinence from CIE, rats continue to show increased mPFC apical but not basal dendritic arborization and no longer display increased spine density (Navarro & Mandyam, 2015). Prolonged abstinence from CIE also results in decreased phosphorylation of NR2B, suggesting NMDA receptors are being internalized, potentially as a compensatory measure against CIE-induced excitotoxicity (Navarro & Mandyam, 2015).

2.3.4 Opioid Peptide Signaling in Withdrawal

Dynorphins are endogenous opioid peptides possessing activity at all opioid receptors but highest affinity for receptors (Chavkin et al., 1982). Dynorphins are distributed widely throughout the central nervous system (Fallon & Leslie, 1986; Watson et al., 1982). They are capable of inducing negative affective states and their dysregulation has been implicated in substance addiction (Shippenberg et al., 2007; Wee & Koob, 2010). One of the proposed functions of the dynorphin-opioid receptor system is to negatively regulate the mesolimbic reward pathway in response to excessive releasing of dopamine. In the VTA, populations of neurons projecting to mPFC, but not NAc, are inhibited by opioid peptides, providing a mechanism for modulating dopamine output pathways (Margolis et al., 2006). Because dynorphin expression is induced by chronic ethanol exposure

in limbic tissues (Lindholm et al., 2000) and its activity at opioid receptors decreases dopamine activity and is associated with dysphoric negative emotional states, it is thought to play a role in alcohol withdrawal and negative reinforcement and thus promoting compulsive ethanol consumption (George F. Koob, 2013; Todtenkopf et al., 2004; Walker et al., 2011). Supporting this theory, administration of opioid receptor antagonists reduces dependence-induced self-administration of ethanol in rats (Walker et al., 2011; Walker & Koob, 2008).

2.3.5 CRF Receptors and Amygdala Overactivation

The transition from impulsive to compulsive ethanol consumption has been attributed to a combination of mPFC-associated cognitive dysfunction and CeA overactivation, driving negative reinforcement through negative affect states (G F Koob, 2008). Anxiety states in alcohol withdrawal can be sensitized by CRF receptor agonists or reduced by CRF receptor antagonism (Overstreet et al., 2004), and this activity can be traced to CeA (Heinrichs et al., 1995). In rats, acute abstinence after prolonged intermittent exposure to ethanol produces recruitment of CRF interneurons to mPFC and is associated with a functional disconnection between mPFC and CeA along with impaired working memory (George et al., 2012). These effects were not observed in rats given continuous access or in rats receiving intermittent access but not in withdrawal. This supports the hypothesis

that alcohol withdrawal-induced negative affect states due to CeA overactivation can drive dysfunctional changes in mPFC and thereby impair executive function, potentially predisposing to compulsive behaviors. Further underscoring this idea, ethanol dependent rats given a CRF antagonist reduce ethanol self-administration following acute withdrawal (Funk et al., 2007).

2.3.6 Dichotomous Projections to Nucleus Accumbens

AUD is characterized by episodic relapses which can be triggered by the presence of alcohol-associated cues. Cue associations develop rapidly for rewarding effects of alcohol and are difficult to extinguish (Ciccocioppo et al., 2001; Field & Duka, 2002; Lê & Shaham, 2002; Sinha & Li, 2007). Alcoholics with short and long term abstinence show increased functional magnetic resonance imaging blood-oxygen-level-dependent imaging responses in mPFC when viewing alcohol-associated cues visual cues compared to controls (Grüsser et al., 2004; Heinz et al., 2007). Activation was highest in individuals that went on to relapse in the following 3 months and the degree of mPFC activation correlated with intake during relapse (Grüsser et al., 2004). Not limited to visual cues, alcohol gustatory cues alone are able to elicit substantial functional magnetic resonance imaging blood-oxygen-level-dependent responses in the mPFC of heavy alcohol drinkers (Filbey et al., 2008).

Targeted ablation of mPFC projections to NAc in rats eliminated cue-induced reinstatement of alcohol seeking, suggesting alcohol-cue associations are given value and salience by mPFC, which is communicated to the mesolimbic reward system via NAc (Keistler et al., 2017). This reinstatement pathway appears to be shared with other drugs of abuse and involves cued activation of excitatory prelimbic mPFC neurons, which then release glutamate onto NAc core (Klenowski, 2018; McFarland et al., 2003). This circuitry is modulated by dopamine D1 receptor expression on NAc projecting prelimbic neurons, which enhance salience of drug-cue associations (Brenhouse et al., 2008; Kalivas et al., 2005).

While the prelimbic mPFC tends to project to the NAc core, the NAc shell receives its mPFC afferents almost exclusively from the infralimbic area (Haber et al., 1995). In contrast to the prelimbic- NAc core projections, the infralimbic-NAc shell projections are modulated by dopamine D2 receptors (Zbukvic et al., 2016). Additionally, while prelimbic projections to NAc core act to increase drug-cue associations and reinstatement, infralimbic projections targeting NAc shell are associated with extinction of alcohol seeking behavior and inactivation of drug-associated cues (J. Peters et al., 2008, 2009; Pfarr et al., 2015). Highlighting this inhibitory role, selective ablation of NAc-shell projecting infralimbic neurons causes excessive alcohol seeking in rats (Pfarr et al., 2015).

2.4 White Matter in Alcohol Use Disorder

Oligodendrocytes have the capacity to wrap hundreds of neuronal axons with electrically insulating myelin, greatly increasing action potential fidelity and conduction velocity. While the majority of myelination occurs in early life, oligodendrocyte precursor cells continue to divide, differentiate, and myelinate in adult brain (Rivers et al., 2008). This process is important for plasticity of neural networks and has been observed in human adults learning new tasks (Bengtsson et al., 2005; Fields, 2005, 2010, 2015; Scholz et al., 2009).

In rodent CIE models of AUD, a decrease in proliferation, differentiation, and survival of mPFC oligodendrocyte precursor cells is observed (A. Kim et al., 2015). Those changes are accompanied by synaptic alterations in dendritic arbors, spine densities, and NMDA receptor subunit expression. In human alcoholics, white matter volume loss and dysfunction are observed and coincide with cognitive deficits affecting decision making, learning, and memory (Chanraud et al., 2007; Demirakca et al., 2011; Pfefferbaum & Sullivan, 2005; Ryan & Butters, 1980). Likewise, decreased expression of genes involved in myelination, including proteolipid protein (PLP), myelin-associated glycoprotein (MAG), and myelin

basic protein (MBP) is seen in postmortem human brain tissue (Lewohl et al., 2005; Liu et al., 2006).

Species	Gene	Identity
Human	CLIC1	67%
Human	CLIC2	66%
Human	CLIC3	51%
Human	CLIC4	-
Human	CLIC5	75%
Human	CLIC6	76%
Mouse	CLIC4	99%
<i>C. elegans</i>	EXC-4	25%
<i>C. elegans</i>	EXL-1	24%
<i>D. melanogaster</i>	CLIC	30%

Table 2.1: Chloride intracellular channel gene family homology.

Protein sequence identity for CLIC4 and the other 5 human chloride intracellular channel genes as well as CLIC4 orthologs in mouse, *C. elegans*, and *D. melanogaster*. Sequence identity obtained through protein BLAST. (<https://blast.ncbi.nlm.nih.gov>).

2.5 Characteristics of Chloride Intracellular Channel 4

Chloride intracellular channels are a small family of 6 highly conserved genes in vertebrates with orthologs in invertebrates (**Table 2.1**). Members of a rare class of metamorphic proteins, chloride intracellular channels can alter their three-dimensional structure under specific redox conditions (Littler et al., 2004, 2005). Although the functions of these proteins are still being elucidated, repeated studies have documented that one of the best characterized members of this family, CLIC4, has diverse roles in development (Chalothorn et al., 2009), apoptosis (Fernandez-Salas et al., 2002; Suh et al., 2004), and membrane trafficking (Chou et al., 2016; Maeda et al., 2008). CLIC4 has been shown to translocate to the nucleus as an early responder to cell stress (Suh et al., 2004) and to modulate transcription in the transforming growth factor beta pathway (Shukla et al., 2009). The gene has highly localized patterns of expression in the nervous system, potentially including white matter tracts (V. Padmakumar et al., 2014), and has been implicated in ion channel activity (Harrop et al., 2001; Littler et al., 2004; Tulk et al., 2000) and membrane trafficking (Chou et al., 2016; Maeda et al., 2008).

CLIC4 was first identified in 1987 as a p64 homolog (Howell et al., 1996) and its crystal structure was published in 2005 (Littler et al., 2005). CLIC4 is a 253 amino acid, 29kDa protein, that like other members of the chloride intracellular channel family, has structural homology with the glutathione S-transferase (GST)

fold superfamily (Littler et al., 2010). GSTs classically catalyze the covalent transfer of glutathione to exogenous substances as part of phase II metabolism and detoxification. Like other GST proteins, chloride intracellular channels contain two major structural domains, an N-terminal mixed α -helix and β -sheet domain and a C-terminal all-helical domain. Unique to members of the Ω subclass of GST proteins, chloride intracellular channels possess a glutaredoxin-like motif and active cysteine in their N-terminal domain which in other members of the Ω -GST class, has been associated with enzymatic redox reactions in lieu of glutathione transferase activity (Board et al., 2000; Littler et al., 2005). This glutathione-dependent oxidoreductase enzymatic activity has been demonstrated *in vitro* for multiple members of the chloride intracellular class, including CLIC4, and was capable of being inhibited by selective chloride channel inhibitors IAA-94 and A9C (Al Khamici et al., 2015).

Perhaps the most unique characteristic of the chloride intracellular channels is their ability to spontaneously modify their tertiary structure in response to changes in the redox state of their environment. Metamorphic proteins possess multiple stable equilibrium conformations and appear to be capable of interconversion in a ligand-free environment (Goodchild et al., 2011). Chloride intracellular channels are prototypical of this behavior, possessing glutaredoxin-like enzymatic activity in their soluble globular reduced state and becoming

membrane-integral when oxidized (Littler et al., 2005). Integration into membranes is thought to be facilitated by rearrangement of the N-terminal domain, which reveals an otherwise hidden, putative non-polar transmembrane domain (Harrop et al., 2001; Littler et al., 2005). In this oxidized state, CLIC4 demonstrates the ability to conduct anions across artificial membranes similar to an ion channel, although this feature is lost with the application of a reducing agent (Littler et al., 2005). However, further electrophysiological evaluation of CLIC4 in artificial membranes suggests the protein forms poorly-selective channels that also permit cations, suggesting classification as a pore may be more accurate than channel (Singh & Ashley, 2007). The mechanisms by which chloride intracellular channels form these pores is currently unknown. Intriguingly, mutation of the N-terminal active site cysteine inhibits both the glutaredoxin-like enzymatic activity of reduced CLIC4 (Al Khamici et al., 2015) and the ability of oxidized CLIC4 to integrate into membranes and conduct ions (Littler et al., 2010).

Expression of CLIC4 is fairly ubiquitous with high expression in vasculature, skin, liver, kidney, and brain (V. Padmakumar et al., 2014). Knowledge of regional and cell type-specific CLIC4 expression in brain is limited, but in situ hybridization data from Allen Brain Atlas suggest expression is highest in olfactory bulbs, cerebellum, and lateral septal complex (Lein et al., 2007; V. Padmakumar et al., 2014). CLIC4 has been identified in a variety subcellular

compartments, depending on specific cell type and conditions, but most commonly include cytoplasm, nucleus, mitochondria, plasma membrane, and intracellular membranes (Berry et al., 2003; Proutski et al., 2002; Suh et al., 2004). CLIC4 contains a nuclear localization sequence in its C-terminus and has been shown to translocate to the nucleus following TNF- α signaling and various cellular stresses including DNA damage, metabolic inhibitors, and inhibitors of transcription and translation (Fernandez-Salas et al., 2002; Suh et al., 2004). CLIC4 also has a p53 response element in its promoter and is upregulated by p53 pro-apoptotic signaling where its translocation to the nucleus accelerates apoptosis (Suh et al., 2004). CLIC4 has also been shown to translocate to the nucleus in order to promote TGF- β signaling by stabilizing phospho-SMAD transcription factors (Malik et al., 2010; Shukla et al., 2009). Considering its rapid induction following acute ethanol and ability to translocate to the nucleus during stress, it is possible *Clic4* may act as a modulator of the gene expression response to ethanol in brain.

2.6 Alcohol Use Disorder Studies in Model Organisms

Established animal models of AUD are numerous, ranging from invertebrates to non-human primates. Invertebrate model organisms such as *Drosophila melanogaster* and *Caenorhabditis elegans* are particularly well suited to high throughput mutation screens and evaluating acute ethanol behaviors such as

sensitivity to sedation and tolerance (Grotewiel & Bettinger, 2015). Rodents, including mice and rats, are commonly used to model more complex behaviors such as voluntary ethanol consumption, withdrawal, and reinstatement. With the abundance of available transgenic mice, candidate gene characterization studies are commonly carried out in mice. Two strains commonly used are the DBA/2J (D2) and C57BL/6J (B6) mice, which display different responses to acute ethanol, withdrawal, and voluntary ethanol consumption. D2 mice are more sensitive to ethanol and show longer periods of ethanol sedation, higher locomotor induction, and more severe withdrawal states compared to B6 mice (Linsenhardt et al., 2009; Lister, 1987; T. J. Phillips et al., 1994). While D2 mice show an aversion to ethanol consumption, B6 mice can show a higher preference for certain concentrations of ethanol over water (Belknap et al., 1993). Aversion in D2 mice appears to be a pre-digestive sensory discrimination phenomena considering the strain will self-administer ethanol if provided intravenously (Grahame & Cunningham, 1997). B6 and D2 mice and crossed hybrid offspring are often contrasted in genomic studies to model diversity of ethanol sensitivity and preference in humans (Farris et al., 2010; Gallaher et al., 1996; Kerns et al., 2005; Metten et al., 1998; Tamara J. Phillips et al., 1994, 1998; Tarantino et al., 1998; Wolen et al., 2012).

Mouse models of voluntary ethanol consumption are diverse and include various manipulations such as continuous or intermittent access, multiple ethanol

concentration choices, and forced ethanol vapor or voluntary drinking. While each paradigm has its own advantages, intermittent ethanol access (IEA), which models frequent repeated binge-withdrawal cycles, produces a higher escalation and overall intake compared to continuous access paradigms (H. C. Becker & Ron, 2014). Two-bottle choice, which pairs a bottle of water with an identical bottle of dilute ethanol, is the most commonly employed voluntary access methodology, but evidence suggests three-bottle choice (3BC) produces even higher escalation of intake (Melendez et al., 2006). Similar to humans, mice display sex differences in ethanol-related behaviors, although somewhat differently. Female mice tend to drink more ethanol than males, especially early in studies, have longer sedation periods, and show less severe withdrawal (J. B. Becker & Koob, 2016). In summary, mice make for useful models of AUD, displaying strain and sex-specific differences in ethanol-related behaviors and having an abundance of transgenic options available for investigating candidate genes.

In the following chapters, a combination of model organisms will be applied in the task of characterizing the molecular and behavioral responses to acute ethanol. This will include the use of *Drosophila* for evaluating sensitivity to ethanol sedation and the gene expression responses to *Clic* knockdown. A combination of D2 and B6 mice will be used to evaluate acute and chronic ethanol exposure-related behaviors, the role of *Clic4*, and the accompanying transcriptome

modifications. Together these approaches provide novel characterization of gene expression contributions to the development of AUD.

Chapter 3

Ethanol Sensitization and the Synaptic

Transcriptome

3.1 Introduction

Alcoholism is a chronic disease characterized by compulsive drug-seeking undeterred by negative consequences, as well as cravings and potential for relapse that persist despite years of abstinence. The endurance of these pernicious behaviors supports the theory that addiction arises from progressive and lasting cellular and molecular adaptations in response to repeated ethanol exposure (Nestler, 2001; Nestler et al., 1993). A more complete comprehension of neuronal plasticity that underlies the transition to compulsive drug use could lead to novel therapeutic strategies for alcohol use disorders.

The morphological specialization of neurons, where synapses appear to be regulated in an individual manner, advocates the need for local mechanisms

controlling synaptic function. Local synaptic protein synthesis is supported by the finding of synthesis machinery at post-synaptic sites, including ribosomes, tRNA, translation factors, endoplasmic reticulum, and Golgi apparatus (Steward & Levy, 1982; Steward & Reeves, 1988). Furthermore, through in situ hybridization (Lyford et al., 1995; Poon et al., 2006) and studies characterizing synapse-enriched subcellular fractions (Chicurel et al., 1993; Matsumoto et al., 2007; Poon et al., 2006; Rao & Steward, 1993) and microdissected neuropil (Cajigas et al., 2012), a number of mRNA species have been identified at synapses. mRNA transport has been shown to occur in an activity dependent manner. For instance, mRNA of the immediate early gene, *Arc*, as well as *GluR1* and *GluR2* transcripts have been shown to be localized to dendrites following NMDA and metabotropic glutamate receptor activation, respectively (Grooms et al., 2006; Steward & Worley, 2001). Also, depolarization extends transport of mRNA for BDNF and its receptor, TrkB, to the distal processes in neuronal cell culture (Tongiorgi et al., 1997). Studies using protein synthesis inhibitors have shown that protein synthesis is required for behavioral and synaptic plasticity, assumedly for establishing enduring modifications (Kang & Schuman, 1996; Steward & Schuman, 2001). Thus, targeting of specific RNAs to dendrites may be an efficient way of rapidly localizing proteins involved in synaptic function. Alterations in dendritic mRNA transport, stability,

or translation could thus modulate synaptic plasticity (Chicurel et al., 1993; Steward & Banker, 1992).

Previous research from our laboratory that examined ethanol regulation of gene expression across a variety of mouse strains has found significant enrichment of genes involved with synaptic functioning and plasticity, reproducibly amongst several brain regions (Kerns et al., 2005; Wolen et al., 2012). There is also evidence to support that adaptive responses underlying ethanol tolerance and dependence are synaptic in nature, in part involving changes in glutamate neurotransmission (Tsai & Coyle, 1998). Ethanol administration has been shown to induce structural synaptic plasticity as well. Alcohol-preferring rats exposed to 14 weeks of continuous access or subjected to repeated deprivations of ethanol exhibited decreased density and increased size of spines in a subpopulation of neurons in the NAc (Zhou et al., 2007). Cortical neurons exposed to chronic intermittent ethanol administration had significant increases in NMDA receptor surface expression (Qiang et al., 2007) and hippocampal cultures receiving prolonged ethanol exposures exhibited increased co-localization of PSD95 and f-actin (Carpenter-Hyland & Chandler, 2006) leading to enlargement of spine heads. Together these data suggest that dendritic spines may be an important target for the adaptive actions of ethanol. Therefore, we investigated whether ethanol

evoked changes to the synaptic transcriptome in a well-characterized model of behavioral plasticity, ethanol locomotor sensitization.

It has been proposed that behavioral sensitization is a process that occurs following repeated drug exposure as the result of neuroadaptations in brain reward systems that contribute to such phenomenon as drug craving and relapse in alcoholics (Piazza et al., 1990; T. E. Robinson & Berridge, 1993). Intermittent administration of many drugs of abuse, including ethanol, propagates the development of long-lasting sensitized responses to their stimulant effects, often measured as augmented locomotor activation in rodent models (Hirabayashi & Alam, 1981; Masur et al., 1986; Shuster et al., 1975). Behavioral sensitization has been associated with neurochemical and molecular adaptations that effect neurotransmission (Kalivas & Stewart, 1991; Vanderschuren & Kalivas, 2000; White & Kalivas, 1998). There is also evidence that brain regions mediating reinforcement and reward undergo neuroadaptations with cocaine or amphetamine sensitization causing increased incentive salience and self-administration of the drug (Horger et al., 1990; Piazza et al., 1990). Increased voluntary consumption of ethanol has also been observed following intermittent repeated exposure (Camarini & Hodge, 2004; Lessov et al., 2001).

We therefore hypothesize that ethanol-induced sensitization, may result, at least in part, from alterations in the synaptic transcriptome, contributing to

synaptic remodeling and plasticity. Here we utilize synaptoneurosomes (Williams et al., 2009) prepared from ethanol sensitized DBA2/J mice to enrich for synaptic mRNAs for the purpose of RNAseq analysis. Our expression profiling reveals that repeated ethanol exposure elicits distinctive changes to the complement of mRNA present at the synapse. Furthermore, our detailed analysis identifies, for the first time, that ethanol behavioral sensitization produces a striking alteration in exon utilization in the synaptic compartment. This analysis of the synaptic transcriptome in response to ethanol sensitization increases our understanding of mechanisms underlying ethanol-induced synaptic plasticity and highlights the complexity of genomic regulation at the subcellular level.

3.3 Materials and Methods

Ethics Statement

All procedures were approved by Virginia Commonwealth University Institutional Animal Care and Use Committee under protocol AM10332 and followed the NIH Guide for the Care and Use of Laboratory Animals (NIH Publications No. 80-23, 1996).

Animals

Male D2 mice were purchased from Jackson Laboratories (Bar Harbor, ME) at 8-9 weeks of age. Animals were housed 4 per cage and had *ad libitum* access to standard rodent chow (#7912, Harlan Teklad, Madison, WI) and water in a 12-hour light/dark cycle (6 am on, 6 pm off). Mice were housed with Teklad corn cob bedding (#7092, Harlan Teklad, Madison, WI) and cages were changed weekly. Subjects were allowed to habituate to the animal facility for one week prior to starting behavioral experiments. Behavioral assays were performed during the light cycle between the hours of 8 am and 2 pm.

Ethanol-Induced Behavioral Sensitization and Tissue

Collection

Ethanol behavioral sensitization was induced as previously described (Costin et al., 2013a; Costin et al., 2013b). Briefly, mice were divided into three treatment groups (n = 16 each): saline-saline (SS), saline-ethanol (SE), and ethanol - ethanol (EE). Mice were acclimated to the behavioral room for 1 hour prior to the start of the experiment on testing days. All locomotor activity was measured immediately following i.p. injection with either saline or ethanol during 10-minute sessions in sound-attenuating locomotor chambers (Med Associates, model ENV-

515, St. Albans, VT). The system is interfaced with Med Associates software that assesses activity using a set of 16 infrared beam sensors along the X-Y plane. Animals received two days of saline injections and placement in the testing apparatus for habituation to the experimental procedure. On test day 3, acute locomotor responses to i.p. saline (SS, SE) or 2.0 g/kg ethanol (EE) were measured. On conditioning days 4-13, animals received daily i.p. injections in their home cages of either saline (SS, SE) or 2.5 g/kg ethanol (EE). On the final testing day 14, the SS group received saline and the SE and EE groups received 2.0 g/kg ethanol and all groups were subsequently monitored in activity chambers for 10 minutes. On day 14 of the behavioral sensitization paradigm, mice were sacrificed by cervical dislocation 4 hours following i.p. injection. Immediately afterward, brains were removed and chilled for one minute in ice-cold 1x phosphate buffered saline. The frontal pole was dissected by making a cut rostral of the optic chiasm and then removing the olfactory bulbs. Excised tissue was stored in a tube on ice for less than 8 minutes before processing for synaptoneurosome isolation.

Synaptoneurosome Preparation

The protocol for preparation of synaptoneurosomes was adapted from Williams *et al.*, 2009 (Williams et al., 2009). Fresh tissue from 4 animals was pooled (approximately 0.45 g) and manually homogenized utilizing a 15 ml Potter-

Elvehjem Safe-Grind® tissue grinder (#358009, Wheaton, Millville, NJ) and diluted 1:10 in synaptoneurosome homogenization buffer. The buffer consisted of 0.35 M nuclease free sucrose (CAS #57-50-1, Acros Organics, NJ), 10 mM HEPES (#15630-056, Life Technologies, Carlsbad, CA), and 1 mM EDTA (#AM9260G, Ambion, Carlsbad, CA), which was brought to a pH of 7.4 and filter sterilized. Immediately before use, 0.25 mM DTT (CAS #3483-12-3, Fisher Scientific, Waltham, MA), 30 U/mL RNase Out (#10777-019, Invitrogen, Carlsbad, CA), and protease inhibitor cocktail containing AEBSF, Aprotinin, Bestatin, E64, Leupeptin, and Pepstatin A (#1862209, Halt, Thermo Scientific, Rockford, IL), were added to buffer. Centrifugation of whole homogenate (WH) at 500 × g for 10 minutes at 4°C removed nuclei and cellular debris, yielding pellet, P1 and supernatant, S1. The S1 fraction was passed through a series of nylon filters with successively decreasing pore sizes of 70, 35, and 10 μm (#03-70, #03-35, #03-10, SEFAR, Buffalo, NY). The filtrate was then diluted with 3 volumes of homogenization buffer and centrifuged at 2000 × g for 15 minutes at 4°C to yield the synaptoneurosome enriched pellet (P2) and a cellular supernatant fraction (S2). Fractions were frozen on dry ice and then stored at -80°C until further processing. Aliquots from each fraction of a synaptoneurosomal preparation were examined for the presence of contaminating nuclei using 4', 6-diamidino-2-phenylindole (DAPI) staining. Representative fields at 20x magnification were assessed for nuclear content.

Transmission Electron Microscopy

Morphological integrity of synaptoneuroosomes was confirmed by transmission electron microscopy. The P2 fraction was washed in PBS and centrifuged at $2000 \times g$ for 8 minutes. The supernatant was decanted and pellet was fixed with 2% glutaraldehyde in 0.1 M sodium cacodylate buffer at room temperature. After initial fixation, the sample was rinsed in 0.1 M cacodylate buffer for 5-10 minutes and then post-fixed in 1% osmium tetroxide in 0.1 M cacodylate buffer for 1 hour, followed by another 5-10-minute rinse in 0.1 M cacodylate buffer. Preparation continued with a serial dehydration with ethanol: 50%, 70%, 80%, 95% - for 5-10 minutes each, followed by 100% ethanol for 10-15 minutes (3x), and incubation in propylene oxide for 10-15 minutes (3x). The sample was then infiltrated with a 50/50 mix of propylene oxide and PolyBed 812 resin (Polysciences, Inc., Warrington, PA) overnight, which was then replaced with pure resin once again overnight. The sample was embedded in a mold, placed in a 60°C oven overnight, and then sectioned with a Leica EM UC6i Ultramicrotome (Leica Microsystems, Wetzlar, Germany), stained with 5% Uranyl acetate and Reynold's Lead Citrate, and examined on JEOL JEM-1230 transmission electron microscope (JEOL USA, Inc., Peabody, MA). Images of various magnifications (2,000x – 10,000x) were captured with the Gatan Ultrascan 4000 digital camera (Gatan, Inc., Pleasanton, CA).

Immunoblotting

Pellets (P1 and P2) and liquid aliquots (WH, S1, and S2) from synaptoneurosomal preparations were used to perform semi-quantitative immunoblotting. Pellets were triturated with NuPAGE LDS (#NP0008, Life Technologies, Carlsbad, CA) diluted to 1x and containing protease inhibitor cocktail (#1862209, Halt, Thermo Scientific, Rockford, IL), while liquid aliquots were lysed directly with 4x LDS with added proteinase inhibitor. Samples were sonicated on ice water until no longer viscous. Protein concentrations were determined using the bicinchoninic acid assay (#23227, Thermo Scientific, Rockford, IL) and absorbance at 562nm. Sample concentrations were balanced using 1x LDS, 10x NuPAGE reducing agent (#NP0004, Life Technologies, Carlsbad, CA) and boiled for 10 minutes. For each synaptoneurosomal fraction, 10 µg of protein was loaded per lane on a 10% or a 4% - 12% NuPAGE bis-tris gel (#NP0303BOX, #NP0322BOX, Life Technologies, Carlsbad, CA). Electrophoresis was performed at 150V followed by transfer to 0.45 µm nitrocellulose membrane for 1.5 hours at 30V on ice. Membranes were incubated with Ponceau S for 10 minutes, and densitometric analysis of staining was performed using ImageJ processing and analysis software (National Institutes of Health). Prior to primary antibody incubation, the membranes were blocked with 5% non-fat dried milk in 1x TBST for 45 minutes. Primary and secondary antibody catalog numbers,

dilutions, and incubation times are provided in **Table S1**. Immunoblots were visualized on GeneMate Blue Autoradiography film (BioExpress, Kaysville, UT) using the Amersham ECL Western Blotting Detection Reagent (#RPN2106, GE Healthcare Life Sciences, Pittsburgh, PA) and quantified using ImageJ. All detected proteins were normalized to the total protein loaded per well as measured by Ponceau S staining. Statistical analysis of immunoblot data was performed by one-way ANOVA across synaptoneurosome fractions followed by Tukey's *post-hoc* analysis.

Quantitative Reverse Transcriptase PCR (qRT-PCR)

Synaptoneurosomal fractions, S2 and P2, prepared from mice subjected to the sensitization protocol were assessed for enrichment of known dendritically-trafficked and somatically-restricted transcripts using qRT-PCR. Total RNA was isolated using the guanidine/phenol/chloroform method (#Cs-502, Stat-60, Tel-Test Inc., Friendswood, TX) and a Tekmar homogenizer as per the STAT-60 protocol. RNA concentration was determined by measuring absorbance at 260 nm and RNA quality was assessed by electrophoresis on an Experion Analyzer (Bio-Rad, Hercules, CA) and 260/280 absorbance ratios. All RNA samples had RNA quality indices (RQI) ≥ 7.6 and 260/280 ratios were between 1.97 and 2.06. cDNA was generated from 995 ng of total DNase-treated RNA and 5 ng of luciferase

mRNA (#L4561, Promega, Madison, WI) using Deoxyribonuclease I (#18068-015, Invitrogen, Carlsbad, CA) and the iScript cDNA kit (#170-8891, Bio-Rad, Hercules, CA) according to manufacturer's instructions. qRT-PCR was performed using the iCycler iQ system (Bio-Rad, Hercules, CA) according to manufacturer's instructions for iQ SYBR Green Supermix (#170-8880, Bio-Rad, Hercules, CA). Primer sequences, annealing temperatures, amplicon sizes, and cDNA dilutions used for each gene are listed in **Table S3.1**. Relative expression was calculated by comparing Ct values to a standard curve produced from S2 fraction cDNA (diluted 1:5, 1:25, 1:125, 1:625). Expression values were normalized to the exogenous internal reference mRNA, luciferase, to control for losses and inefficiencies of downstream processing (Johnson et al., 2005). Statistical analysis of qRT-PCR data was performed using a Student's t-test between the two fractions.

RNAseq Library Preparation and Sequencing

RNAseq data has been deposited with the Gene Expression Omnibus resource (GSE73018). Total RNA isolated for qRT-PCR was also used for gene expression profiling using RNAseq performed by the VCU Genomics Core Laboratory. To avoid non-biological experimental variation that arises from sample batch structure, supervised randomization of samples prior to each processing stage (RNA extraction, library amplification, and lane assignment) was

performed. A total of 4 biological replicates, each representing a pool from 4 animals, was obtained for each treatment group/fraction (**Figure 3.1**; SSS, SES, EES, SSP, SEP, EEP). Preparation of cDNA libraries was conducted following standard protocols using TruSeq RNA Sample Preparation Kit (#RS-122-2001, Illumina, San Diego, CA). Briefly, mRNA was isolated from total RNA using poly-T oligo-attached magnetic beads and then fragmented in the presence of divalent cations at 94°C. Fragmented RNA was converted into double stranded cDNA followed by ligation of Illumina specific adaptors. Adaptor ligated DNA was amplified with 15 cycles of PCR and purified using QIAquick PCR Purification Kit (#28104, Qiagen, Venlo, Netherlands). Library insert size was determined using an Agilent Bioanalyzer. Library quantification was performed by qRT-PCR assay using KAPA Library Quant Kit (#KK4835, KAPA, Wilmington, MA). RNAseq libraries were analyzed using Illumina TruSeq Cluster V3 flow cells and TruSeq SBS Kit V3 (#FC-401-3001, Illumina, San Diego, CA), with six libraries of different indices pooled together in equal amounts loaded on to a single lane at a concentration of 13 pM and sequenced (2 x 100 paired end reads) on an Illumina HiSeq 2000. Sample EE6_P2 was removed from subsequent analyses due to over-amplification artifacts. A summary of RNAseq metrics can be found in **Table S3.2**.

RNAseq Alignment

FASTQ formatted sequence files were aligned using TopHat2 v2.0.8 (D. Kim et al., 2013) with GRCm38/mm10 reference genome and annotations obtained from the UCSC genome table browser (<https://genome.ucsc.edu/cgi-bin/hgTables>) (Karolchik, 2004). The B6 reference genome (mm10) was edited to include D2 single nucleotide polymorphisms (Wang et al., 2016). Aligned BAM files produced by TopHat2 were validated for mapping quality with Samtools v0.1.9 (Li et al., 2009) and for completeness using BamUtil v1.0.13 (<http://genome.sph.umich.edu/wiki/BamUtil>). BAM files were converted to sorted SAM files for downstream feature count-based analysis with Samtools.

Differential Gene Expression Analysis

Raw read counts were produced from each SAM file using the python package HTSeq v0.6.1 (Anders et al., 2012) script *htseq-count* with the read overlap handler set to *union*. Resulting raw count files were analyzed for differential gene expression (DGE) between ethanol sensitized (EE) or acutely exposed (SE) animals and ethanol naïve (SS) animals within either the synaptic P2 fractions or the cellular supernatant S2 fractions using the R (<https://www.R-project.org>) package edgeR v3.10.2 (M. D. Robinson et al., 2010) with a negative binomial generalized log-linear model approach (McCarthy et al., 2012). Lowly expressed genes were

filtered out if not present in at least three libraries with counts per million of 3.4 or greater, corresponding with approximately 5 total counts in the smallest library. Genes meeting a false discovery rate (FDR) cutoff of 0.10 were considered significantly altered and used in downstream bioinformatic analysis.

Differential Exon Usage Analysis

A GFF annotation file containing collapsed exon counting bins was prepared from the UCSC GRCm38/mm10 GTF file using the DEXSeq v1.16.10 (Anders et al., 2012) Python script *dexseq_prepare_annotation.py*, with gene aggregation disabled. The number of reads overlapping each exon bin were then counted using the DEXSeq Python script *dexseq_count.py*, the GFF file, and each sample's SAM file. Differential exon usage (DEU) analysis was then carried out for the same contrasts studied in our differential gene expression analysis using the DEXSeq R package standard analysis workflow. Ensembl transcript IDs produced in the DEXSeq results files were translated to gene symbols using the R package BiomaRt v2.32.0 (Durinck et al., 2009). Genes with transcripts possessing at least 1 differentially utilized exon bin with an adjusted p-value (*padj*) less than 0.01 were considered to be significantly altered and were used in downstream bioinformatic analysis.

Bioinformatic Analysis

Functional enrichment analyses for DGE and DEU results were performed using ToppFun, available as part of the ToppGene suite of web-based applications (toppgene.cchmc.org) (Chen et al., 2009). Mouse gene symbols were submitted and analyzed for over-representation of genes that belong to Gene Ontology (GO) categories (molecular function, biological processes, and cellular component), mouse phenotypes and biological pathway databases including the Kyoto Encyclopedia of Genes and Genomics (KEGG) (Carbon et al., 2019; Kanehisa, 2000) and Reactome (Jassal et al., 2020). Only categories with p-values less than 0.01 and possessing between 3 and 1000 total genes were considered. The webtool REVIGO (Supek et al., 2011) was used for data reduction by semantic similarity, and visualization of GO terms lists resulting from this analysis.

RNA Binding Protein Enrichment Analysis

Genes possessing DEU between EEP and SSP groups ($p_{adj} < 0.01$) were intersected with the genes possessing basal DEU between SSP and SSS groups ($p_{adj} < 0.01$) in order to produce a list of genes with synapse-specific DEU that was also regulated by ethanol sensitization. The same was done to produce a synaptic sensitization-induced DGE gene list using FDR cutoffs of 0.1. These two lists of genes were then intersected with gene list obtained from two public databases of

known and predicted RNA binding proteins (RNABP): RBPDB (Cook et al., 2011) and ATtRACT (Giudice et al., 2016). The synaptic ethanol-sensitive DEU gene list was also intersected with a list of mRNA targets of the RNA binding protein fragile X mental retardation protein (FMRP), which was obtained from **Table S3.2A** of Darnell et al. (Darnell et al., 2011). For RNABP and FMRP enrichment analyses, the R package GeneOverlap (version 1.16.0; <http://shenlab-sinai.github.io/shenlab-sinai/>) was used to calculate odds ratios for relative enrichment of synaptic ethanol sensitive DEU genes and Fisher's exact tests to calculate enrichment p-values.

Sequence Motif Analysis

Chromosomal coordinates for the differentially utilized exon bins from the synaptic sensitization-induced DEU gene lists used in the RNABP analysis were provided to BEDTools v2.26.0 (Quinlan & Hall, 2010) in order to obtain their respective nucleotide sequences. Sequences for the 475 exon bins (**Table S12**) containing a minimum of 8 base pairs were then supplied to the web-based motif discovery tool MEME (Bailey et al., 2009) to search for known or novel motifs common between them. Any motifs identified that met an E-value cutoff of 0.05 were aligned to the CISBP-RNA database of RNABP motifs and specificities using the MEME Suite tool Tomtom (Gupta et al., 2007). Database motif alignments were considered significant if the alignment score had an E-value ≤ 0.05 .

3.4 Results

3.4.1 Synaptoneurosome Fraction Characterization

D2 mice were chosen for these studies due to their characteristic sensitivity to ethanol psychomotor stimulation and development of sensitization (T. J. Phillips et al., 1994). Distance traveled on test days 3 and 14 was compared and a significant increase in activity on day 14 was interpreted as an induction of ethanol sensitization (**Figure 3.1a, b**). Daily i.p. injections of 2.5 g/kg ethanol elicited an augmented locomotor response to 2.0 g/kg ethanol on day 14 as compared to day 3 (two-way repeated measures ANOVA, $F_{\text{Treatment}[2,45]} = 96.76, p < 0.001, F_{\text{Day}[1,45]} = 77.47, p < 0.001, F_{\text{Interaction}[2,45]} = 16.89, p < 0.001, n = 16$). Frontal pole brain tissue obtained from mice in this experiment was utilized in preparation of synaptoneurosome enriched samples.

The synaptoneurosomal fractionation protocol (**Figure 3.2a**) was validated in preliminary studies by transmission electron microscopy (**Figure 3.3a**). As suggested previously (Williams et al., 2009), the intact pre- and post-synaptic terminals, identified by transmission electron microscopy, provide for selective extraction of synaptic mRNAs. Absence of intact nuclei throughout synaptoneurosomal fractions was verified by 4'-6-Diamidino-2-phenylindole (DAPI) staining (**Figure 3.2b**), while

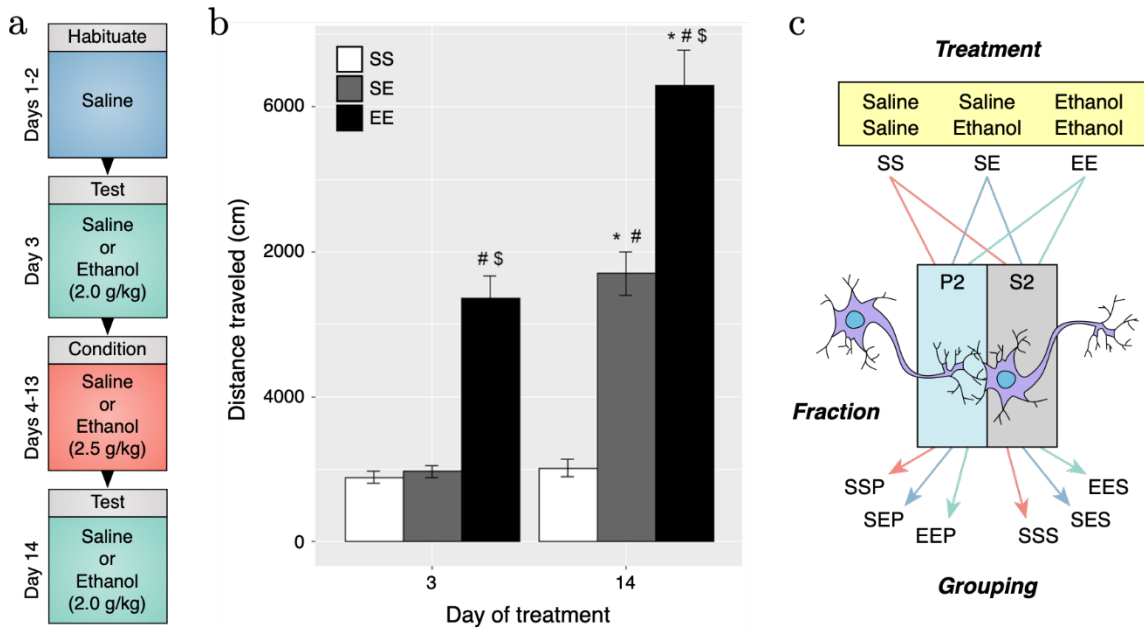


Figure 3.1. Ethanol behavioral sensitization in male D2 mice.

(a) Experimental protocol and timeline for induction of behavioral sensitization. (b) Repeated ethanol exposure induced behavioral sensitization as measured by locomotor activity on day 14 (EE) as compared to acute ethanol administered on day 3 (EE) and day 14 (SE). (c) Experimental groupings used for RNA sequencing and bioinformatic analysis were derived from ethanol treatment type and specific cellular fraction. (# $p < 0.001$ compared to SS within same day, \$ $p < 0.001$ compared to SE within same day, * $p < 0.001$ compared to same treatment on day 3, repeated measures two-way ANOVA with Tukey's post hoc analysis)

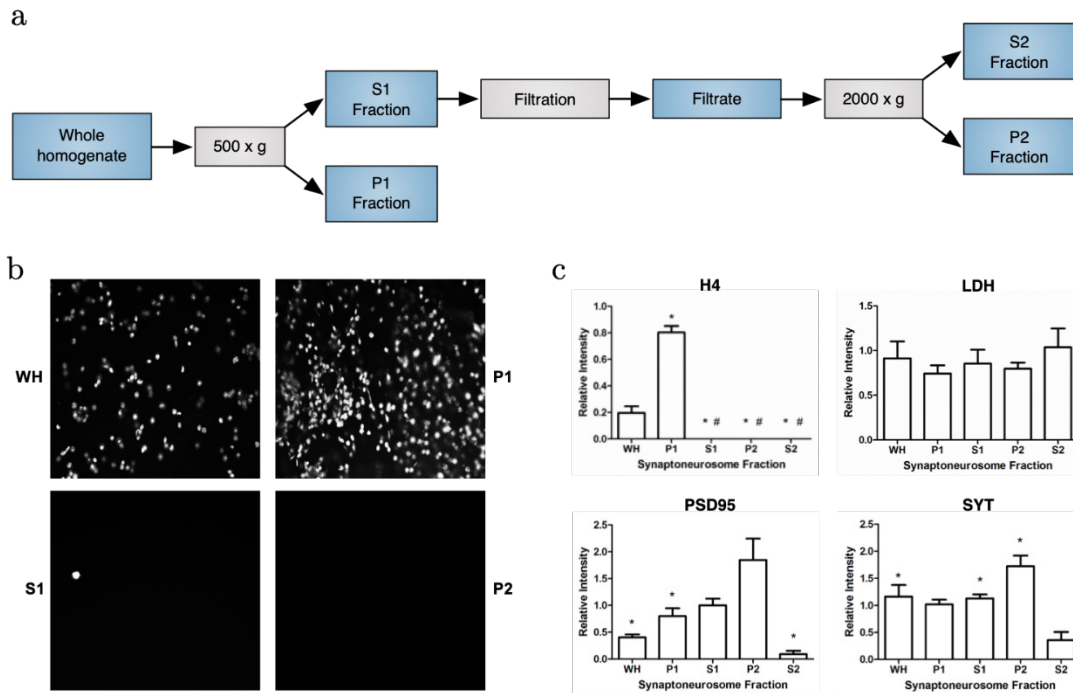


Figure 3.2. Characterization of synaptoneurosome preparations. (a) Schematic depicting synaptoneurosome preparation. Whole homogenate (WH) processed from pooled frontal pole tissue of four mice was used in the centrifugation/filtration scheme depicted here. The initial pellet (P1) contained cellular debris and nuclei. The supernatant from the initial centrifugation (S1) was filtered and subjected to a second centrifugation. The pellet, P2, was enriched for synaptic elements and dendritically targeted RNA as compared to the supernatant, S2, which contained the remainder of the somatodendritic RNA. (b) DAPI staining of synaptoneurosome fractions at 20x magnification indicating that most, if not all the nuclei were removed during the initial centrifugation step to produce the P1 pellet. (c) Quantification of immunoblots probing subcellular protein markers across synaptoneurosome fractions (H4 = nuclear; LDH = cytosolic; PSD95 = post-synaptic; SYT = presynaptic).

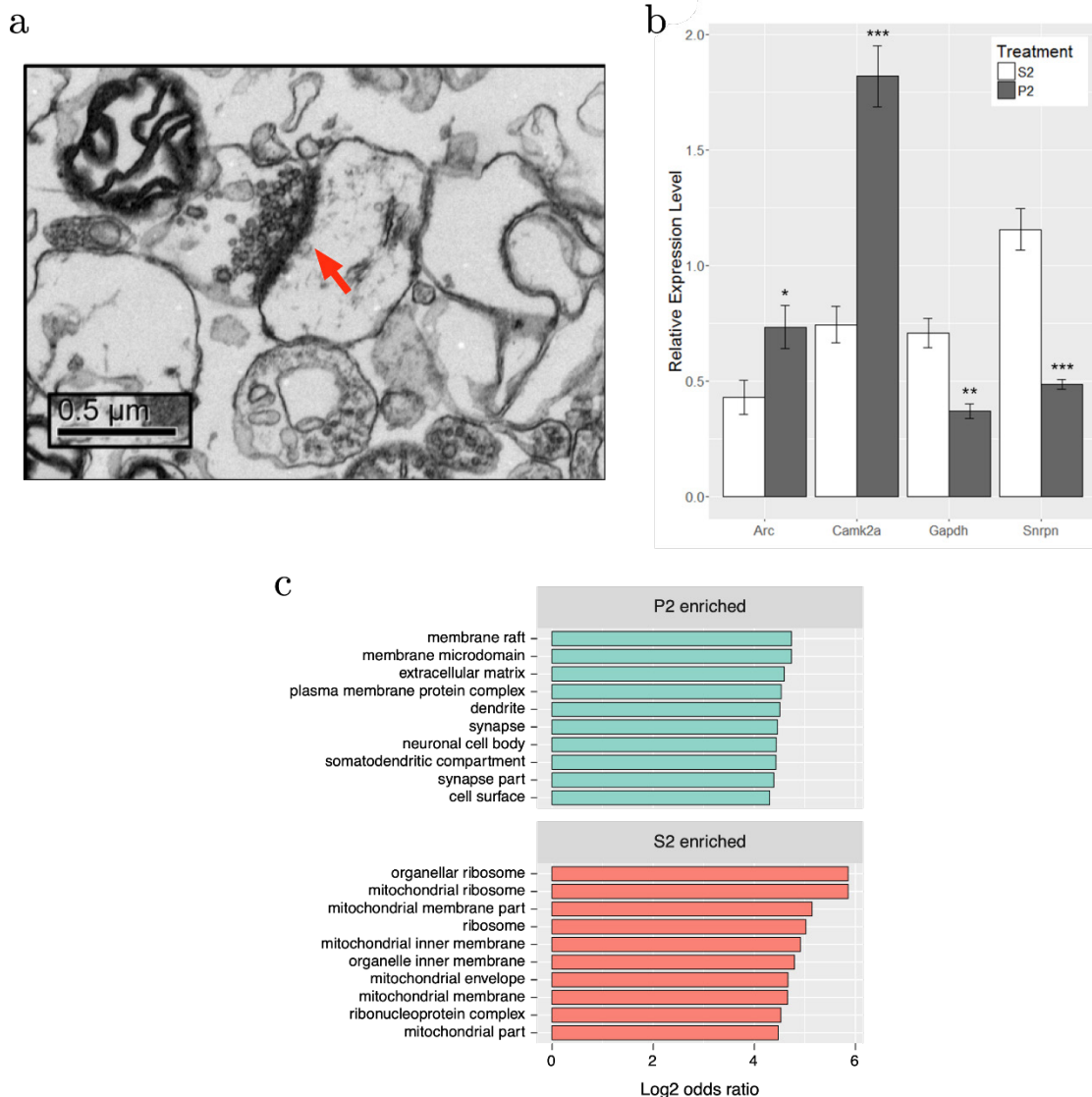


Figure 3.3. Synaptoneurosomes display distinct RNA populations. (a) Representative electron micrograph from P2 fraction observed at 10,000x magnification. Post-synaptic density is labeled by red arrow and presynaptic elements with synaptic vesicles can be observed immediately adjacent. (b) RNA isolated from S2 and P2 fractions of behaviorally sensitized mice was assayed for transcripts of known subcellular localization to ensure enrichment of synaptic RNAs. *Camk2a* and *Arc* are transcripts known to be synaptically targeted, while *Gapdh* and *Snrpn* are somatically restricted. Paired Student's t-test between fraction for each gene, *Camk2a* ($t[7] = 6.941$, $***p = 0.0002$), *Arc* ($t[7] = 2.646$, $*p = 0.0331$), *Gapdh* ($t[7] = 4.181$, $**p = 0.0041$), *Snrpn* ($t[7] = 8.439$, $****p < 0.0001$), $n = 8$. (c) Top 10 GO Cellular Compartment categories according to p-value as derived from functional enrichment analysis of the untreated P2 enriched gene list (SSP vs. SSS), sorted by log₂ of the categories' odds ratio.

immunoblotting for subcellular protein markers was used to ascertain purity of the preparation (**Figure 3.2c**). Together these data indicate P2 fractions contain synaptic elements enriched for the synaptic protein markers, synaptotagmin and PSD-95 (one-way ANOVA, $F_{\text{SYT}}[4,10] = 9.83$, $p = 0.0017$, $F_{\text{PSD95}}[4,10] = 11.09$, $p = 0.0011$, $n = 3$), and are devoid of appreciable nuclear contamination (one-way ANOVA, $F_{\text{H4}}[4,10] = 125.3$, $p < 0.0001$, $n = 3$),

To ensure enrichment in experimental tissues, total RNA isolated from S2 and P2 fractions of mice subjected to the ethanol behavioral sensitization paradigm was evaluated by qRT-PCR (**Figure 3.3b**). P2 fractions had higher relative expression levels of known synaptically targeted transcripts, *CamK2a* and *Arc* (Burgin et al., 1990; Link et al., 1995; Lyford et al., 1995), while transcripts known to be somatically restricted, *Gapdh* and *Snrpn* (Litman et al., 1994; Poon et al., 2006), were more abundant in the S2 fraction (Student's paired *t*-test, $t_{\text{CamK2a}}[7] = 6.941$, $p = 0.0002$, $t_{\text{Arc}}[7] = 2.646$, $p = 0.0331$, $t_{\text{Gapdh}}[7] = 4.181$, $p = 0.0041$, $t_{\text{Snrpn}}[7] = 8.439$, $p < 0.0001$, $n = 8$).

RNAseq was used to evaluate global gene expression in the S2 and P2 fractions (**Table S3.3**). DGE analysis (**Table S3.4, S3.5**) demonstrated widespread and highly significant differences in P2 versus S2 samples at the gene level in saline control samples (SSP_SSS), with 1829 genes differentially expressed at an FDR ≤ 0.1 and log2 fold-change ≥ 1 or ≤ -1 . Of these, 1408 were found to be enriched (>2 -

fold increased expression) in the P2 fraction (**Table S3.5**) and 421 enriched in the S2 fraction (**Table S3.5**). Of note, our RNAseq data faithfully replicated the qRT-PCR results of **Figure 3.3b**, even though derived from a totally separate experiment and synaptoneurosome preparation (**Table S3.6**). This supports the rigor of our RNAseq studies. Functional enrichment analysis of the P2 enriched gene list revealed significant over-representation of cellular categories related to the structure of the synapse (**Figure 3.3c**) and molecular or biological categories relating to calcium ion binding, cell adhesion and growth factor binding among others relevant to the synapse (**Table S3.5**). In contrast, the S2 fraction showed cellular category enrichment relating to protein synthesis and mitochondria (**Table S3.5**). These results establish that, in contrast to the cellular supernatant S2 fraction, the P2 synaptoneurosome fraction was enriched for mRNA relevant to synaptic function.

3.4.2 Sensitization Alters the Synaptic Transcriptome

To focus our attention on functional reorganization of the synapse occurring with acute ethanol or ethanol sensitization, we identified treatment-responsive DGE within cellular fractions through a gene-level analyses in edgeR. For these analyses, we used only an FDR cutoff (≤ 0.1) without further filtering for fold-change. **Figure 3.4a** and **Table S3.7** show that more than twice as many genes

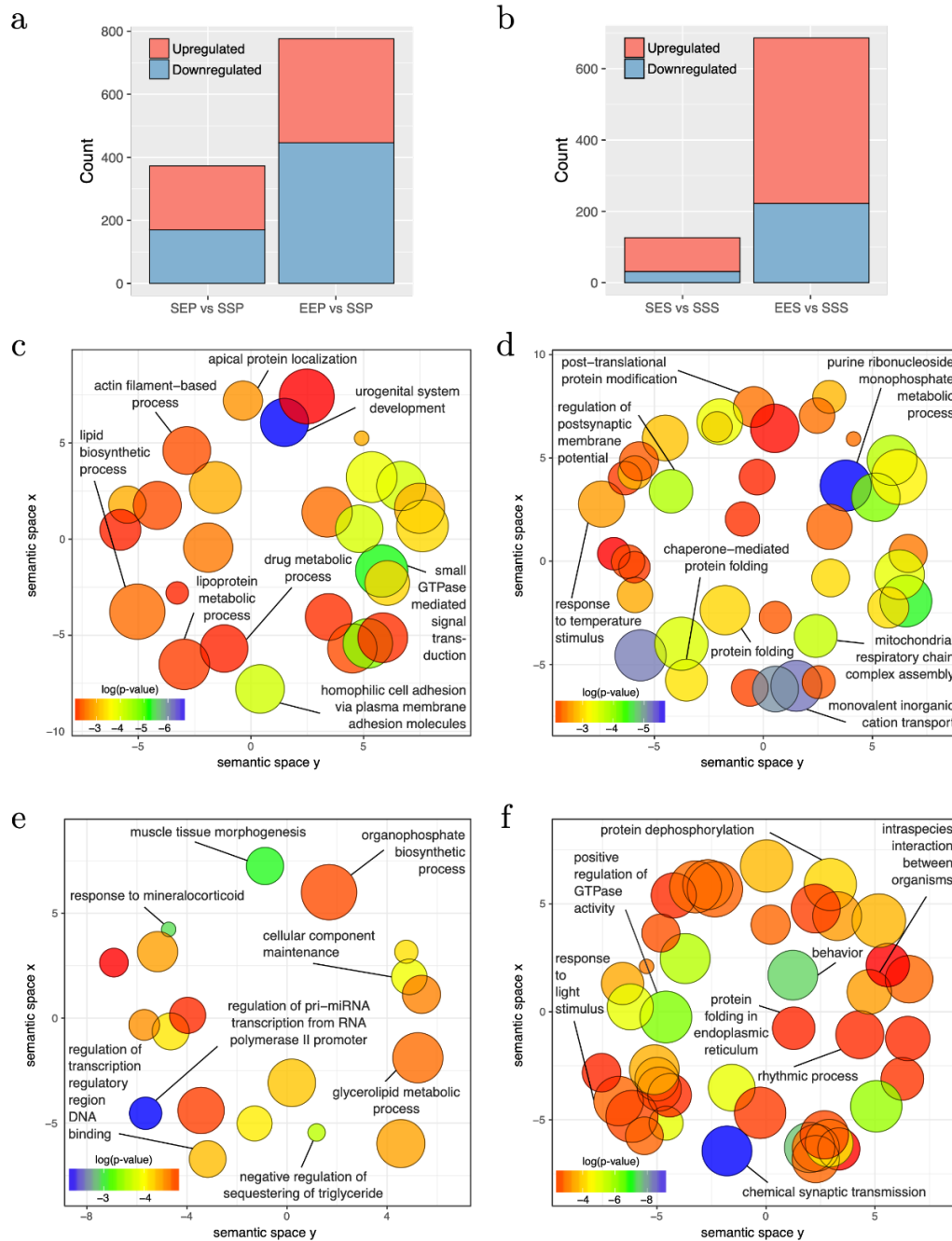


Figure 3.4. DGE following acute ethanol exposure or sensitization. The number of genes found to be significantly altered (FDR < 0.1) by sensitization and acute exposure to ethanol treatments in the (a) P2 fraction and (b) S2 fractions. Scatterplots of representative GO Biological Process categories derived from functional enrichment analysis of genes regulated by acute ethanol (c,e) or ethanol sensitization (d,f) in the P2 fraction (c,d) and S2 fraction (e,f). Scatterplots depict semantic similarity on axes, dispensability by size, and log₁₀ p-value as color.

responded to ethanol sensitization (EEP vs SSP; n=776) as to acute ethanol (SEP vs. SSP; n=375) in the P2 fraction. The S2 fraction (**Figure 3.4b** and **Table S3.8**) showed an even larger divergence between acute and repeated ethanol exposures with 686 genes regulated by sensitization (EES vs. SSS) and 126 responding to acute ethanol (SES vs. SSS).

Functional over-representation analysis of these DGE groups showed striking divergence between responses to acute vs. sensitizing ethanol treatments within both the P2 and S2 compartments. REVIGO semantic similarity analysis was used to group similar GO Biological Process categories and thus reduce the complexity of the functional group analysis. **Figure 3.4d** demonstrates functional clusters relating to postsynaptic membrane potential, post-translational protein modification, protein folding and molecular chaperones and mitochondrial respiratory function in the EEP vs. SSP comparison. In contrast, none of these clusters are present in the SEP vs. SSP analysis of acute ethanol responses (**Figure 3.4d**), which did show categories related to actin filament function and small GTPase signal transduction (**Figure 3.4c**). Similarly, the EES vs. SSS and SES vs. SSS comparisons showed functional dissimilarity with each other and the P2 comparisons for the most part (**Figures 3.4e, 3.4f**) except for the occurrence of clusters relating to molecular chaperone function in the EES vs. SSS comparison, similar to that seen in the P2 sensitization response (**Figure 3.4d**). Complete details

of all functional over-representation studies for these group comparisons are contained in **Tables S3.6** and **S3.7**. Overall, this gene level functional analysis suggests that ethanol sensitization produces a striking synaptic transcriptome response with changes in expression groups affecting energy production, protein trafficking/folding, and postsynaptic membrane currents.

3.4.3 Sensitization is Accompanied by Differential Splicing

Since differential splicing and transcript utilization are prominent in the nervous system, we performed an exon-level analysis of treatment effects within the P2 and S2 compartments using DEXSeq. We used a more stringent statistical threshold (adjusted p-value ≤ 0.01) to define DEU due to the nearly 30-fold greater number of exons detected (n = 356,131; **Table S3.9**) compared to the number of genes detected with edgeR (n = 11,764; **Table S3.3**). DEXSeq analysis revealed widespread alternative splicing events in the frontal pole S2 and P2 of ethanol sensitized mice. 1067 exons were differentially utilized in the P2 fraction following ethanol sensitization (EEP vs. SSP), representing 746 unique genes (**Figure 3.5a**, **Table S3.10**). In contrast, only 42 exons representing 36 genes were differentially utilized in the acute ethanol exposure group (SEP vs. SSP; **Figure 3.5a**, **Table S3.10**). In the somatic fractions of sensitized mice, 6179 exons representing 2627 genes were differentially utilized (EES vs. SSS), whereas no

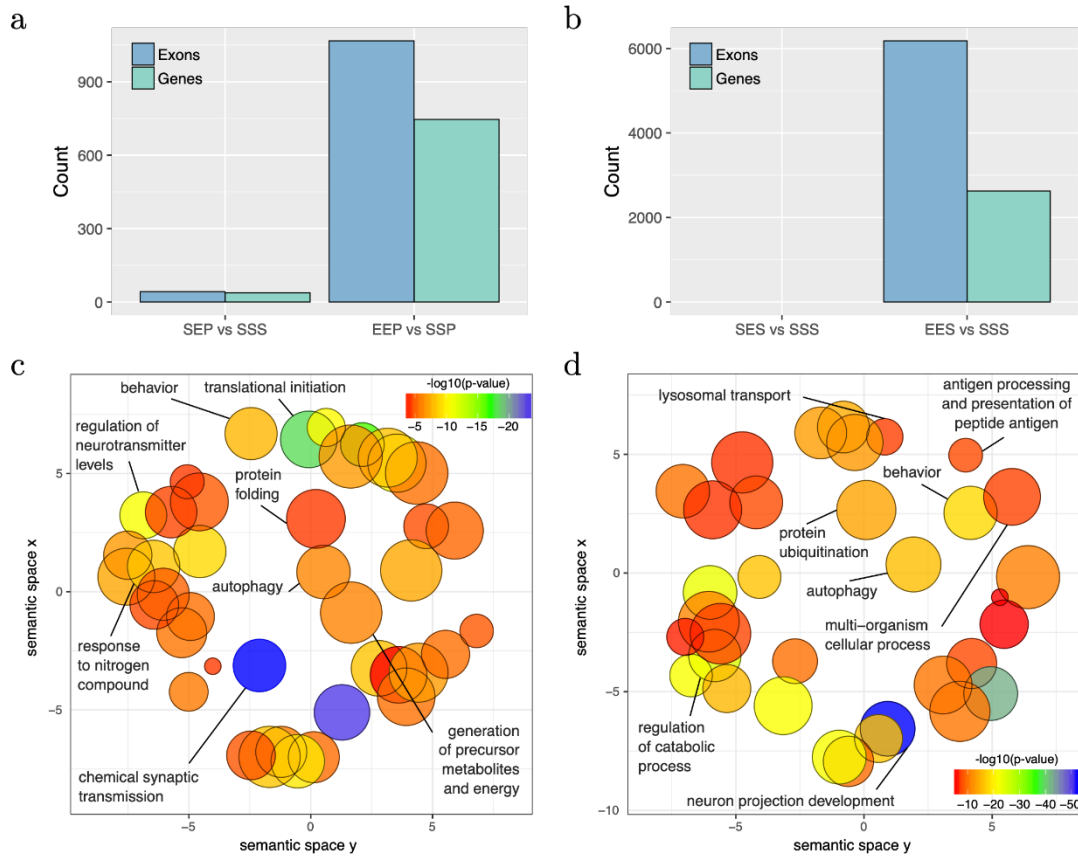


Figure 3.5. DEU following acute ethanol exposure or sensitization. The number of differentially utilized exons ($p_{adj} < 0.01$) and unique genes possessing a minimum of one differentially utilized exon observed in the P2 (a) and S2 (b) fractions following acute ethanol exposure or sensitization. GO reduction plots depicting clustering of top biological processes associated with ethanol sensitization and acute exposure induced DEU are displayed for the P2 (c) and S2 (d) fractions.

exons passed our statistical threshold in the acute ethanol exposure group (**Figure 3.5b, Table S3.11**).

Functional enrichment analysis of P2 genes affected by ethanol sensitization-induced DEU revealed perturbed GO Biological Processes ($p < 0.01$) relevant to translation regulation, mRNA processing, protein stability, and synaptic function (**Figure 3.5c, Table S3.10**). In contrast, GO Biological Processes affected by sensitization ($p < 0.01$) in the S2 fraction were primarily involved in catabolism, autophagy, and regulation of cellular morphology (**Figure 3.5d, Table S11**). Over-representation analysis was not performed for the acute ethanol exposure groups due to the low level of affected exons.

3.4.4 Enrichment of RNA Binding Protein Targets

To further evaluate the RNA processing and translation-related functional categories present in the ethanol sensitization-dependent P2 DEU functional enrichment analysis, the significant P2 DEU and DGE gene lists were analyzed for enrichment in RNA binding proteins using two publicly available databases, RBPDB and ATtRACT. To focus more conservatively on synaptic mRNA regulated by ethanol sensitization, we used the intersection of EEP vs SSP and SSP vs. SSS gene or exon datasets for these analyses. The DGE (**Table S3.4**) and DEU (**Table S3.12**) gene lists showed a modest but significant overlap with each other

(OR = 2.3, $p = 1 \times 10^{-5}$) as did the databases of RBPDB and ATtRACT (OR = 8.8, $p = 9.6 \times 10^{-63}$) (**Figure 3.6a**). However, the DGE list was not enriched for RNABPs from RBPDB (OR = 0.3, $p = 1$) or ATtRACT (OR = 1, $p = 0.59$) nor was the DEU list enriched for RNABPs from RBPDB (OR = 0.3, $p = 1$) or ATtRACT (OR = 1.3, $p = 0.22$) (**Figure 3.6a**).

The same sensitization-induced synaptic DGE and DEU gene lists were then evaluated for enrichment of RNA targets of a synaptically ubiquitous RNABP, FMRP. FMRP has previously been identified as being involved in ethanol regulation of GABA_B receptor membrane abundance (Wolfe et al., 2016). The DGE gene list was not found to be enriched in FMRP targets (OR = 1.4, $p = 0.07$) whereas the DEU gene list showed marked over-representation for FMRP targets (OR = 7.2, $p = 1.1 \times 10^{-56}$) (**Figure 3.6b**).

Due to the lack of enrichment of RNABPs but over-representation of RNABP targets in the sensitization-induced synaptic DEU gene list, the possibility for novel or known sequence motifs governing RNABP target preference was investigated within the differentially utilized exon bins. Exon bin sequences were supplied to the web-based motif discovery tool MEME and 5 novel sequence motifs were detected within the exon list having E-values ≤ 0.05 (**Table 3.1**, **Table S3.13**). Of these, 4 were also found to have high sequence alignment with known

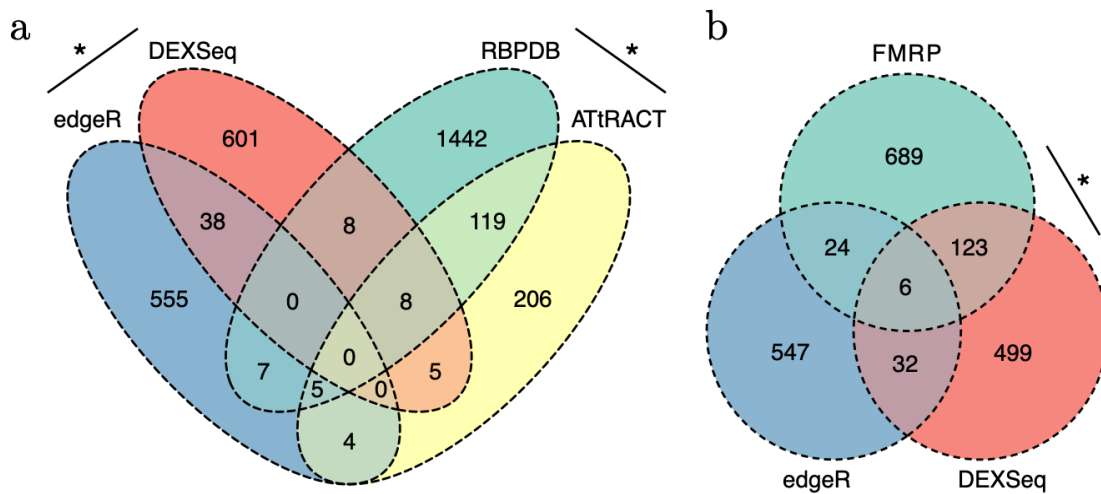


Figure 3.6. Synapse-Specific DEU is enriched in RNABP targets. Ethanol sensitization altered synaptic exon usage for targets of RNA binding proteins. Ethanol sensitization did not enrich gene expression or differential exon usage (a) of RNA binding proteins at synapses. Synaptic DEU but not DGE were enriched for targets of FMRP following ethanol sensitization (b) (* $p < 0.05$, Fisher's exact test).

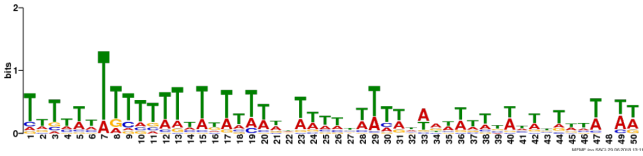
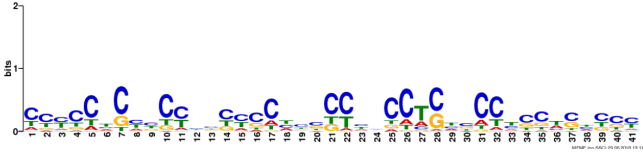
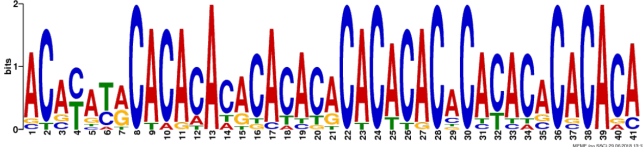
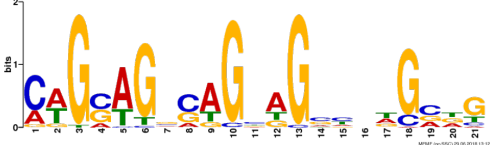
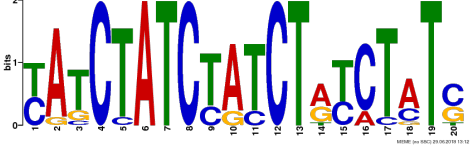
Motif	Logo	E-v alue	Similar motifs
1		1×10^{-170}	Gm10110
2		3.6×10^{-93}	Srsf4
3		3.8×10^{-13}	Celf3 Celf4 Hnrp11 Rbm38
4		1.2×10^{-8}	None known
5		2.5×10^{-8}	Hnrpdl

Table 3.1. Sequence motif discovery. Motifs found in P2 ethanol sensitization-regulated exons. Motifs are ranked by E-value and nucleotide letter sizes in logos are proportionate to relative frequency within motif sequence. Four of the novel motifs have high sequence similarity with known or predicted RNABP target sequence preferences (E-value ≤ 0.05).

RNABP sequence preferences ($E \leq 0.05$) from the CISRNA-BP database. These findings suggest that a discrete set of RNABPs may regulate synaptic trafficking of ethanol sensitization-responsive transcripts.

3.5 Discussion

The studies contained here provided the first genomic analysis of acute ethanol and ethanol sensitization regulation of the synaptic transcriptome. Using a well-characterized synaptoneurosomal preparation, we validated enrichment of synapse-related mRNA. RNAseq analysis showed that both acute ethanol and ethanol sensitization, a model of behavioral plasticity, produced unique changes in the synaptic transcriptome. In particular, ethanol sensitization produced increased synaptic expression of genes that function in protein synthesis and folding and dendritic structure, among others. We also demonstrated, using an exon-level analysis, a striking preponderance of differential exon utilization occurring following ethanol sensitization. The genes showing DEU with ethanol sensitization were over-represented for targets of specific RNA binding proteins, including FMRP. Thus, ethanol sensitization has a major impact on the synaptic transcriptome in both regulation of gene expression and transcript composition. The genes identified here as regulated by ethanol sensitization in the synaptic transcriptome may provide unique understanding of the mechanisms underlying

synaptic plasticity contributing to behavioral changes occurring with chronic ethanol exposure.

Neurons are highly specialized polarized cells, whose dendritic and axonal arborizations contain thousands of synapses that function and change individually in response to stimulation (Steward et al., 1998; Steward & Levy, 1982; Wallace et al., 1998). It has been proposed that activity-dependent synaptic plasticity requires the transport and translation of specific mRNA species, creating a unique complement of proteins that are able to function in response to a specific stimulus (Bramham & Wells, 2007). Comparing the somatic and synaptic transcriptomes in response to acute or sensitizing treatments of ethanol, we were able to detect compartmentalized differences in ethanol regulation of gene expression. Through our initial characterization studies, we are confident in our assessment that the differences observed when analyzing the P2 and S2 fractions are a survey of ethanol's effect on gene expression in distinct subcellular locations. The exact means by which ethanol is exerting its regulation of the synaptic transcriptome has yet to be determined. Conceivably, ethanol could be affecting synaptic transcript abundances through overall modulation of gene expression that could have a global effect on mRNA levels within the cell, and ultimately, through the mere altered availability of transcript, results in changes at the synapse. Our data indicates that this is not an adequate explanation, as we were

able to detect distinct gene sets representing different biological function categories in the P2 and S2 fractions. Furthermore, there was a striking lack of overlap between functional categories regulated by acute versus sensitizing ethanol treatments, despite both assays being done at the same time frame post-ethanol exposure. This is clear evidence of reorganization of the synaptic transcriptome with chronic ethanol exposure.

The trafficking and localization of transcripts to the synapse offers another possible means of regulatory control. Synaptic tagging is a process whereby synaptic activation induces a transient synapse-specific change that allows the synapse to capture mRNA or proteins required for long-term plasticity, which has explicitly been studied for its role in long-term potentiation (Frey & Morris, 1997). The exact physical nature of the synaptic tag has not been absolutely defined, but candidate molecular tags that have been proposed include post-translation modifications to existing synaptic proteins, alterations to protein conformational states, initiation of localized translation or proteolysis, and reorganization of the local cytoskeleton (Doyle & Kiebler, 2011; Kelleher et al., 2004; Martin & Kosik, 2002) (Martin and Kosik, 2002;Kelleher et al., 2004;Doyle and Kiebler, 2011). All of these mechanisms have the potential of being initiated by signaling events that result from membrane receptor activation. For instance, one pharmacological effect of ethanol is the release of dopamine in the NAc, which when acting at

dopamine D1-like receptors increases activity of adenylyl cyclase, thereby increasing cAMP levels and PKA activity. It has been shown that PKA activation is required for the formation of the synaptic tag (Barco et al., 2002; Casadio et al., 1999). The premise that signaling cascades downstream of ethanol could alter the ability of activated synapses to capture dendritically targeted mRNA requires examination.

Regardless of the exact mechanisms for synaptic localization of mRNA, our data here clearly suggests that differential activation or expression of RNA binding proteins by ethanol sensitization may be a major mechanism for restructuring the synaptic transcriptome to produce enhanced locomotor activation following repeated ethanol exposure. Our motif binding overrepresentation analysis of DEU results adds supportive evidence for ethanol sensitization utilizing specific mRNA binding proteins for modulating the synaptic transcriptome by identifying 5 novel consensus sequences with high similarity to known or predicted RNABP targets. Furthermore, this mechanism is strongly supported by our finding that genes with ethanol sensitization-induced DEU in the synaptic fraction are strongly over-represented for targets of the mRNA binding protein FMRP. FMRP is a known RNA-binding protein involved in mRNA transport and regulation of synaptic protein translation, as well as dendritic spine development (Cruz-Martin et al., 2012; Darnell et al., 2011; Michaelsen-Preusse et al., 2018). Prior studies on ethanol

and FMRP have shown that the protein can regulate an acute ethanol-induced alteration in GABA type B receptor dendritic expression (Wolfe et al., 2016). Spencer and colleagues also showed that chronic ethanol exposure altered expression of NMDA, Kv4.2 and KChIP3 in hippocampus in a FMRP-dependent fashion, possibly by altering phosphorylation of FMRP and its translational inhibitory properties (Spencer et al., 2016). Our studies here greatly extend this connection between ethanol, FMRP and synaptic plasticity. **Figure 3.6** demonstrates that 20% (129/660; $p=1.1 \times 10^{-56}$) of the genes showing ethanol sensitization-induced DEU and enriched in the P2 fraction also overlapped with presumed FMRP target mRNA. This utilization of FMRP targeting by ethanol sensitization clearly implicates this subset of genes in mechanisms of ethanol-induced synaptic plasticity and may have implications for overlap of AUD with other neurological disorders.

Another major finding in these studies is that repeated dosing of ethanol to produce sensitization in D2 males induces substantially more differential gene expression than acute ethanol in both the P2 and S2 fractions. Strikingly, differential exon usage was almost exclusively seen in the ethanol sensitized mice. The bioinformatics analysis of our P2 candidate gene list indicated that transcripts altered in response to repeated ethanol are significantly enriched for biological functions associated with postsynaptic membrane potential, posttranslational

protein modifications, protein folding and molecular chaperones, and mitochondrial function. Previously our laboratory has shown that ethanol regulates transcription and mRNA abundance of molecular chaperones in vitro and in vivo (Kerns et al., 2005; Miles et al., 1991, 1994). The present study extends these findings by providing evidence that this regulation may be localized or at least occurring at the synapse. The robust expression response to ethanol sensitization is striking in that some of our prior studies have documented actual habituation of some expression responses (*Sgk1*) to acute ethanol following ethanol sensitization induction (Costin et al., 2013). Acute ethanol induced significantly fewer expression changes that represented distinct biological categories including actin filament and small GTPase signal transduction. In a similar study of synaptic transcriptional events following acute ethanol, Wolfe et al. evaluated hippocampal synaptoneurosome DGE and DEU 45 minutes after a single acute exposure to ethanol (2.4g/kg) in B6 mice (Wolfe et al., 2019). Despite using different mouse strains, ethanol doses, and time points, our findings have commonality including identification of altered GTPase-related processes in response to acute ethanol in the synaptic fractions.

The large expression responses to both acute ethanol and ethanol sensitization with gene-level analysis of our RNAseq data was in striking contrast to our finding that ethanol sensitization alone led to robust alterations of exon

usage in both the synaptoneurosome and somatic fractions. Very few exons were differentially utilized following acute ethanol. However, the categories of genes altered by ethanol sensitization either at the gene level or exon utilization show functional overlap with biological processes of RNA translation, RNA processing, and cellular energetics. This functional over-representation is consistent with altered demands on synaptic activity and synaptic protein synthesis with sensitization. However, the striking predominance of exon utilization regulation by sensitization suggests that a form of transcriptional plasticity accompanying the synaptic and behavioral plasticity seen with repeated ethanol exposure. The mechanism(s) for such differential exon utilization may be linked to the need for trafficking mRNA to the synapse. Such a response is suggested by our finding that sensitization-responsive DEU genes were over-represented for FMRP target mRNA, but that at the gene level, sensitization did not evoke an over-representation of FMRP targets in the synaptic transcriptome (data not shown). The mechanism whereby sensitization might alter promoter utilization, splicing or mRNA stability in producing such a robust DEU response at the synapse remains to be determined.

In a prior study, Most et al. reported microarray analysis of expression changes in a synaptoneurosome preparation from amygdala in B6 mice following prolonged ethanol oral consumption (Most et al., 2015). That study also identified

changes relating to protein synthesis in the ethanol-regulated synaptic mRNA. However, there was no clear connection to a form of plasticity in their studies, although progressive ethanol consumption is thought to involve synaptic plasticity. Furthermore, those studies did not involve an exon-level analysis so direct comparison to our results here is not possible. Regardless, Most et al. did find a much more vigorous ethanol-responsive gene expression regulation in the synaptoneurosome as compared to a total cellular lysate. Their studies thus complement our findings on the dramatic response to ethanol at the level of the synaptic transcriptome. Together, our studies emphasize the importance of analyzing ethanol transcriptional responses at a more precise cellular and sub-cellular level so as to more clearly identify biological mechanisms and consequences. A minor drawback to both our current studies and those of Most et al. is the lack of validation of RNAseq results by additional techniques such as qRT-PCR or Western blot analysis, or preferably, by cellular resolution techniques such as in situ hybridization or immunohistochemistry. Such studies were not a major goal of the current report, where we have focused on network- or pathway-level finding rather than single genes. We did provide at least a partial cross validation of our molecular findings in our studies on select candidate genes shown in **Figure 3b** and **Table S3.6**. However, future detailed cellular validation studies are clearly needed.

Using expression analysis, our study is the first to characterize regulation of the synaptic transcriptome by ethanol (or any exogenous drug) in an in vivo model of synaptic plasticity. With repeated intermittent exposure to ethanol that resulted in a sensitized response, we observed changes to the complement of mRNA present at the synapse and alterations in the exonic composition of synaptic mRNA that we hypothesize contribute to the development of the behavioral phenotype in D2 mice. The individual genes and functional groups (e.g. molecular chaperones) identified in these studies provide important new information regarding the mechanisms of ethanol-induced synaptic plasticity. Perhaps most importantly, however, our studies have identified that ethanol sensitization uniquely regulates exon utilization at the synapse in a manner that implicates specific RNA binding protein targeting, such as by FMRP. Functional analyses will be required to further validate these results with the ultimate goal of disrupting synaptic targeting of specific transcripts or groups of transcripts in order to causally relate this mechanism to synaptic plasticity and modulation of ethanol behaviors.

Supplemental Tables:

<https://www.frontiersin.org/articles/10.3389/fgene.2018.00402/full#supplementary-material>

Chapter 4

Drosophila Clic Knockdown Alters the Transcriptome

4.1 Introduction

CLICs are a family of evolutionarily conserved proteins with unique metamorphic properties and a host of highly diverse, yet poorly understood biological functions. Vertebrates possess 6 highly similar chloride intracellular channel paralogs and orthologs can also be found in invertebrates including *Caenorhabditis elegans* and *Drosophila melanogaster* (Littler et al., 2010). The biological functions of CLICs have been difficult to ascertain, but insight has been gained through knockout models in mice and *C. elegans*. Although viable, animals deficient for CLICs exhibit a diverse array of phenotypes including defective excretory canal formation in *C. elegans* (Berry et al., 2003) and impaired angiogenesis (Chalothorn et al., 2009; Ulmasov et al., 2009), and wound healing in

mice (V. C. Padmakumar et al., 2012). Work in knockout models has been complemented by *in vitro* studies and the overall list of functions associated with CLICs now includes roles in ion channel activity (Harrop et al., 2001; Littler et al., 2004; Tulk et al., 2000), membrane trafficking (Chou et al., 2016; Maeda et al., 2008), apoptosis (Fernandez-Salas et al., 2002; Suh et al., 2004), TGF-beta signaling (V. C. Padmakumar et al., 2012; Rønnov-Jessen et al., 2002; Shukla et al., 2009), tubulogenesis (Berry et al., 2003; Chalothorn et al., 2009; Chou et al., 2016), innate immunity (He et al., 2011; Tang et al., 2017), and oxidoreductase enzymatic activity (Al Khamici et al., 2015) among others. Unfortunately, little progress has been made in identifying the molecular mechanisms by which CLICs engage in these diverse biological processes and much remains to be elucidated.

As members of a rare class of metamorphic proteins, CLICs can alter their three-dimensional structure in a ligand-free environment in response to changes in redox conditions (Goodchild et al., 2011; Littler et al., 2004, 2005). Under oxidizing conditions, CLICs can rearrange their tertiary structure and spontaneously insert into membranes where they demonstrate an ability to conduct ions across membranes through an unknown mechanism (Harrop et al., 2001; Littler et al., 2004; Tulk et al., 2000). The selectivity of CLICs for anions, let alone chloride, has been challenged suggesting the channels may better resemble membrane pores (Singh & Ashley, 2007). Under reducing conditions, CLICs tend

towards a soluble globular conformation which has been associated with enzymatic oxidoreductase activity *in vitro* (Al Khamici et al., 2015). This finding is not entirely surprising considering the structural homology of CLICs and omega class GST enzymes (Dulhunty et al., 2001; Harrop et al., 2001). General features of CLICs such as their resemblance to omega class GSTs, ability to interconvert structures and conduct ions across membranes are largely conserved between vertebrates to invertebrates (Littler et al., 2008). One major distinction between invertebrate and vertebrate CLICs is the presence of a two-cysteine redox active site, which is disrupted in *C. elegans* paralogs *exl-1* and *exc-4*, but maintained in *Drosophila Clic*. This active site has been linked to binding of CLICs to lipid bilayers after oxidation, which is true of vertebrate and *Drosophila* CLICs, but not *C. elegans* (Littler et al., 2008). This active site motif may also be necessary for glutathione binding and oxidoreductase enzymatic activity (Al Khamici et al., 2015).

Growing evidence has linked CLICs to ethanol-related behaviors and identified them as a potentially important risk factor for AUD. Expression of *Clic4* is downregulated in the brains of postmortem human alcoholics (Liu et al., 2006) and part of an ethanol-responsive gene network in mouse PFC (Farris & Miles, 2013). *Clic4* has been shown to be induced in mouse brain by acute ethanol (Bhandari et al., 2012; Kerns et al., 2005) and overexpression of *Clic4* in PFC decreased sensitivity to ethanol sedation in D2 male mice (Bhandari et al., 2012).

In the same study, transposon disruption of *Drosophila Clic* and mutation of *C. elegans exc-4* were also shown to decrease ethanol sedation sensitivity. In a separate study, RNAi knockdown of *Drosophila Clic* replicated these findings by reducing sensitivity to ethanol sedation (Chan et al., 2014). These findings are significant considering the possible role of low initial ethanol sensitivity as a risk factor in the development of AUD in humans (Schuckit, 1994; Schuckit & Smith, 1996). Similar to many of the other biological functions associated with CLICs, the molecular mechanisms by which they alter ethanol sensitivity is presently unknown.

CLICs are a unique class of proteins with an increasingly diverse array of associated biological functions. With relevance to fields of development, AUD, cancer biology, and immunology, CLICs are a subject of increasing interest and biomedical research. Unfortunately, little is presently known about the molecular interactions of CLICs and it is unlikely the extent of their biological roles has been fully explored. The present study has taken steps to address these gaps by using the power of *Drosophila* genetics to knock-down *Clic* expression selectively in neurons and characterizing the consequent transcriptomic response. Since Chan et al. (Chan et al., 2014) have previously shown that this approach reduced sensitivity to ethanol sedation, we expected that study of transcriptome networks resulting from *Clic* knockdown would not only add to our knowledge on *Clic* function, but might also increase our understanding of the neurobiology underlying ethanol

sedation sensitivity in the fly. Our findings provide validation for published roles for CLICs, identify potentially novel functions and genetic interactions that shed light on the nature of chloride intracellular channel biology, and show a remarkable conservation across transcriptome responses relating to ethanol sedation sensitivity in *Drosophila*.

4.2 Methods

***Drosophila* Husbandry, Genetics, and Behavioral Studies**

Drosophila neuron-selective Gal4 driver strain *elav/+* and *Clic* RNAi-targeting strain *v105975/+* were reared, crossed, and evaluated for sensitivity to ethanol sedation as previously described (Chan et al., 2014). Flies were placed in sealed plastic containers containing 95% O₂ twice daily to induce hyperoxia. Survival following repeated hyperoxia exposures was evaluated as previously described (Jones et al., 2014).

RNA Extraction and Microarray Preparation

RNA was extracted from fly heads as previously described (Jones et al., 2014). Microarray preparation performed per standard Affymetrix protocol using GeneChip *Drosophila* Gene 1.0 ST arrays (ThermoFisher Scientific #902155).

Hybridization, washing, and scanning performed per manufacturer specifications by VCU Massey Cancer Center Tissue and Data Acquisition and Analysis Core.

Microarray Analysis

All microarray data processing, statistical analysis, and bioinformatics were performed in R v3.5.1 (R Development Core Team & Team, 2016) using R Studio v1.1.456 (RStudio Team, 2016) unless otherwise stated. Microarray CEL files were preprocessed with the R package Oligo v1.44.0 (Carvalho & Irizarry, 2010) for quality control visualization and background subtraction and normalization was performed with the default robust multi-array average (RMA) method. Release 36 of the corresponding Affymetrix *Drosophila* Gene 1.0 ST array transcript annotations were used. Differential gene expression analysis was performed with the R package Limma v3.36.5 (Ritchie et al., 2015) using gene-level linear model fitting and empirical Bayesian smoothing of standard errors per the default workflow. P-values were adjusted using the false discovery rate method (Benjamini & Hochberg, 1995) and a cutoff of less than or equal to 0.05 was applied for significant differential expression. Plotting for these analyses was performed with the R package ggplot2 v3.0.0 (Wickham, 2016). PCA plotting performed by ggbiplot R package v0.55 (Vu, 2011) with computed normal confidence ellipses feature enabled.

Bioinformatics

Functional enrichment analysis of differentially expressed genes found with Limma analysis was performed using the web-based tool DAVID (<https://david.ncifcrf.gov/>) (Huang et al., 2009). Databases examined included the KEGG (Carbon et al., 2019; Kanehisa, 2000) and GO categories of Biological Processes, Cellular Components, and Molecular Functions. A p-value cutoff of 0.01 was applied to all GO terms and terms with > 90% redundancy were removed. Significantly enriched terms were visually explored using the R package GOplot v.1.0.2 (Walter et al., 2015) to produce the representative plots in **Figure 4.3**. The web-based tool GeneWeaver (<https://geneweaver.org/>) was used to perform an integrative genomic analysis across multiple published *Drosophila* gene sets (Baker et al., 2012). Using the HiSim Graph tool, differentially expressed genes from the present *Clic* knockdown were found to have significant Jaccard similarity with four published *Drosophila* ethanol exposure (Kong et al., 2010; Morozova et al., 2006; Urizar et al., 2007) and sedation sensitivity (Morozova et al., 2007) gene sets (GS137794, GS75550, GS137795, and GS75562 respectively). These four gene sets were combined to create a union set of ethanol-sensitive genes, which was then compared to the *Clic* knockdown-altered genes using a Fisher's exact test-based method provided in the R package GeneOverlap v.1.16.0 (Shen, 2013). Genes found to overlap between the ethanol-sensitive union and *Clic* knockdown

sets were submitted for bioinformatic analysis by DAVID in order to identify enriched functional terms common between ethanol and *Clic* knockdown-sensitive genes.

DRSC Integrative Ortholog Prediction Tool (https://www.flyrnai.org/cgi-bin/DRSC_orthologs.pl) was used to obtain human orthologs for the *Clic* knockdown differentially expressed gene list (Hu et al., 2011). In cases where multiple orthologs were found for a single *Drosophila* gene, only the top ortholog according to parameters *w_score*, *best_rev*, *sim_score*, and *identity* was used. The top 150 up and downregulated orthologs were then provided to the CLUE web-based tool for Connectivity Map (CMap) analysis (<https://clue.io/>), which compares the input transcriptomic signature with that of 476,251 transcriptomic signatures obtained from in vitro exposure of 9 human cell lines to 27,927 distinct chemical or RNAi perturbagens (Subramanian et al., 2017). Only perturbagen signatures having connectivity scores (τ) > 90 or < -90 are reported here.

4.3 Results

4.3.1 Differential Gene Expression Following *Clic* Knockdown

A neuron-specific Gal4 expressing *Drosophila* strain (*elav/+*) was crossed to a UAS-dependent *Clic*-targeting RNAi strain (*v105975/+*), producing a neuronally-

selective *Clic* knockdown strain (elav/v105975, **Figure 4.1**). To identify genes dysregulated by *Clic* knockdown, total RNA was extracted from fly heads for each strain and analyzed using Affymetrix Genome 2.0 Arrays, which quantifies expression of more than 18,500 *Drosophila* transcripts. Principal component analysis (PCA) of robust multi-array average (RMA) corrected probeset intensities revealed clear separation of the elav/v105975 knockdown and elav/+ control fly strain samples (**Figure 4.2a**).

Differential gene expression analysis of the two strains identified 1,450 genes with expression after applying an FDR cutoff of 0.05 (**Figure 4.2b, Table S4.1**). Differentially expressed genes represent 9.7% of the total genes assayed, and although split fairly evenly, show a trend towards overall downregulation. Human orthologs for the top 20 differentially expressed genes according to FDR include multiple cytochrome p450 enzymes (Cyp) as well as examples of membrane-bound (Abcg2, Elovl7, Ntm, and Glipr111) and translation-associated (Mrpl37 and Srsf3)

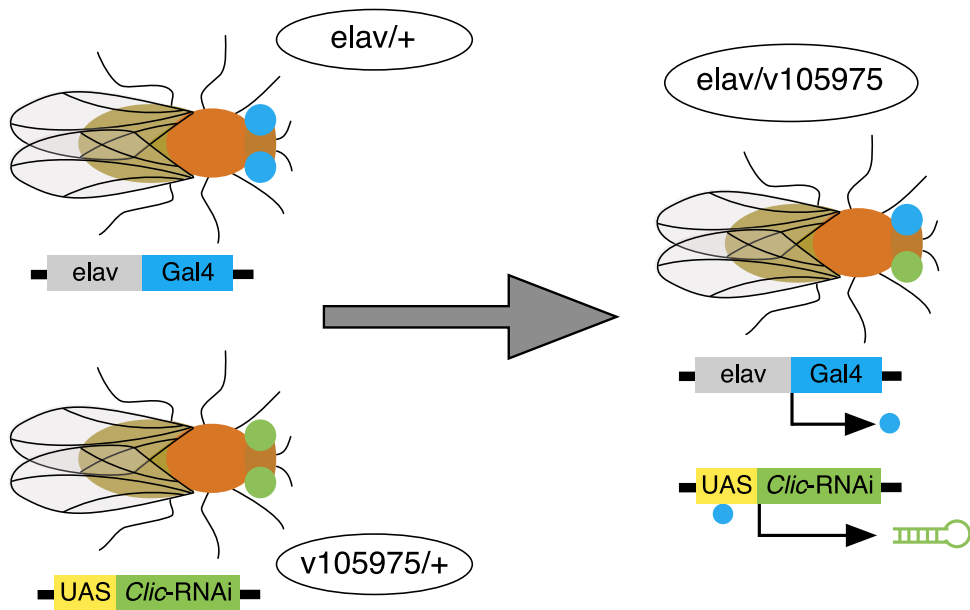


Figure 4.1. Overview of *Clie* knockdown approach. Schematic depicting breeding scheme for neuronal-specific Gal4 expression under the *elav* promoter driving UAS activated *Clie*-RNAi expression in *Drosophila*.

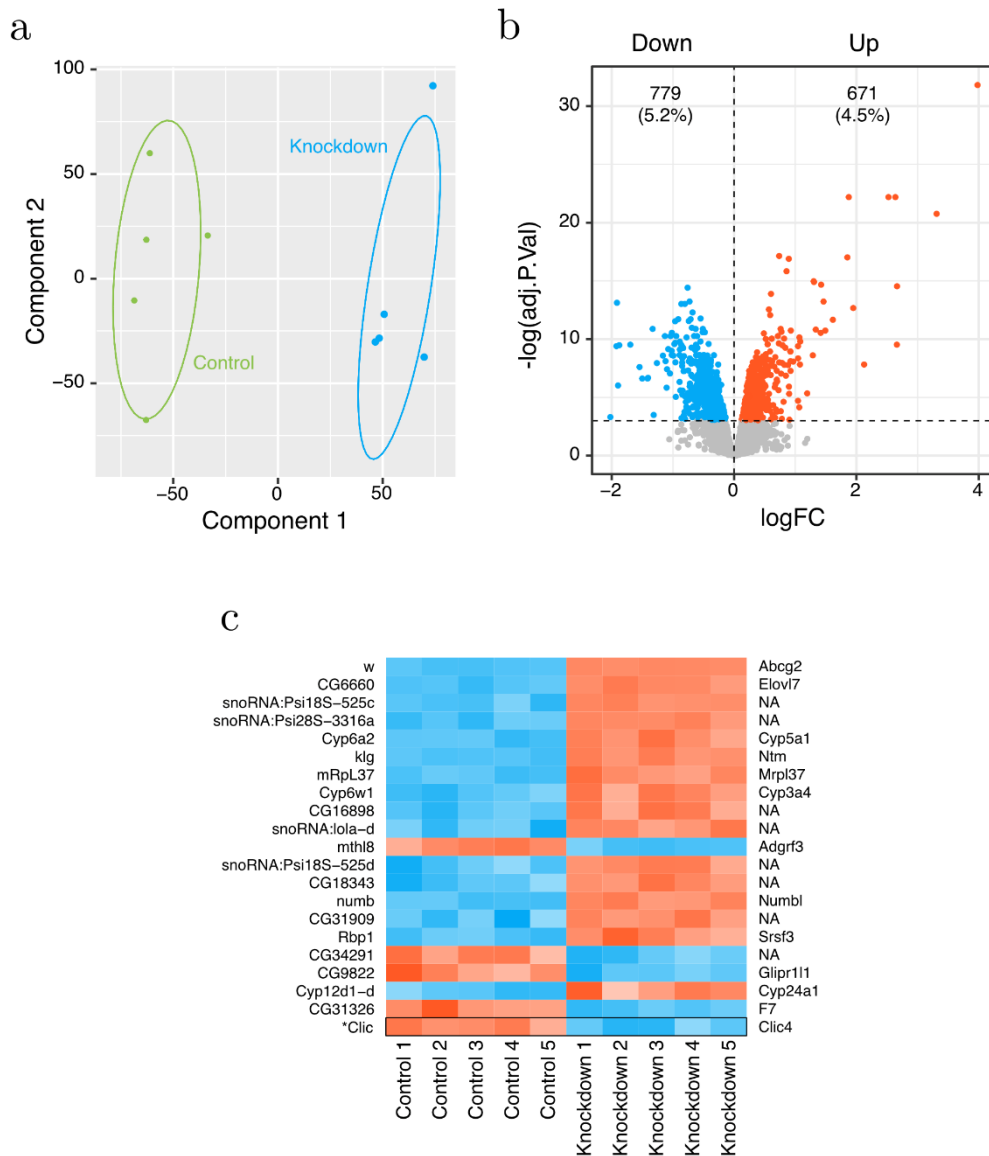


Figure 4.2. *Clic* knockdown-responsive gene expression. (a) PCA plot depicting expression profiles for control (*elav/+*) and *Clic* knockdown flies (*elav/v105975*) with normal confidence ellipses. (b) Volcano plot for complete differential gene expression results, highlighting significantly downregulated (blue) and upregulated (red) genes (FDR < 0.05). (c) Heatmap of top 20 differentially regulated genes, ranked by FDR. Fly genes are listed on left and corresponding human orthologs on right (NA indicates no clear ortholog). *Clic* expression added to bottom row of heatmap for clarity.

proteins (**Figure 4.2c**). The knockdown strain (elav/v105975) has twice the number of copies of selectable marker gene mini-white (*w*) as the control strain (elav/+), rendering it the top differentially expressed gene as expected. The knockdown target gene, *Clic*, was expressed at 59% of elav/+ control fly levels.

To assess the possibility of RNAi expression leakage in the Gal4-UAS system, v105975/+ RNAi-only controls were run alongside the elav/v105975 knockdown and elav/+ Gal4-only control strains during differential gene expression analysis. Unexpectedly, v105975/+ controls showed a 15% reduction in *Clic* expression compared to elav/+ controls, suggesting expression of RNAi molecules is occurring in the absence of a Gal4 driver (**Table S4.1**). While the knockdown magnitude was much lower than the elav/v105975 knockdown strain, it did result in substantial differential gene expression (**Figure 4.3a**). However, nearly all of genes altered by the v105975/+ RNAi-only control are also altered by the elav/v105975 Gal4-driven knockdown. Specifically, only 54 genes are differentially expressed between the v105975 RNAi-only control and elav/v105975 knockdown strain, and only 14 of those are not also differentially expressed between the elav/v105975 knockdown and elav/+ control strains (**Figure 4.3b**). Effectively serving as a lower dose and less neuronally-specific knockdown, the v105975 RNAi-only control was omitted from the rest of the bioinformatic analyses to focus on the elav/v105975 knockdown.

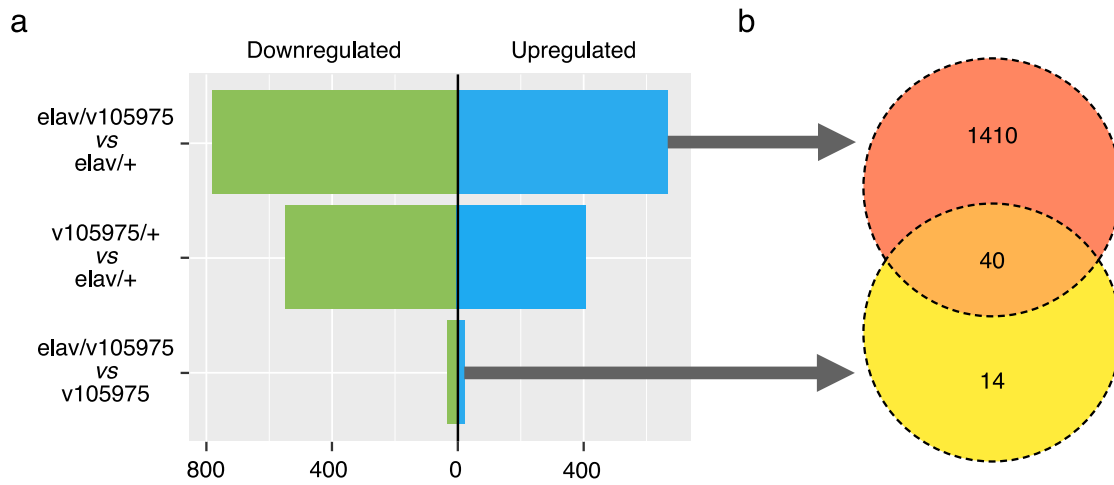


Figure 4.3: Differential Gene Expression by Strain. (a) Differentially regulated genes (FDR < 0.05) for each possible fly strain contrast. (b) Genes differentially expressed between knockdown (elav/v105975) and RNAi-only control (v105975) are also altered in the knockdown vs Gal4-only control (elav/+) contrast.

4.3.2 Perturbed Oxidation-Reduction and Cytoplasmic

Translation

To objectively screen the large list of differentially expressed genes for meaningful biological patterns, functional over-representation analysis was performed using the GO classification system. Twenty-three non-redundant GO terms with p-values < 0.01 were identified from all three GO categories (Biological Processes, Molecular Functions, & Cellular Components) and reflected trends observed in the top 20 differentially expressed genes (**Figure 4.4a, Table S4.2**). The top 6 overrepresented GO terms according to p-value included Biological Processes Cytoplasmic Translation and Oxidation-Reduction Process, Molecular Functions Heme Binding, and Cellular Components Membrane, Cell Junction, and Nucleolus (**Figures 4.4a-d**). Differentially expressed genes localized to the nucleolus and those involved in cytoplasmic translation, oxidation-reduction processes, and heme binding are largely downregulated whereas those localized to membranes or cell junctions are mostly upregulated (**Figures 4.4a-c**).

Despite having large z-scores for overall direction of regulation (**Figures 4.4a,b**), terms such as Oxidation-Reduction Process and Cell Junction possess examples of genes with opposing directions of regulation, highlighting the

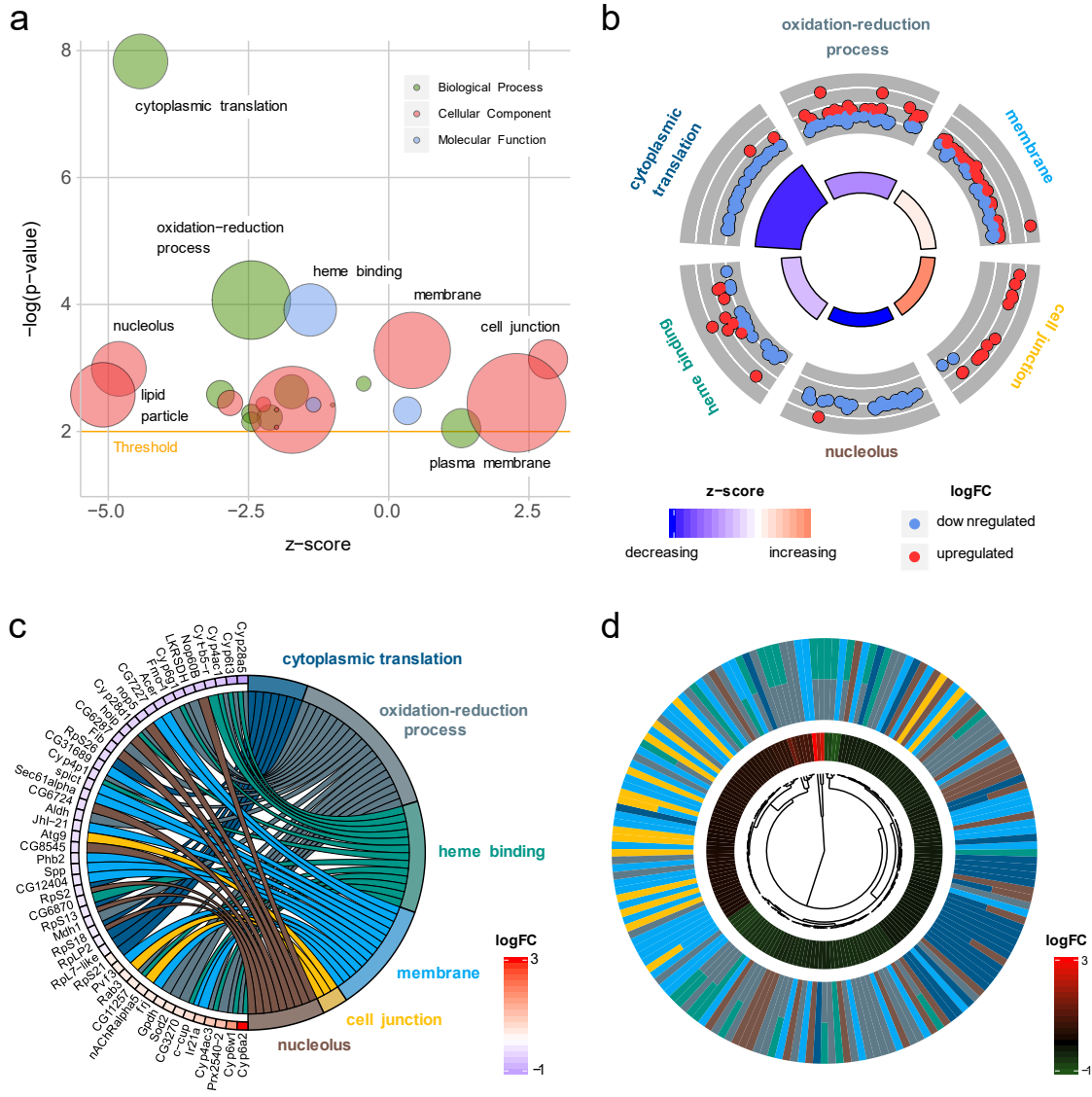


Figure 4.4. GO Terms Enriched by *Clic* Knockdown. (a) GO terms significantly affected by *Clic* knockdown with a p-value cutoff set to 0.01. Bubble radius is proportionate to term size in total number of genes and z-score represents overall direction of regulation of differentially expressed genes. (b) Circle plot depicting top 6 GO terms according to enrichment p-value. Outer ring corresponds to regulation of individual genes (logFC) within a term while inner ring corresponds to term enrichment p-value (bar height) and direction of regulation z-score (color). (c) Top 6 GO terms and top 50 differentially regulated genes from union of all 6 terms' gene sets, depicted by gene name. (d) Hierarchical clustering according to logFC expression value of all differentially expressed genes in the top 6 GO terms. GO terms are color coded for all figure panels.

complex but specific molecular responses to *Clic* knockdown (**Figure 4.4c**). For example, Cyp genes are particularly overrepresented among top *Clic* knockdown-responsive genes, but show considerable variation in direction of regulation, despite a low overall z-score for their parent term Oxidation-Reduction Process. Unsupervised hierarchical clustering of the top 6 GO terms by gene expression reveals strong clustering within GO terms but clustering is also apparent between Cell Junction and Membrane and Heme Binding and Oxidation-Reduction Process terms (**Figure 4.4d**). This likely points to co-regulation of genes with similar or interacting biological functions.

4.3.3 Overlap with Ethanol Regulated Genes

To gain further insight into the biological functions associated with *Clic*, the knockdown gene expression profile was screened against the large database of other transcriptomic studies available through GeneWeaver (Baker 2012). The most similar gene sets identified, having significant Jaccard Index scores ($p < 0.05$), were obtained from 4 transcriptomic studies related to ethanol exposure (Kong et al., 2010; Morozova et al., 2006; Urizar et al., 2007) and sedation sensitivity (Morozova et al., 2007) in *Drosophila* (**Figure 4.5a**). A union of these ethanol-responsive gene sets was intersected with the *Clic* knockdown-responsive gene set and a significant

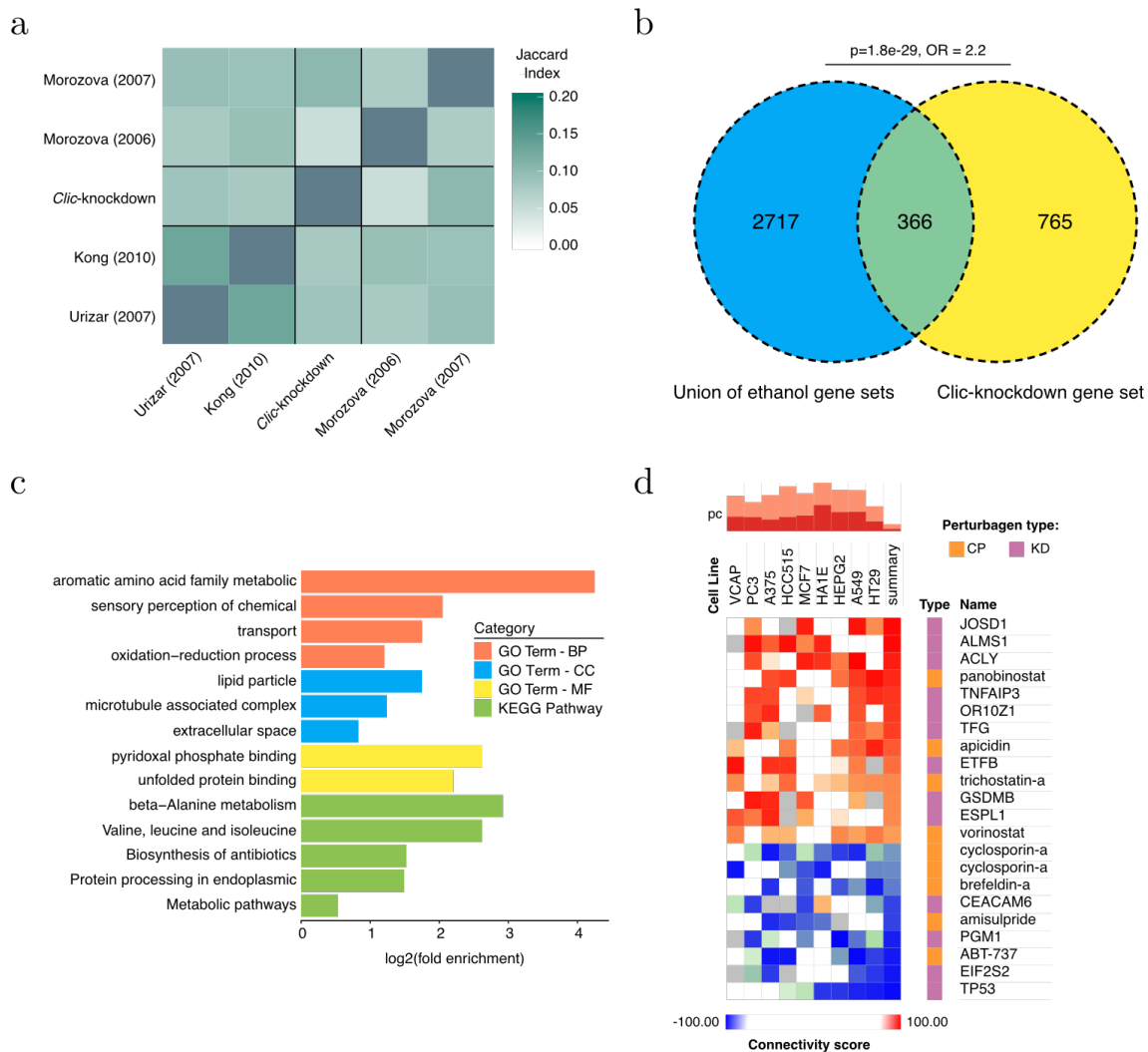


Figure 4.5. Gene Sets Overlapping with *Clic* Knockdown. (a) Heatmap showing Jaccard similarity between the *Clic* knockdown-sensitive gene set and 4 *Drosophila* ethanol-related gene sets obtained through GeneWeaver. Genes shared between the union of the 4 ethanol-related gene sets and the *Clic* knockdown-responsive gene set shown in (b) along with their GO functional enrichment analysis (c). (d) CMap analysis of perturbagen transcriptomic signatures with high positive (red, $\tau > 90$) and negative (blue, $\tau < 90$) connectivity with the *Clic* knockdown transcriptomic signature among 9 human cell lines. Assayed perturbagens include compounds (CP) and gene knockdowns (KD).

overlap of 366 genes ($p = 1.8 \times 10^{-29}$, OR = 2.2) was found (**Figure 4.5b**, **Table S4.3**). These genes were overrepresented in multiple GO terms and KEGG pathways, including metabolic and redox processes, sensory perception, protein processing, and transport among others (**Figure 4.5c**).

How *Clic* modulates resistance to ethanol sedation is not known and being a member of generally poorly understood class of proteins, identification of selective pharmacological activators and inhibitors for more direct investigation is challenging. Using the cloud-based CLUE platform for CMap analysis, the transcriptomic signature of *Clic* knockdown was correlated with transcriptomic signatures of over 19,000 small molecules previously tested in human cell lines. This approach was an attempt to produce a list of small molecules with transcriptomic signatures positively or negatively connected to the signature of *Clic* knockdown, thereby identifying potentially novel pharmacological modulators of *Clic* function. The CMap screen was able to identify 22 perturbagens, either chemical small molecules or RNAi, that showed significant connectivity ($\tau > 90$ or < -90) with transcriptomic signature of *Clic* knockdown (**Figure 4.5d**). Among chemical perturbagens, *Clic* knockdown was positively connected with histone deacetylase inhibitors (HDI) apicidin, panobinostat, trichostatin-a, and vorinostat and negatively connected to immunosuppressant cyclosporin-a, unfolded protein stress response inducing brefeldin-a, dopamine

receptor antagonist amisulpride, and pro-apoptosis *Bcl-2* inhibitor ABT-737 (**Figure 4.5d**). RNAi knockdown signatures with high connectivity to *Clic* knockdown included genes associated with cytoskeleton and membrane dynamics (*Josd1, Alms1, Tfg*), apoptosis (*Tnfrsf3, Gsdmb, Tp53*), metabolism (*Pgm1, Acly, Etfb*), and translation (*Eif2s2*) among others (**Figure 4.5d**).

4.3.4 Ethanol Sensitivity Altered by Knockdown and Hyperoxia

Considering the overrepresentation of differentially expressed genes related to oxidation-reduction processes (**Figure 4.4**), it is plausible that *Clic* knockdown flies may have a selective vulnerability or resistance to oxidative stress such as hyperoxia. However, under hyperoxic conditions, knockdown flies show only a slight resistance, having a mean survival time of 175 hours compared to 171 hours for controls (**Figure 4.6a**). Having previously shown that *Drosophila Clic* knockdown increased resistance to ethanol sedation (Chan et al., 2014), *Clic* knockdown flies were next tested for a possible combined knockdown-hyperoxia effect on ethanol sedation sensitivity. While the control strain showed no change in resistance to ethanol sedation over 3 days in ambient conditions (**Figure 4.6b**), *Clic* knockdown flies replicated previous findings and showed an increased resistance to ethanol sedation across all days (**Figure 4.7a-c**). In contrast to ambient

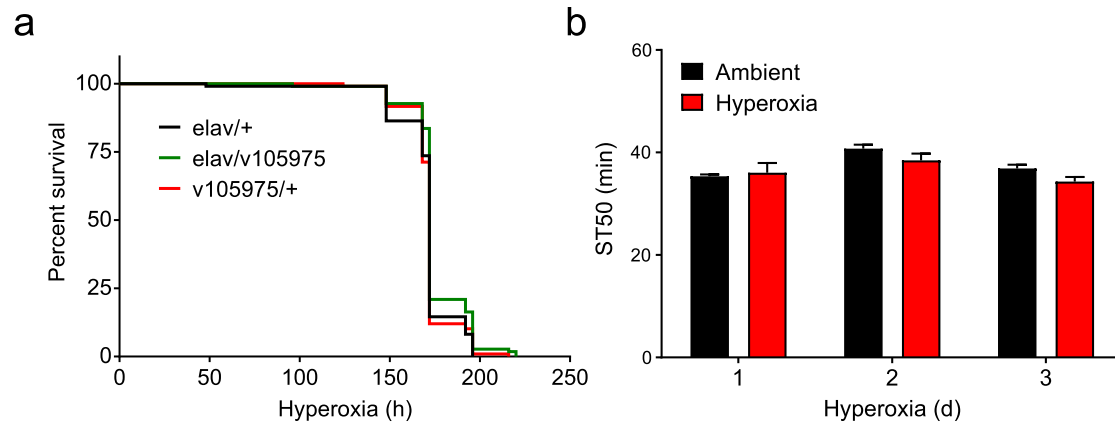


Figure 4.6: Hyperoxia Survival. (a) Survival analysis for flies exposed to continuous hyperoxia grouped by strain. (b) Ethanol sedation times for control flies (*elav/+*) under ambient and hyperoxic conditions for 3 days.

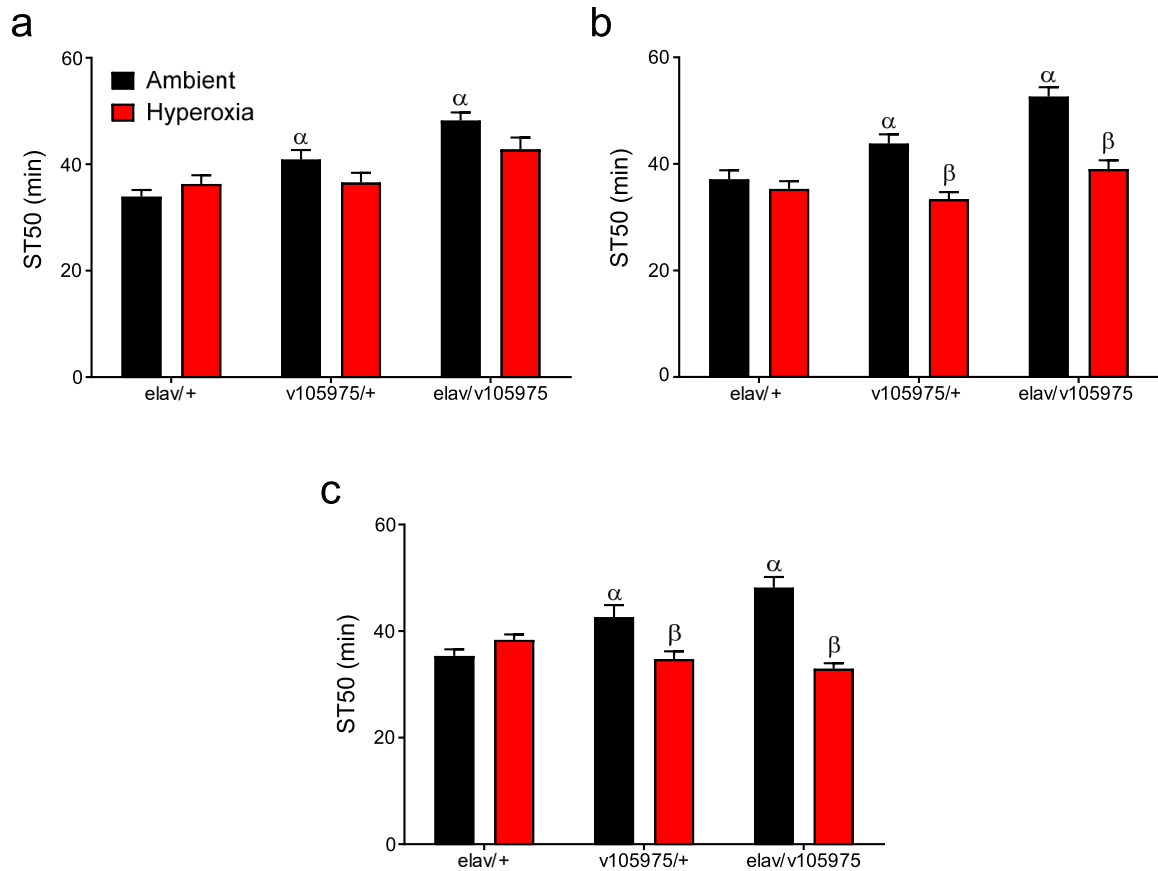


Figure 4.7. Ethanol Sensitivity Under Hyperoxia. Time for 50% of tested flies to display sedation (ST50) after exposure to ethanol vapor and hyperoxia twice-daily for three days. (a) Day 1: Effect of Genotype ($p < 0.0001$) but not hyperoxia ($p = 0.0950$) and no interaction ($p = 0.0626$). ^αEffect of genotype under ambient conditions: ST50 longer in v105975/+ and elav/v105975 compared to control elav/+ ($p < 0.0001$ - 0.0477). (b) Day 2: Effects of hyperoxia ($p < 0.0001$) and genotype ($p < 0.0001$) with a significant interaction ($p = 0.0021$). ^αEffect of genotype under ambient conditions: ST50 was longer in v105975/+ and elav/v105975 compared to control elav/+ ($p < 0.0001$ - 0.0358). ^βWithin genotype, hyperoxia decreased ST50 ($p < 0.0001$ - 0.0003). (c) Day 3: Effect of hyperoxia ($p < 0.0001$) but not genotype ($p < 0.0791$), and a significant interaction ($p = 0.0001$). ^αEffect of genotype under ambient conditions: ST50 was longer in v105975/+ and elav/v105975 compared to control elav/+ ($p < 0.0001$ - 0.0172). ^βWithin genotype, hyperoxia decreased ST50 ($p < 0.0001$ - 0.0078). Strain and hyperoxia conditions evaluated with two-way ANOVAs and post-hoc testing performed with Bonferroni corrected *t*-tests.

conditions, *Clic* knockdown flies exposed to 1 day of hyperoxia did not show an enhanced resistance to ethanol sedation (**Figure 4.7a**). Furthermore, the blunting of resistance to ethanol sedation in the knockdown flies increased with day of exposure, ultimately lowering their resistance below that of control flies (**Figure 4.7a-c**). For an additional genetic control in these sensitive behavioral tasks, an RNAi-only group lacking Gal4 (*v105975/+*) was also assessed and exhibited an intermediate phenotype between the Gal4 control (*elav/+*) and knockdown (*elav/v105975*) strains (**Figure 4.7a-c**).

4.4 Discussion

The present study constitutes the first published transcriptomic profiling of a chloride intracellular channel genetic manipulation. We targeted *Clic*, the sole *Drosophila* chloride intracellular channel gene, for RNAi knockdown and performed differential gene expression and bioinformatic analysis to gain insight into the genes and biological processes perturbed by *Clic* reduction and to better understand the role of this gene in acute ethanol sedation sensitivity. Chloride intracellular channels are an enigmatic class of proteins, having characteristics of metamorphic proteins (Littler et al., 2004), ion channels (Tulk et al., 2000), and redox enzymes (Al Khamici et al., 2015). While previous studies have sought to identify chloride intracellular channel functions through more direct lines of

investigation, such as *in vitro* assays of enzymatic reduction (Al Khamici et al., 2015) and ion channel efflux capabilities (Tulk et al., 2000), the present study has taken a more discovery-oriented approach by seeking to identify genes that respond to a reduction in *Clic* expression. Impressively, a neuronally-selective 41% knockdown of *Clic* altered the expression over 9% of the known *Drosophila* genome. Over-representation analysis of these differentially regulated genes identified several enriched GO terms including Oxidation-Reduction *Biological Process* and Membrane *Cellular Component* as well as significant overlap with gene sets from *Drosophila* ethanol sedation sensitivity and exposure studies. Extending our findings from *in silico* to *in vivo*, we evaluated *Clic* knockdown flies for sensitivity to ethanol sedation in the presence of hyperoxia and observed a blunting of sensitivity. Taken together, the studies published here provide additional evidence for known chloride intracellular channel functions as well as potentially novel functions meriting further investigation.

One potentially surprising finding from this study is the presence of altered gene expression and ethanol sedation sensitivity in the RNAi-only control fly strain. While inducible gene expression systems are invaluable for producing temporally and spatially precise genetic manipulations, they are often prone to leakage and the Gal4-UAS system is no exception. Leakage has previously been described for both Gal4 inducers and UAS transgenes, but extent of leakage is

difficult to predict and can vary according to fly strain and age among other factors (Poirier et al., 2008). Here we observe an intermediate phenotype in RNAi-only controls that falls between the knockdown and Gal4 strains in terms of gene expression and sensitivity to ethanol sedation. While the differential gene expression observed in the RNAi-only control is substantial, these are almost entirely the same set of genes differentially expressed in the knockdown strain. However, leaked expression does complicate interpretation of the neuron-selectivity of the knockdown. Although the majority of the knockdown is occurring under the neuron-specific *elav*-Gal4 inducer, some component of the gene expression or ethanol sedation changes may be occurring in other cell types. This is an unfortunate caveat to many inducible genetic systems and must be interpreted carefully.

Overrepresentation analysis performed on *Clic* knockdown-responsive genes yielded multiple enriched GO terms of interest that both highlight known functions related to chloride intracellular channels but also point to possibly novel, undescribed roles. Chloride intracellular channels are known to interact with membranes, forming intracellular channels (Littler et al., 2004; Weng et al., 2009), associating with membrane domains undergoing tubulogenesis (Berry et al., 2003; Bohman et al., 2005), and promoting membrane trafficking (Chou et al., 2016; Maeda et al., 2008). These activities correspond well to the GO term hits, Lipid

Particle and Membrane. Furthermore, CMap analysis identified knockdown of *Josd1*, *Alms1*, and *Tfg*, three genes with functions linked to cytoskeleton and membrane dynamics, as being highly connectivity to the *Clic* knockdown signature. A similar GO term hit, Cell Junctions, has relevance to vertebrate *Clic* orthologs, which have been shown to be enriched at junctions between dividing cells, where they are potentially regulating cytoskeletal organization (Berryman & Goldenring, 2003).

The GO term Oxidation-Reduction Process was enriched by *Clic* knockdown-sensitive genes and may reflect a known role of chloride intracellular channels in carrying out oxidoreductase reactions (Al Khamici et al., 2015). Although evidence for this function is limited to observation *in vitro*, it has been long suspected based on the homologous omega class glutathione S-transferase structure of chloride intracellular channels (Harrop et al., 2001; Littler et al., 2010). Also reproducing known roles for chloride intracellular channels, *Clic* knockdown showed high connectivity on CMap analysis with the apoptosis-blocking drug ABT-737 and with pro-apoptosis gene p53. It has been shown that chloride intracellular channels have a p53 binding element in its promoter, upregulate in response to various cell stressors including DNA damage, and has been shown to traffic to the nucleus as an early responder to cell stress where it also participates in apoptosis (Fernandez-Salas et al., 2002; Suh et al., 2004). A potentially novel

association of *Clic* identified in this study is protein translation, for which Cytoplasmic Translation was the top GO term from the overrepresentation analysis and was enriched almost exclusively by downregulated genes. In concordance with this, CMap analysis showed a strong negative connectivity between the *Clic* knockdown signature and translation initiation factor, *Eif2s2*. Also potentially novel, CMap analysis identified multiple histone deacetylase inhibitors with strong connectivity to *Clic* knockdown.

Chloride intracellular channels are highly conserved evolutionarily and vertebrates possess a family of 6 paralogs (Littler 2010). *Drosophila Clic* has high sequence similarity to vertebrate orthologs including *Clic4*, which has been shown to be regulated by ethanol (Bhandari et al., 2012; Kerns et al., 2005) and capable of decreasing ethanol sedation sensitivity when overexpressed in mouse brain (Bhandari et al., 2012). Neuronal *Drosophila Clic* knockdown has previously been shown to decrease ethanol sedation sensitivity (Chan et al., 2014), consistent with our findings here, showing a conservation of function between mouse and *Drosophila* orthologs. Of note, the decreased sensitivity to ethanol sedation is obtained through opposing genetic manipulations in mice and flies, overexpression and knockdown, respectively. As hypothesized previously, this difference in phenotype expression may be due to species-specific differences in number and presence of chloride intracellular channel paralogs or the

experimentally targeted cell types or brain regions (Bhandari et al., 2012). Novel to this body of work, we show that the while *Clic* knockdown decreases sensitivity to ethanol sedation, this effect is reversed by hyperoxia in a time-dependent manner. Considering hyperoxia had no effect on the control strain, this decrease in ethanol sedation sensitivity with time in the knockdown strain suggests that genes altered by *Clic* knockdown, which are otherwise protective against ethanol sedation, are also regulated on some level by hyperoxia. A possible mechanism for this interaction is the oxidoreductase enzymatic activity reported of vertebrate chloride intracellular channels *in vitro* (Al Khamici et al., 2015). Metabolism of ethanol produces ROS and cellular oxidative stress, which *Clic* may be protective against. This possibility is underscored by overrepresentation of genes related to GO oxidation-reduction processes in both the *Clic* knockdown-responsive gene set and GeneWeaver overlap analysis with ethanol-related *Drosophila* gene sets. A possible explanation for the interaction of effects between hyperoxia and *Clic* knockdown: Knocking down *Clic* upregulates genes and pathways related to the oxidative stress response, which translate to decreased vulnerability to ethanol-related ROS and sensitivity to ethanol sedation. However, combining this upregulation of cellular stress pathways with those also responding to hyperoxia results in a maladaptive hyperresponsivity, resulting in increased cellular stress and sensitivity to ethanol sedation.

Remarkably, nearly one third of genes responsive to *Clic* knockdown were found to be shared with a union set of published ethanol sedation sensitivity-related *Drosophila* genes. Three of these gene sets display ethanol regulation during acute exposure (Kong et al., 2010; Morozova et al., 2006; Urizar et al., 2007) while the fourth represents genes differentially expressed between strains artificially selected for high and low ethanol sedation sensitivity (Morozova et al., 2007). This intersection between *Clic* knockdown-responsive and ethanol-regulated genes suggests a role for *Clic* in molecular pathways governing ethanol sedation sensitivity and the acute response to ethanol. Functional enrichment of the shared gene set implicates a variety of possible processes including amino acid metabolism, oxidation-reduction, sensory perception, protein processing, and transport.

Employing the Gal4-UAS gene-switch system, this study is the first to characterize the transcriptome following genetic manipulation of a chloride intracellular channel gene. Bioinformatic analysis of knockdown-induced differentially regulated genes provided support for existing evidence that *Clic* is involved in oxidation and reduction processes and has roles near cellular membranes. Novel to this work, we also identified an enrichment of *Clic* knockdown-sensitive genes related to cytoplasmic translation and heme binding and associated with the nucleolus and cell junction. We have also determined that

an interaction between hyperoxia and *Clic* expression modulates ethanol sedation sensitivity. Taken together, these studies add to the growing body of literature supporting *Clic* genes as important for ethanol-related behaviors and also being involved in redox-related processes.

Supplemental Tables:

Table S4.1: Differentially Expressed Genes

Table S4.2: Enriched Gene Ontology Terms

Table S4.3: GeneWeaver Ethanol Gene Sets

Chapter 5

Clic4 Modulates Ethanol and Anxiety-like

Behaviors

5.1 Introduction

Increasing evidence has linked chloride intracellular channels, and specifically vertebrate ortholog *Clic4*, with ethanol-related behavior and the brain's molecular response to ethanol. *Clic4* was found to be downregulated in postmortem frontal cortex tissue of human alcoholics that consumed more than 80g/day of ethanol per day (6 standard drinks) when compared to abstinent or social drinking controls (Liu et al., 2006). *Clic4* was also found to be part of ethanol-responsive gene network in postmortem hippocampus tissue obtained from individuals meeting DSM-IV criteria for either alcohol abuse or dependence (Farris et al., 2015). In a microarray meta-analysis of multiple mouse strains displaying diverse levels of ethanol preference, mice predisposed to high levels of

voluntary alcohol drinking showed an increase in *Clic4* expression in whole brain (Mulligan et al., 2006). F1 female B6 x FVB/NJ hybrid mice displayed upregulation of *Clic4* in laser-captured VTA dopaminergic neurons following three weeks of a drinking in the dark binge model of voluntary ethanol consumption (Marballi et al., 2016). In male D2 mice, *Clic4* is upregulated in PFC 4 hours after 2g/kg (Kerns et al., 2005) and 4g/kg (Bhandari et al., 2012) i.p. injections of ethanol. Additionally, mouse *Clic4* is located in a quantitative trait locus QTL for alcohol preference (Ap3q) for a 15-day two-bottle choice voluntary ethanol consumption task (Tarantino et al., 1998). Mouse *Clic4* is also positioned within two QTLs associated with anxiety-like behavior measured in elevated plus maze and open field tasks (Kazuhiro Nakamura et al., 2003; Thifault et al., 2008).

Behavioral studies characterizing chloride intracellular channels are limited but what has been published implicates mouse *Clic4* and invertebrate orthologs in ethanol sedation sensitivity. Two independent transposon disruptions of *Drosophila* ortholog *Clic* produced reduced sensitivity to ethanol sedation, an effect that was rescued by transposon reversion (Bhandari et al., 2012). This effect on ethanol sedation sensitivity has been replicated with a neuron-selective *Clic* RNAi (Chan et al., 2014). Mutation of *C. elegans* orthologs *Exc-4* and *Exl-1* produces different phenotypes, with *Exc-4* mutation reducing sensitivity to ethanol sedation and *Exl-1* increasing acute functional tolerance (Bhandari et al., 2012). In D2 mice,

neuron-selective overexpression of *Clic4* in mPFC decreased sensitivity to ethanol sedation in a loss of righting reflex (LORR) task (Bhandari et al., 2012).

Considering the mounting evidence supporting ethanol-regulated expression and modulation of ethanol sedation sensitivity with vertebrate *Clic4* and invertebrate orthologs, further investigation is merited to identify the extent to which *Clic4* modulates ethanol-related behaviors and to initially characterize the cellular site(s) for such *Clic4* action. This includes whether *Clic4* modulates ethanol behaviors differently in males and females, if it influences voluntary ethanol consumption, and in which cell types and brain regions does it have roles. While D2 mice show altered ethanol LORR following *Clic4* overexpression, that strain of mice is strongly averse to voluntary ethanol consumption. In the present study, we use ethanol preferring B6 mice to characterize ethanol and anxiety-like behaviors following *Clic4* knockout specifically in oligodendrocytes. Oligodendrocytes were prioritized in this study due to evidence suggesting higher expression of *Clic4* compared to other CNS cell types, which included *in situ* hybridization data (V. Padmakumar et al., 2014), single cell RNAseq databases (Marques et al., 2016; Zeisel et al., 2015), and confocal double-labeling immunofluorescence data (Chapter 6). Considering altered ethanol sedation sensitivity resulted from overexpression of *Clic4* in D2 mice (Bhandari et al., 2012), we hypothesized oligodendrocyte-specific deletion of *Clic4* in B6 mice would also

alter ethanol sedation sensitivity. Ethanol sensitivity is inversely correlated with risk of developing AUD in humans (Schuckit, 1994; Schuckit & Smith, 1996), therefore we also hypothesized *Clic4* deletions would reduce voluntary ethanol consumption.

5.2 Methods

Ethics Statement

All procedures were approved by Virginia Commonwealth University Institutional Animal Care and Use Committee under protocol AM10332 and followed the NIH Guide for the Care and Use of Laboratory Animals (NIH Publications No. 80-23, 1996).

Animals

Male and female mice were group housed on corn cob bedding (Teklad #7092) with a 12-hour light/dark cycle (7am on, 7pm off) and provided *ad libitum* access to food (Teklad #7912) and water with weekly cage changes. All animals taking part in behavioral studies were permanently transferred to Sani-Chips bedding a minimum of one week before testing. *Clic4^{lox/lox}* animals were obtained on a mixed background from Dr. Stuart H. Yuspa at the National Cancer Institute

and backcrossed to B6 mice for 7 generations within our colony. Plp-promoted tamoxifen-inducible Cre mice on a 100% B6 background (Plp-Cre-ER^T, Jackson Laboratory #005975) were crossed to *Clic4*-floxed mice to produce inducible global *Clic4* deletions in oligodendrocytes. Experimental animals included homozygous *Clic4*-floxed mice either null (Cre-) or heterozygous for Cre (Cre+). Between 8-11 weeks of age, oligodendrocyte-specific *Clic4* deletions were induced through either stereotactic microinjection of adeno-associated virus (AAV) carrying Cre into *Clic4*-floxed mice or by i.p. tamoxifen injection into *Clic4*-floxed Plp-Cre-ER^T mice. Tamoxifen (Sigma-Aldrich #T5648) was delivered through 5 daily 75mg/kg i.p. injections in a sunflower oil vehicle (Sigma-Aldrich #S5007) and provided to both Cre- and Cre+ animals. Injections of 0.5 μ l of either AAV8-MBP-eGFP-T2A-iCre (Vector Biolabs #1538, 1×10^{13} GC/ml) or AAV8-MBP-eGFP control (Vector Biolabs #1553, 1×10^{13} GC/ml) were performed under isoflurane anesthesia using a Neurostar robotic stereotaxic instrument. Injection coordinates for mPFC relative to bregma were 1.3mm rostral, 0.3mm bilaterally, and 1.75mm ventrally. Animals were then single housed after completion of tamoxifen injections or receipt of virus and given 4 weeks to recover before being used in behavioral studies. Effectiveness of viral vector to delete *Clic4* was evaluated by immunolabeling CLIC4 protein in Cre+ and Cre- viral injected mice. Cell type-specificity of the viral vectors was validated by co-labeling eGFP with mature oligodendrocyte marker CC1. Viral-

mediated deletions were validated for correct injection coordinates in all animals by visualizing eGFP expression in 40µm paraformaldehyde fixed and cryosectioned brain slices. Animals were dropped from the study if either of the bilateral injection locations were incorrect.

Western Blotting

Male and female *Clic4*-floxed Plp-Cre-ER^T mice 4 weeks and 6 months post-tamoxifen treatment were euthanized by cervical dislocation and decapitation and frontal cortex was microdissected and immediately flash frozen. Protein was extracted from frontal cortex in RIPA Buffer (Alfa Aesar #J63324) with Halt Protease and Phosphatase Inhibitor Cocktail (ThermoFisher Scientific #78440). 10 µg of protein was loaded per well, separated by SDS-PAGE in a 4-12% Bis-Tris Polyacrylamide Gel (ThermoFisher Scientific #NP0329BOX), and transferred onto PVDF membrane. Membranes were air dried and blocked with LiCor Intercept (TBS) Blocking Buffer (#927-60001). Overnight primary antibody incubation and 1-hour secondary antibody incubation were performed. Images taken with Odyssey Imaging Scanner and quantified with FIJI distribution (Schindelin et al., 2012) of ImageJ (Rasband, 2015). Expression values were normalized to loading control GAPDH and then to Cre- controls. Membranes were probed serially for CLIC4, MBP, and PLP with stripping performed in between. Stripping was

performed with LiCor NewBlot IR Stripping Buffer (#928-40028). Sample sizes include 5 animals per group.

Immunofluorescence

Mice were perfused with 1x PBS followed by 4% paraformaldehyde before brain extraction and 24-hour post-fixation. Cryoprotection performed in 30% sucrose and brains flash frozen then cut on a Leica 3050S cryostat at 20 μm per section, unless otherwise stated. Antigen retrieval performed for 15 minutes at 80°C in 10mM citrate buffer (pH6) before blocking with a 10% goat serum and 0.2% Triton X-100 solution for 30 minutes at room temperature. Free floating sections incubated overnight with primary antibodies at 4°C and secondary antibodies applied for 2 hours at room temperature. Mounting performed using VECTASHIELD Hardset with DAPI (#H-1500). Sample sizes include 3 sections per animal and 3 animals per group.

Antibodies

The following antibodies were used for immunofluorescence: anti-CLIC4 (1:100; Cell Signaling Technology #D2A7D), anti-CC1 (1:200; Millipore, OP80), AlexaFluor 488 anti-mouse (1:1000; ThermoFisher Scientific #A21121), and AlexaFluor 594 anti-rabbit (1:300; ThermoFisher Scientific #A11012).

The following antibodies were used for Western blotting: anti-GAPDH (1:7500; Millipore #MAB374), anti-PLP (1:5000; Abcam #ab9311), anti-MBP (1:10000; Abcam #ab7349), 680LT Mouse IgG1 (1:50000; LiCor #926-68050), 800CW Mouse IgG2a (1:30000; LiCor #926-32351), 800CW Rabbit (1:30000; LiCor #926-32211), and 800CW Rat (1:30000; LiCor #926-32219).

Microscopy

Confocal images were taken on a Zeiss LSM700 with a 63x oil objective. Pinhole was set to 1 airy unit and scan zoom set to 1x. Image processing performed with FIJI distribution (Schindelin et al., 2012) of ImageJ (Rasband, 2015).

Behavioral Assays

Three Bottle Choice Intermittent Ethanol Access (3BC-IEA) - Mice were given 24-hour free access to three identical bottles containing 0%, 15%, and 30% ethanol in water (v/v) every other day for 5 weeks (below, ethanol access in blue). Access began two hours prior to onset of the 12-hour dark cycle. Due to well-established sex effects for ethanol behaviors in B6 mice, which were not the focus of this study, statistical testing was performed separately within males and females for this and other ethanol behavior tasks. First day of drinking was removed from analysis due to novelty effects. Ethanol consumption was analyzed using unpaired Student's t-

tests to compare Cre⁺ and Cre⁻ average daily ethanol choice, total and 15% intake. 15% ethanol choice was calculated as the ratio of g/kg consumed of 15% to 30%. Sample sizes for the Plp-Cre-ER^T study include 15-22 per group. Sample sizes for the AAV8-MBP-Cre study include 4-9 per group.

Tastant Preference Study – Mice were given 24-hour free access to two identical bottles containing water and either quinine or saccharin. Animals were randomized into two equal groups either drinking saccharin first or quinine first. Daily volume readings were taken and adjusted for evaporation. After 3 days of continuous access, tastant type was switched for both groups and 3 additional days of drinking was recorded. For the Plp-Cre-ER^T mice 25 μ M quinine and 1mM saccharin were used. For AAV8-MBP viral injected mice, 50 μ M quinine and 1mM saccharin were used. Preference was calculated as the ratio of tastant volume to water consumed. Analysis of average daily preference values was performed using type III ANOVAs. Sample sizes for the Plp-Cre-ER^T study include 7-9 per group and time point. Sample sizes for the AAV8-MBP-Cre study include 4-9 per group and time point.

Ethanol Metabolism – Animals were given a 4g/kg i.p. injection of 20% w/v ethanol in normal saline and retro-orbital blood draws were taken using glass

capillary pipettes and EDTA-treated microtainer collection tubes (Becton Dickson #365974) at 15, 30, 60, and 90-minute time points, switching sides after each draw. Animals were euthanized following the final blood draw. Whole blood was centrifuged at 500g for 10 minutes at 4°C to pellet cells and supernatant was analyzed for blood ethanol content (BEC) using an Analox AM1 Analyser. BEC values were analyzed by computing a linear mixed model with the nlme R package (Pinheiro et al., 2020) and performing type III ANOVA Wald chi-square tests with the car package (Fox & Weisberg, 2019). Sample sizes for the Plp-Cre-ER^T study include 4-6 per group and time point.

Light/Dark Box Test – Mice were habituated to the behavioral room for 1 hour before beginning task. Mice were then placed into separate Med Associates Inc. locomotor boxes with dark inserts for a single 10-minute testing period. Placement was in light chamber side with heads facing entry hole for dark chamber. Med Associates provided software was used to calculate time and distance traveled in each compartment based on infrared beam breaks. Percent time in light was calculated as the ratio of time spent in the light chamber to the total duration of the test. Analysis was performed within-sex during the first 5-minute bin of activity in the behavior boxes using unpaired Student's t-tests to compare Cre+

and Cre- animals. Sample sizes for the Plp-Cre-ER^T study include 12-15 per group. Sample sizes for the AAV8-MBP-Cre study include 4-9 per group.

Ethanol-Induced Anxiolysis - Mice were given a 2g/kg i.p. injection of 20% w/v ethanol in normal saline, placed in home cages for 5 minutes, and then evaluated for anxiety like behavior as described in the light/dark box test methodology. Analysis was performed within-sex on the first 5 minutes of activity in the behavior boxes using type III ANOVAs to evaluate effects of ethanol and genotype and Tukey's HSD for post-hoc testing. Sample sizes for the Plp-Cre-ER^T study include 3-6 per group.

Loss of righting reflex (LORR) – Animals were given a 3.8g/kg i.p. injection of 20% ethanol v/v in normal saline and time for LORR onset was recorded. Animals were then placed supine in V-shaped troughs and duration for return of righting reflex was measured. Animals with onset times greater than 4 minutes were considered LORR failures and removed the study. Statistical analysis was performed within-sex using unpaired Student's t-tests to compare Cre⁺ and Cre⁻ animals. Sample sizes for the Plp-Cre-ER^T study include 14-17 per group. Sample sizes for the AAV8-MBP-Cre study include 4-9 per group.

Statistics – Statistical analysis was performed in R v3.6.2 (R Development Core Team & Team, 2016) using R Studio v 1.2.5033 (RStudio Team, 2016). Base R statistical functions were used unless otherwise noted and plotting was performed with the ggplot2 package (Wickham, 2016). An alpha level of 0.05 was set for determination of significance.

5.3 Results

5.3.1 Global Oligodendrocyte-specific *Clic4* Deletion

Clic4-floxed mice were crossed to mice possessing tamoxifen-inducible Cre under the mature oligodendrocyte-selective *Plp* promoter to produce an oligodendrocyte-selective, inducible *Clic4* deletion model. Immunofluorescent co-labeling of CLIC4 protein and mature oligodendrocyte marker CC1 qualitatively revealed most CLIC4 expression to be knocked down in oligodendrocytes by 1 week and virtually all expression lost at 1-month post-tamoxifen (**Figure 5.1**). Similarly, Western blot analysis indicated a 40.5% knockdown of CLIC4 protein in Cre⁺ male ($t(7.76) = -11.24$, $p < 0.001$) and female ($t(4.66) = -9.51$, $p < 0.001$) mouse frontal cortex 1 month after tamoxifen administration (**Figure 5.2a**). Knockdown of CLIC4 protein levels was sustained 6 months after tamoxifen (**Figure 5.2b**), with Cre⁺ males showing a 34.3% reduction in expression ($t(7.68) = -9.86$, $p < 0.001$) and

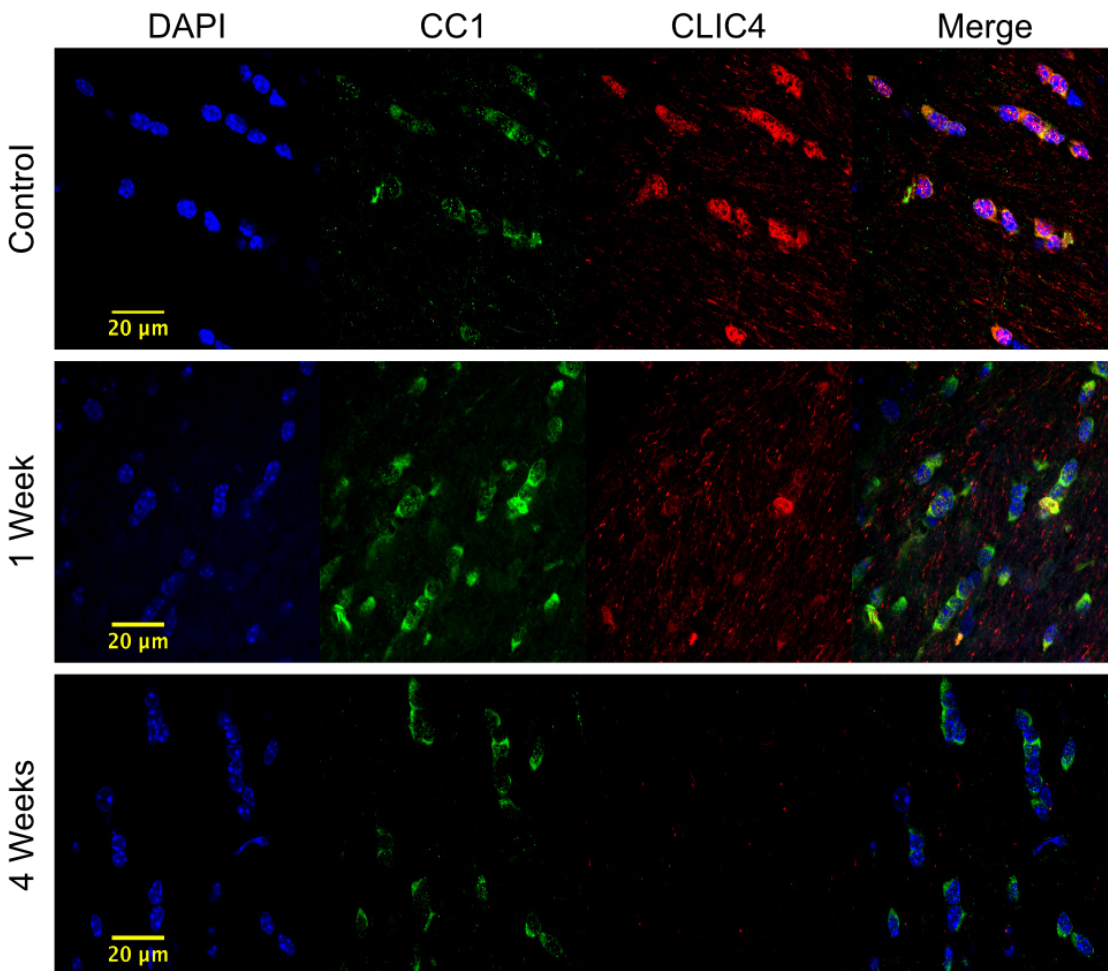


Figure 5.1. Validation of *Clic4* deletion. 63x Confocal microscope images depicting loss of CLIC4 protein expression in mature CC1+ oligodendrocytes in corpus callosum myelin ventral to PFC. Cre- controls (top) and Cre+ animals shown 1 week (middle) and 4 weeks (bottom) after tamoxifen administration.

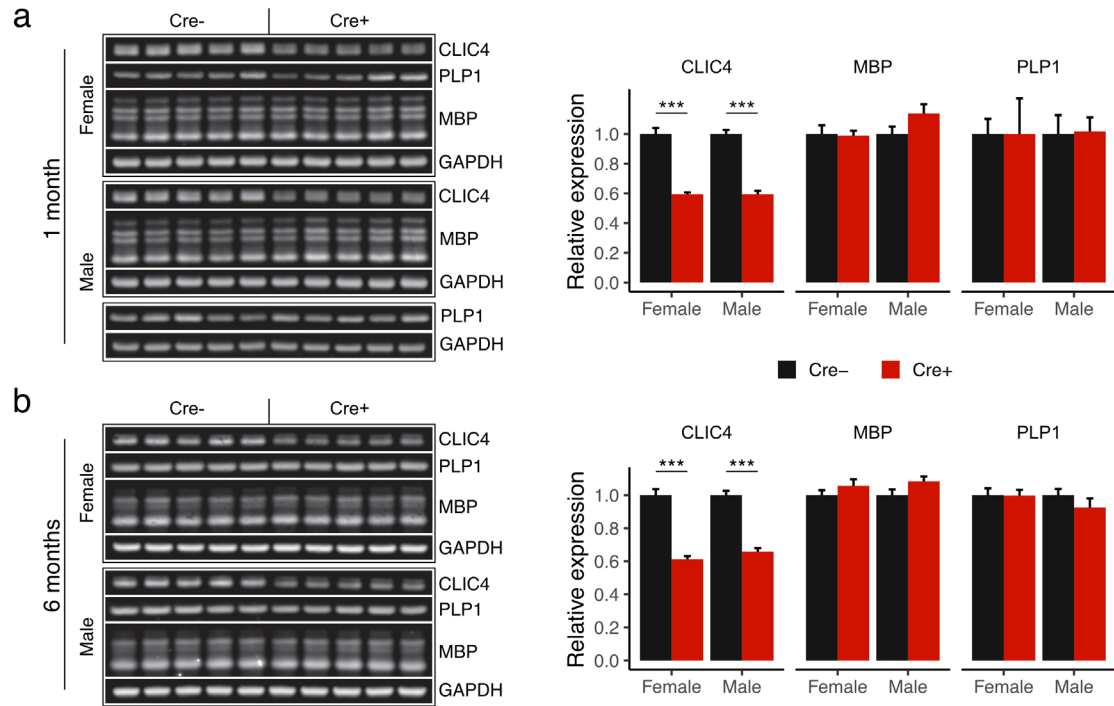


Figure 5.2. Western blot assessment of *Clic4* deletion. Western blots analysis of frontal cortex CLIC4 protein and major myelin proteins PLP and MBP expression 1 month (a) and 6 months (b) after tamoxifen delivery to *Clic4*-floxed *Plp*-Cre-ER^T mice and controls. Quantification plots for each time point depicted on right with expression values relative to GAPDH and Cre- controls (black bars). Box outlines surrounding Western blot scan images denote individual membranes. Within each membrane, serial stripping and re-probing was performed for each gene of interest with GAPDH being re-probed each time. Significance levels indicated by *** $p < 0.001$.

females showing a 38.7% reduction ($t(5.90) = -9.37$, $p < 0.001$).

To assess potential damage to myelin or myelinating oligodendrocytes, expression levels of the two most abundant myelin proteins, MBP and PLP, were also examined. PLP expression was unaffected by genotype at 1 month post-tamoxifen (**Figure 5.2a**) in males ($t(7.40) = 0.11$, $p = 0.91$) and females ($t(5.39) = 0.00$, $p = 1.00$) and also at 6 months (**Figure 5.2b**) in males ($t(7.14) = -1.13$, $p = 0.30$) and females ($t(7.79) = -0.05$, $p = 0.96$). Similarly, MBP expression was unaffected by genotype at 1 months post-tamoxifen in males ($t(7.60) = 1.73$, $p = 0.12$) and females ($t(6.28) = -0.16$, $p = 0.87$) and at 6 months in males ($t(7.79) = 1.84$, $p = 0.10$) and females ($t(7.49) = 1.14$, $p = 0.28$).

5.3.2 Ethanol Consumption Altered by *Clic4* Deletion

Male and female Plp-Cre-ER^T *Clic4*-floxed mice were evaluated for voluntary ethanol consumption in a 3BC-IEA study for a period of 5 weeks. Female Cre⁺ mice consumed 2.3g/kg more total ethanol per day (**Figure 5.3a-b**) than Cre- controls ($t(509.73) = 3.64$, $p < 0.001$) whereas male mice did not show a significant difference ($t(557.69) = -1.42$, $p = 0.16$). This increase in total ethanol consumption in Cre⁺ females was largely due to a 4.2g/kg increase in daily 15% ethanol intake (**Figure 5.3c**, $t(401.98) = 7.21$, $p < 0.001$) and a 14.9% increase in 15% ethanol choice (**Figure 5.3d**, $t(430.10) = 5.10$, $p < 0.001$). While males did not show a difference

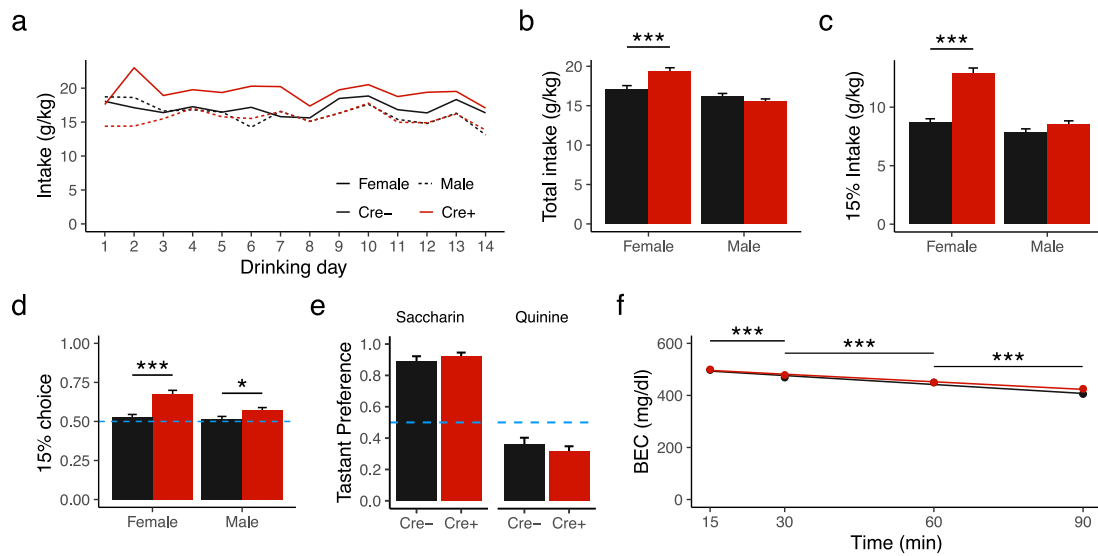


Figure 5.3. Ethanol consumption is altered by *Clic4* deletion. (a) Total ethanol intake (15% + 30%) by drinking day using the 3BC-IEA voluntary consumption paradigm in Cre+ and Cre- animals. (b) Average daily total and 15% (c) ethanol intake across the entire study. (d) Ethanol choice as a ratio of 15% to 30% intake in g/kg. (e) Preference for saccharin or quinine over water in a three-day two-bottle choice voluntary consumption task. (f) Blood ethanol levels evaluated at 4 time points following a single 4g/kg i.p. injection of ethanol with displayed p-values indicating effect of time. Significance levels indicated by * $p < 0.05$ & *** $p < 0.001$.

in 15% ethanol intake (**Figure 5.3c**, $t(573.98) = 1.59$, $p = 0.11$), similar to females, the Cre⁺ animals did show a 5.6% increase in 15% ethanol choice (**Figure 5.3d**, $t(573.96) = 2.18$, $p = 0.03$). Plp-Cre-ER^T *Clic4*-floxed mice were evaluated for changes in taste preference, which could potentially skew ethanol preference and consumption in the 3BC-IEA study. There was a significant effect of tastant type on preference, such that mice had a higher preference for the non-caloric sweetener saccharin than bitter-tasting quinine (**Figure 5.3e**, $F(1,30) = 193.3$, $p < 0.001$). However, there was no effect of sex ($F(1,30) = 1.0$, $p > 0.05$) or genotype ($F(1,30) = 0.0$, $p > 0.05$) and no interactions. Ethanol metabolism was also evaluated in these mice to ensure differences in ethanol-related behaviors due to genotype were not due to *Clic4* deletion-related metabolic differences. Mice were given a 4g/kg i.p. injection of ethanol and BEC values were measured at 15, 30, 60, and 90 minutes. While there was a significant effect of time on BEC (**Figure 5.3d**, $X^2 = 1583.2$, $p < 0.001$), there were no differences in sex ($X^2 = 0.5$, $p < 0.001$) or genotype ($X^2 = 0.3$, $p < 0.001$).

5.3.3 Anxiety-like Behavior Altered by *Clic4* Deletion

Basal anxiety-like behavior was assessed in Cre⁺ and Cre⁻ male and female mice using a light/dark box test. Cre⁺ male mice showed a 5.3% increase in time spent in light (**Figure 5.4a**, $t(34) = 2.26$, $p = 0.03$) compared to Cre⁻ mice, while

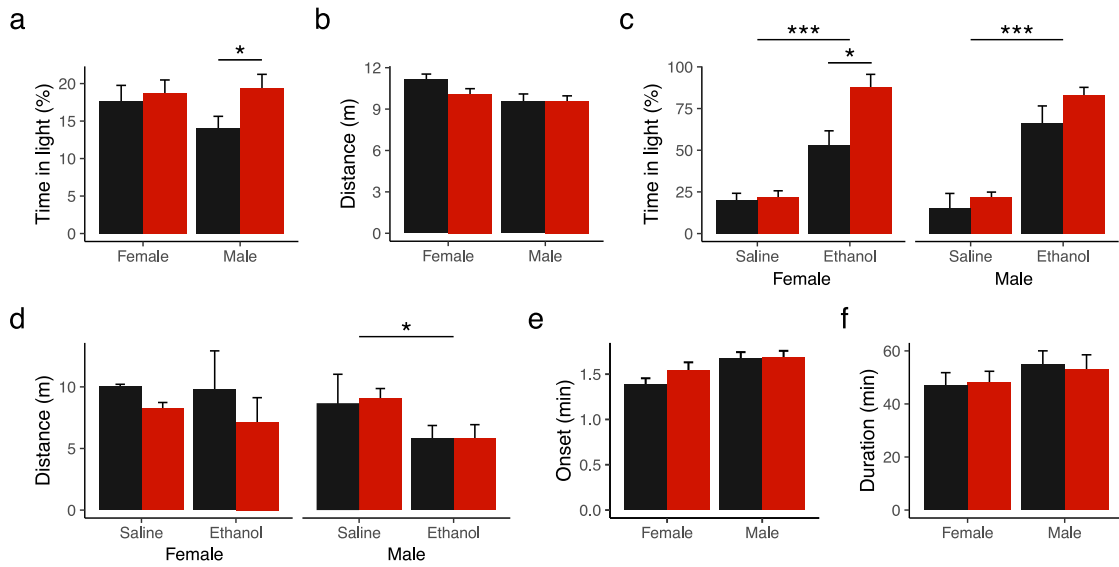


Figure 5.4. Deletion of *Clic4* alters anxiety-like behavior. (a) Basal anxiety-like behavior assessed as percent time spent in light chamber during first 5 minutes of light/dark box test and total distance traveled in all chambers in Cre⁺ and Cre⁻ animals (b). (c) Percent time spent in light chamber and total distance traveled in all chambers (d) during first 5 minutes of light/dark box test after an i.p. injection of saline or 2g/kg ethanol. (e) Onset and duration (f) of LORR following a 3.8 g/kg i.p. injection of ethanol. Significance levels indicated by *p<0.05 & ***p< 0.001.

female mice showed no difference due to genotype ($t(26.90) = 0.41, p = 0.69$). In terms of total distance traveled in all chambers, there was no genotype effect in male (**Figure 5.4b**, $t(23.75) = 0.042, p = 0.97$) or female mice ($t(27.99) = -1.90, p = 0.07$).

To assess anxiolytic effects of ethanol in the absence of *Clic4*, male and female mice were given an i.p. injection of 2g/kg and evaluated with the light/dark box test. There was a large effect of treatment such that ethanol treated males spent 56.8% more time in light than saline treated animals (**Figure 5.4c**, $F(1,14) = 74.91, p < 0.001$) and females spent 49.4% more time light ($F(1,10) = 71.4, p < 0.001$). In female mice, there was a significant interaction between treatment and genotype ($F(1,10) = 8.04, p = 0.02$), such that in the ethanol treated females, Cre⁺ mice spent more time light than Cre⁻ animals by 35.1% (Tukey's HSD; $p = 0.01$). Locomotor behavior was also assessed in the ethanol-induced anxiolysis task and was found to be unaltered by treatment (**Figure 5.4d**, $F(1,10) = 0.17, p = 0.68$) or genotype ($F(1,10) = 1.91, p = 0.20$) in females. In males, there was no effect of genotype on total distance traveled ($F(1,14) = 0.02, p = 0.88$), but ethanol treated animals showed minor locomotor depression, traveling an average of 3.1 fewer meters than saline treated ($F(1,14) = 5.74, p = 0.03$).

LORR onset and duration were measured in male and female mice after a 3.8g/kg i.p. injection of ethanol in order to evaluate ethanol sedation sensitivity.

LORR onset times did not differ between Cre⁺ and Cre⁻ males (**Figure 5.4f**, $t(28.83) = 0.08$, $p = 0.74$) or females ($t(27.17) = 1.02$, $p = 0.32$). Similarly, LORR duration was unaffected by genotype in males ($t(27.94) = -0.37$, $p = 0.72$) or females ($t(26.17) = -0.16$, $p = 0.87$).

5.3.4 Ethanol Consumption Altered by mPFC *Clic4* Deletion

Having established that global *Clic4* deletion in oligodendrocytes alters ethanol and anxiety-like behaviors, mPFC was targeted next to begin dissecting out brain regional contributions to these behaviors. AAV8-MBP-eGFP-T2A-iCre and control AAV8-MBP-eGFP viruses were injected into adult *Clic4*-floxed mouse mPFC in order to induce regionally, temporally, and cell type-specific deletions of *Clic4* (**Figure 5.5a**). Successful deletion of CLIC4 was validated by visualizing immunolabeled CLIC4 protein in mPFC sections from Cre⁺ and Cre⁻ viral vector injected animals (**Figure 5.5b**). Cell type-specificity was verified by co-labeling eGFP with mature oligodendrocyte marker CC1 (**Figure 5.5c**)

Voluntary ethanol consumption was assessed in male and female virus injected mice using the 3BC-IEA model. Average daily total ethanol intake was reduced in Cre⁺ male mice by 2.8g/kg (**Figure 5.6a-b**, $t(93.82) = -3.04$, $p = 0.003$) but unaffected in females ($t(183.46) = -0.88$, $p = 0.38$). This reduction in total ethanol

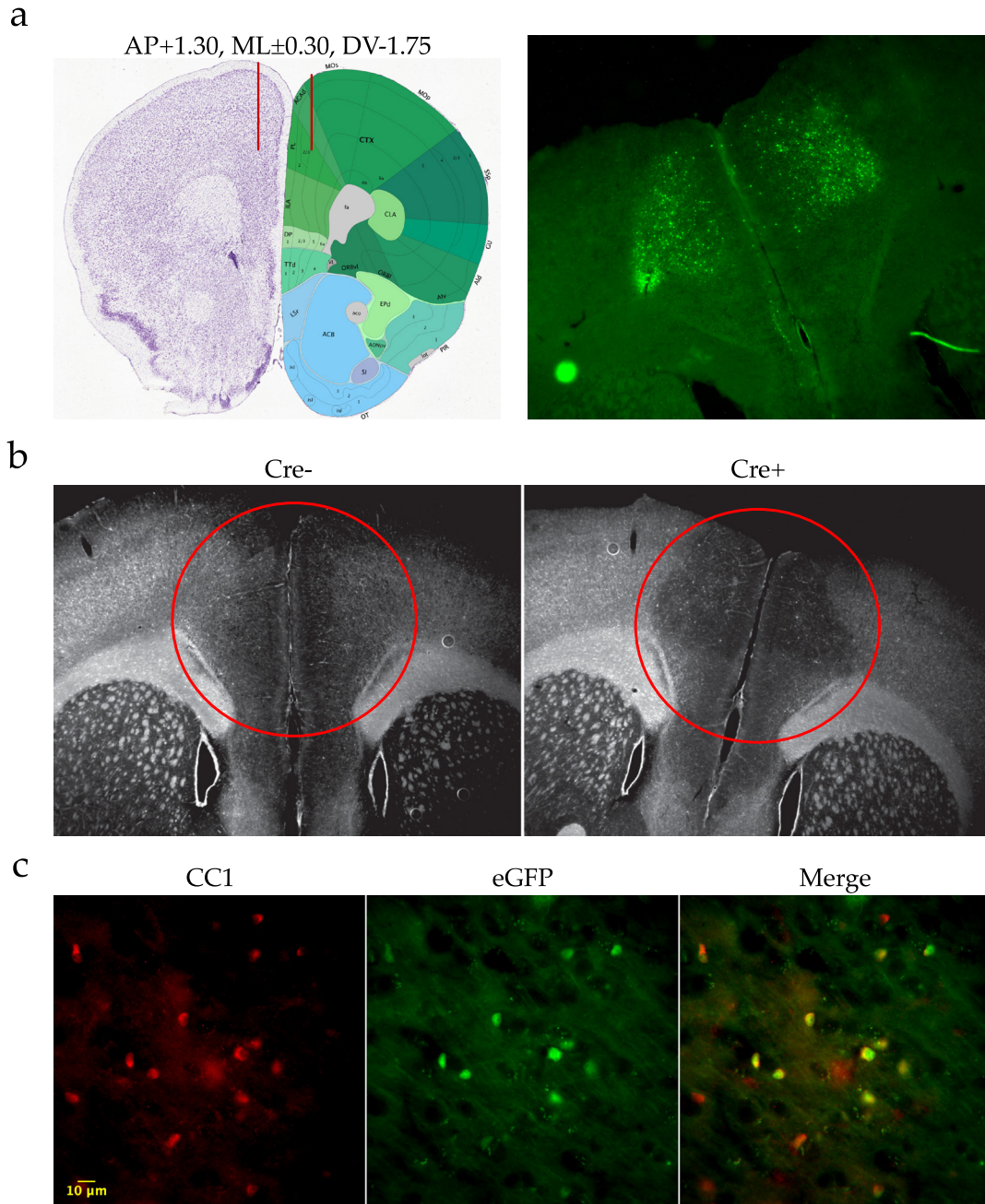


Figure 5.5. Validation of mPFC deletion of *Clic4* in oligodendrocytes. (a) AAV8-MBP-eGFP-Cre and AAV8-MBP-eGFP control virus were microinjected into mPFC of *Clic4*-floxed mice. Targeting scheme (left, adapted from Allen Brain Mouse Atlas) and example eGFP fluorescence in mPFC (right; mPFC, 2.5x widefield). (b) CLIC4 immunofluorescence in mPFC for animals that received either Cre- or Cre+ virus (mPFC, 2.5x widefield). (c) Co-localization immunofluorescence microscopy for mature oligodendrocyte marker CC1 and eGFP expression from virus (mPFC, 40x water immersion widefield).

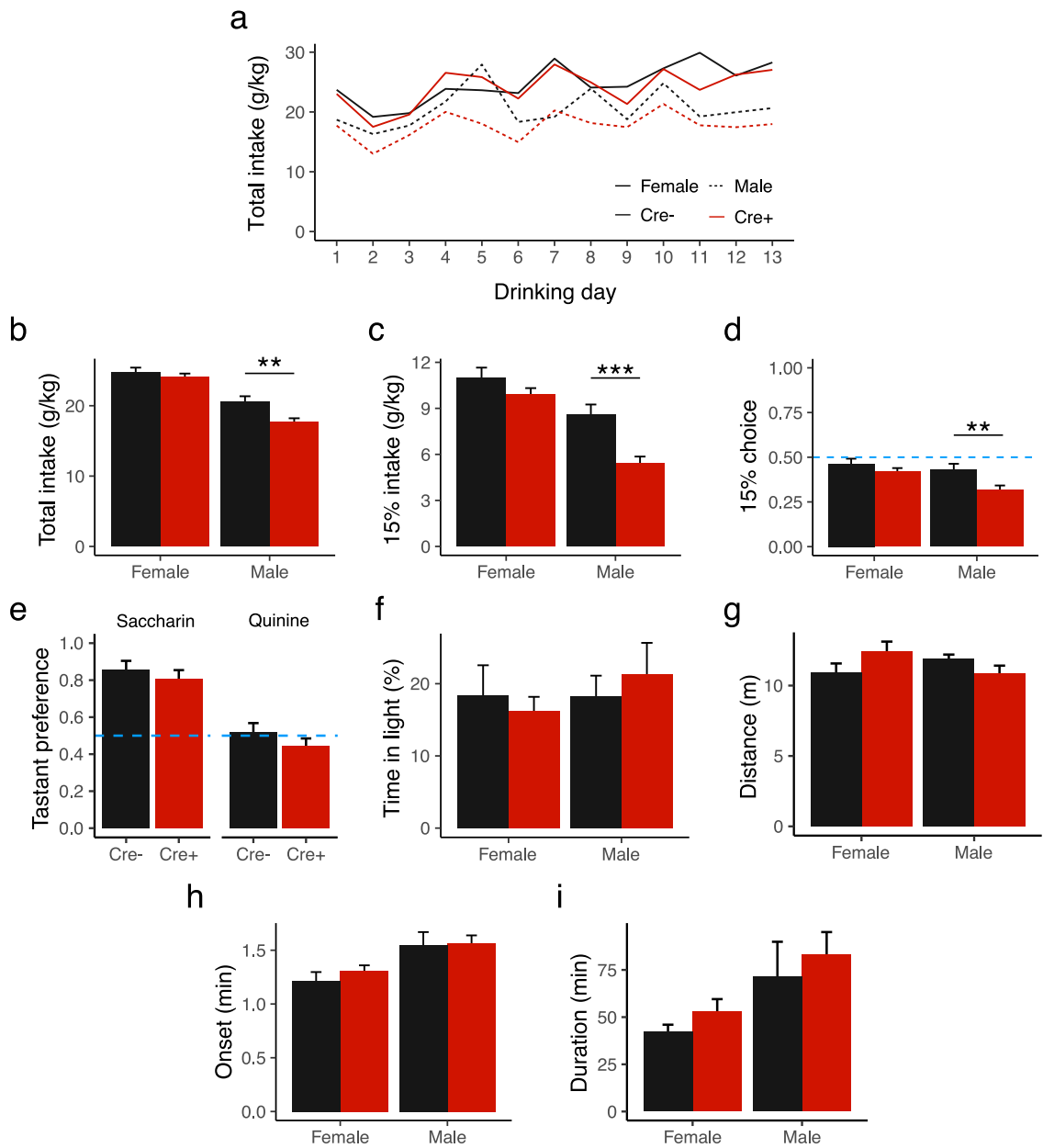


Figure 5.6. Characterization of mPFC oligodendrocyte *Clic4* deletion. (a) Total ethanol intake (15% + 30%) by drinking day in a 3BC-IEA voluntary consumption paradigm in Cre+ and Cre- mice. (b) Average daily total and 15% (c) ethanol intake across the entire study. (d) Ethanol choice as a ratio of 15% to 30% intake in g/kg. (e) Preference for saccharin or quinine over water in a three-day two-bottle choice voluntary consumption task. (f) Basal anxiety-like behavior assessed as percent time spent in light chamber during first 5 minutes of light/dark box test and total distance traveled in all chambers in Cre+ and Cre- animals (g). (h) Onset and duration (i) of LORR following a 3.8 g/kg i.p. injection of ethanol. Significance levels indicated by ** $p < 0.01$ & *** $p < 0.001$.

consumption in Cre⁺ males was associated with less 15% ethanol intake (**Figure 5.6c**, $t(96.17) = -4.09$, $p < 0.001$), but no change in 15% choice over 30% (**Figure 5.6d**, $t(228.37) = -0.65$, $p = 0.52$). Female mice showed no change in 15% ethanol intake ($t(157.82) = -1.36$, $p = 0.17$) or choice in response to viral-mediated *Clic4* deletion ($t(160.47) = -1.22$, $p = 0.22$).

Tastant preference was assessed in viral-injected animals to control for possible taste-related effects of the deletion which could bias ethanol consumption behavior. Preference for quinine and saccharin over water was assessed in a 3-day continuous access two-bottle choice task. There was an effect of tastant type with animals strongly preferring saccharin (**Figure 5.6e**, $F(1,23) = 26.17$, $p < 0.001$), but no effect of sex ($F(1,23) = 0.50$, $p = 0.48$), *Clic4* deletion ($F(1,23) = 0.40$, $p = 0.53$), and no interactions.

Basal anxiety-like behavior was assessed in ethanol-naïve viral injected mice using the light/dark box test. Time spent in light was unaffected by viral-mediated deletion of *Clic4* in mPFC oligodendrocytes for male (**Figure 5.6f**, $t(10.0) = 0.59$, $p = 0.57$) and female mice ($t(8.56) = -0.46$, $p = 0.66$). Locomotor behavior in the light/dark box test was also unaffected by *Clic4* deletion in male (**Figure 5.6g**, $t(9.55) = -1.76$, $p = 0.11$) and female mice ($t(13.92) = 1.65$, $p = 0.12$).

Ethanol sedation sensitivity was assessed by LORR following a 3.8g/kg i.p. injection of ethanol. Time to LORR onset was not affected by viral-mediated *Clic4*

deletion in males (**Figure 5.6h**, $t(5.15) = 0.12$, $p = 0.91$) or females ($t(9.93) = 1.01$, $p = 0.34$). LORR duration was also unchanged between Cre⁺ and Cre⁻ virus injected male (**Figure 5.6i**, $t(5.52) = 0.52$, $p = 0.62$) and female ($t(12.44) = 1.41$, $p = 0.18$) mice.

5.4 Discussion

This set of experiments represents the first published behavioral characterization of a chloride intracellular channel gene knockout in vertebrates. Global deletion of *Clic4* in oligodendrocytes produced altered ethanol and anxiety-like behaviors in male and female mice. This includes increased ethanol consumption in females and increased preference for 15% over 30% ethanol. Cre⁺ untreated male and ethanol-treated female mice showed less anxiety-like behavior in the light/dark box test compared to Cre⁻ controls. These phenotypes did not result from altered taste preference or ethanol kinetics, which were evaluated separately. While ethanol sedation sensitivity has been previously associated with *Clic4* overexpression in D2 mouse PFC (Bhandari et al., 2012) and disruption in invertebrates (Bhandari et al., 2012; Chan et al., 2014), this is the first study to show direct modulation of voluntary ethanol consumption by *Clic4*. Furthermore, this is the first study to identify *Clic4* as a modulator of anxiety-like behaviors in mice, an interesting finding considering its location within two known QTLs associated with anxiety-like behavior in mice (K. Nakamura & Kubota, 1996; Thifault et al.,

2008). Taken together, these experiments highlight the importance of *Clic4* as a unique modulator of ethanol and anxiety-like behaviors.

In considering the results of this study, support for our initial hypotheses is mixed. We were unable to detect altered sedation sensitivity through either global or mPFC-specific oligodendrocyte *Clic4* deletions and this is likely a consequence of mouse strain or targeted cell type. The published study reporting altered sensitivity to ethanol sedation following overexpression of *Clic4* was performed with D2 mice (Bhandari et al., 2012), which compared to B6 mice, have a much lower preference for ethanol consumption (Metten et al., 1998) and a higher sedation sensitivity to acute ethanol (Linsenbardt et al., 2009; Lister, 1987). Additionally, the study involving D2 mice utilized a neuronal-selective approach whereas the present study targeted oligodendrocytes. In terms of ethanol consumption behaviors, our initial hypothesis that *Clic4* deletion would decrease drinking was found to be true of male mice receiving mPFC-specific deletions but not for females or global oligodendrocyte deletions. Considering that our initial hypothesis was based on results from mPFC-specific overexpression of *Clic4*, this latter result provides interesting new evidence for brain region-specific roles for *Clic4*.

The mechanisms underlying *Clic4* modulation of behavior do not appear to be accompanied by gross alterations of myelin or oligodendrocyte abundance and

survival, considering expression of the two most abundant myelin proteins, MBP and PLP, is unperturbed both at 1 and 6-months post-deletion of *Clic4*. We cannot, however, rule out ultrastructural changes that do not affect myelin abundance, which could be potentially assessed with electron microscopy. This otherwise raises the question of how *Clic4* might be modulating ethanol and anxiety-like behaviors in oligodendrocytes, if not by affecting myelin abundance or stability. In addition to the role of supporting saltatory conduction of action potentials, another important role of myelin is providing trophic support to myelinated axons for long term stability. Oligodendrocytes support the highly metabolically active underlying axons by engaging in direct neurotransmission within the axon segment and shuttling proteins and glycolytic metabolites across the axo-myelinic space (Micu et al., 2018; Nave, 2010). The importance of the supportive role of myelin is highlighted by the effects of mutating myelin genes, which can lead to axon swelling and degeneration (Griffiths et al., 1998; Lappe-Siefke et al., 2003). *Clic4* has associated functions in retromer complex-mediated vesicle trafficking (Chou et al., 2016) and cell surface expression of neurotransmitter receptors (Maeda et al., 2008), suggesting a possible role for *Clic4* in supporting the axo-myelinic synapse. Potentially supporting this idea, oligodendrocytes express glutamate neurotransmitter receptors on myelin (Micu et al., 2018) and the same

receptors are known to be trafficked to plasma membrane by the retromer-complex, at least in neurons (Temkin et al., 2017) .

Another possible mechanism by which *Clic4* and other chloride intracellular channels may be altering ethanol-related behaviors is by responding to oxidative damage and cellular stress. Ethanol metabolism produces reactive oxygen species (ROS) capable of damaging various cellular components including proteins, DNA, and lipids. Cumulative ethanol-induced ROS from chronic intake can cause significant cellular damage and even neurotoxicity in the brain (Zhong et al., 2012). Notably, *Clic4* has been shown to upregulate and translocate to the nucleus in response to various cellular stressors including ROS, metabolic inhibitors, TNF- α , and DNA damage (Fernandez-Salas et al., 2002; Suh et al., 2004; Xu et al., 2013). In an *in vitro* study of glioma cell apoptosis, *Clic4* upregulated in response to H₂O₂ and RNAi knockdown of *Clic4* enhanced apoptosis in its presence (Xu et al., 2013). Furthermore, chloride intracellular channels undergo redox-activated conformational changes (Littler et al., 2004, 2005, 2010) and have been shown to exhibit glutaredoxin-like activity *in vitro* by reducing oxidized dithiol groups (Al Khamici et al., 2015). Although the exact mechanism by which CLIC4 responds to oxidative damage has not been established, it appears to provide some level of protection either as a signal transducer for the cellular stress response or as an oxidoreductase enzyme. This role may be especially important in

oligodendrocytes, which show a particular vulnerability to oxidative stress, having a high basal burden of ROS due to the required rate of lipid metabolism needed to produce and maintain large networks of myelin (McTigue & Tripathi, 2008).

Intriguingly, narrowing the anatomical breadth of *Clic4* deletion to just mPFC resulted in a very different set of behavioral alterations. The sustained increase in total ethanol consumption and preference for 15% ethanol, which was observed in female global oligodendrocyte *Clic4* deletion mice, was not observed in the mPFC-specific *Clic4* deletion mice. In contrast, mPFC-specific *Clic4* knockout mice showed a decrease in total ethanol consumption specifically in males. Additionally, anxiety-like behavioral phenotypes observed in the global *Clic4* deletions were absent in the mPFC-specific deletion. One possible explanation for the disparity in findings is that oligodendrocyte *Clic4* is modulating ethanol and anxiety-like behaviors differentially in brain regions other than mPFC. This hypothesis is reasonable when considering that although CLIC4 expression is high in oligodendrocytes, mPFC is relatively sparse of oligodendrocytes, myelin, and *Clic4* expression when compared to other brain regions (**Figure 5.7**). Not unique to PFC, *Clic4* expression has also been shown to be ethanol-induced in VTA (Kerns et al., 2005; Marballi et al., 2016) and is part of an ethanol-responsive gene network in hippocampus (Farris et al., 2015). Likewise, the role of *Clic4* in modulating

anxiety-like behaviors may instead be localized to other limbic structures such as amygdala, hippocampus, or NAc. Supporting this possibility, *Clic4* profiling through the Genotype-Tissue Expression (GTEx) Project Portal (www.gtexportal.org) reveals significant expression in each of these regions and at higher levels than frontal cortex or anterior cingulate mPFC (**Figure 5.8**).

In summary, global deletion of *Clic4* in oligodendrocytes alters ethanol consumption and anxiety-like behavior in a sex-specific manner. This represents the sum of effects from deleting *Clic4* in multiple brain regions, which are unlikely to be uniform considering the functional heterogeneity of the brain. Our results suggest at least part of the ethanol consumption phenotype is mediated by mPFC, but complex regulation of behavior by *Clic4* is occurring in other brain regions as well. As such, *Clic4* is a novel modulator of ethanol consumption and anxiety-like behavior in mice, exhibiting dichotomous functions between sexes and brain regions.

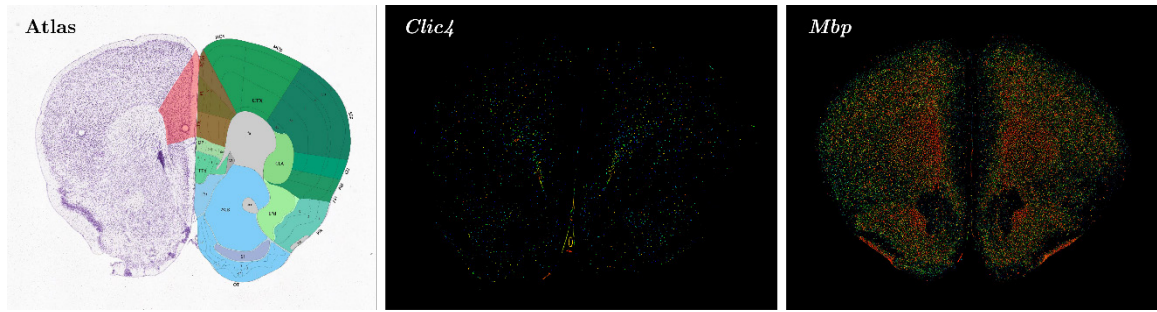


Figure 5.7. mPFC expression of *Clic4*. Mouse mPFC brain regions targeted for viral injection include anterior cingulate cortex, prelimbic, and infralimbic (left, shaded red). *Clic4* (middle) and *Mbp* (right) *in situ* hybridization expression data from approximate location of atlas reference image. Images downloaded from Allen Brain Atlas Mouse Brain Atlas (Lein et al., 2007).

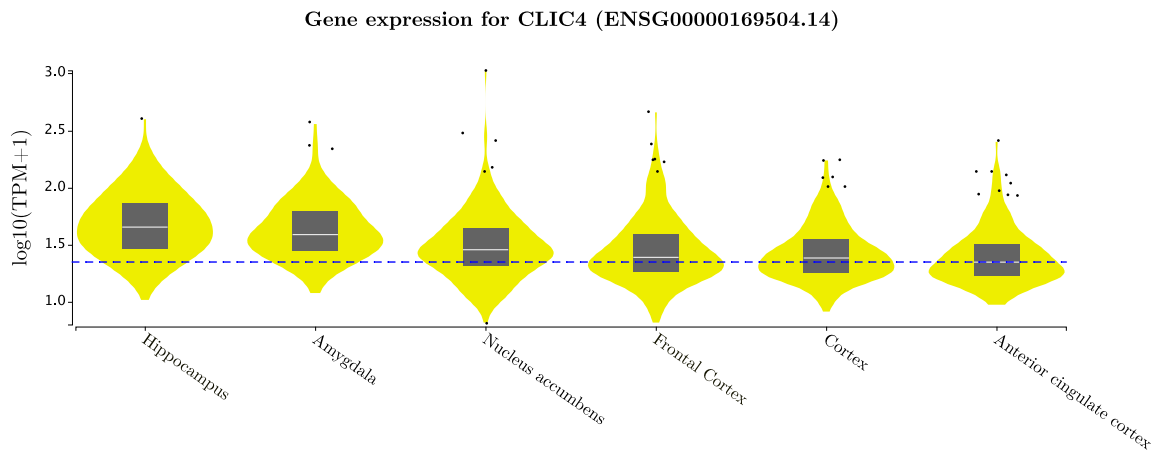


Figure 5.8. Brain region-specific *Clic4* expression. Human *Clic4* mRNA expression data obtained from GTEx and plotted according to brain region. Dashed line indicates expression level of *Clic4* in anterior cingulate cortex mPFC brain region for reference. Image downloaded from GTEx (Lein et al., 2007) and modified for font visibility.

Chapter 6

Clic4 Gene Expression Characteristics

6.1 Introduction

Clic4 expression in various tissues and cell types has been fairly well documented with the exception of brain. Outside of brain, *Clic4* displays a fairly ubiquitous pattern of tissue expression which is notably higher in heart, lung, liver, kidney, and skin (Fernández-Salas et al., 1999). CLIC4 protein has been identified in a variety of cell types, depending on organ system, but consistently shows high expression in vascular endothelial cells (V. Padmakumar et al., 2014). CLIC4 has been detected in multiple subcellular compartments, including cytoplasm, nucleus, mitochondria, plasma membrane, and intracellular membranes such as vesicles and endosomes (Berryman & Goldenring, 2003; Chou et al., 2016; Ponsioen et al., 2009; Proutski et al., 2002; Suh et al., 2004). CLIC4 localization appears to be highly dynamic, showing subcellular translocation following redox changes (Littler et al., 2005), cellular stress (Fernandez-Salas et al.,

2002; Suh et al., 2004; Xu et al., 2013), TGF- β signaling (Malik et al., 2010; Shukla et al., 2009), and RhoA-associated cytoskeleton remodeling (Elisabetta Argenzio et al., 2018; Ponsioen et al., 2009),

Despite the wealth of published data on CLIC4 tissue-specific expression, little is known about CLIC4 expression in brain. What is known is largely limited to publications of single-cell RNAseq databases and tissue expression atlases. Based on Allen Brain Atlas *in situ* hybridization data (Lein et al., 2007), Padmakumar et al. noted that *Clic4* expression in adult mouse brain is generally low and sparse in contrast to other tissues (V. Padmakumar et al., 2014). The group observed that *Clic4* expression was highest along axonal tracks and in lateral septal nucleus, olfactory bulbs, and cerebellum. While it was not possible to ascertain cell type-specific expression characteristics the data, the authors hypothesized expression would be high in these areas due to the abundance of *Clic4* along white matter tracts. Supporting this theory, web-based tools for interrogating single cell RNAseq expression databases consistently report myelinating oligodendrocytes as the highest *Clic4* expressing cell type in brain (Marques et al., 2016; Zeisel et al., 2015; Zhang et al., 2014). Despite this compelling evidence for expression in oligodendrocytes, direct experimental assessment of CLIC expression in brain is still lacking.

Clic4 has been shown to be up-regulated by acute ethanol in D2 mouse PFC (Bhandari et al., 2012; Kerns et al., 2005) but Kerns et al. showed little response or actual decreased *Clic4* expression on microarray analysis in male B6 mice. Considering the ability of *Clic4* to modulate ethanol behaviors in B6 mice discussed in Chapter 5, we might also expect to see ethanol-regulated expression in PFC of this strain as well. Furthermore, considering *Clic4* translocates to the nucleus during cellular stress (Suh et al., 2004) and to enhance TGF- β pathway gene expression (Shukla et al., 2009), we believe *Clic4* may be modulating ethanol-related behaviors, at least in part, by influencing gene expression. We will evaluate both of these hypotheses in this chapter by employing a combination of qRT-PCR and microarray analysis in wild type and oligodendrocyte-specific *Clic4* knockout B6 mice exposed to acute ethanol. The overall goal of the work described in this chapter is to 1) identify cellular expression characteristics of CLIC4 in PFC, 2) assess ethanol-responsiveness of *Clic4* expression in B6 mouse PFC, and 3) characterize the transcriptomic signature of *Clic4* in PFC and how it is affected by acute exposure to ethanol.

6.2 Methods

Ethics Statement

All procedures were approved by Virginia Commonwealth University Institutional Animal Care and Use Committee under protocol AM10332 and followed the NIH Guide for the Care and Use of Laboratory Animals (NIH Publications No. 80-23, 1996).

Animals

Male and female mice were group housed on corn cob bedding (Teklad #7092) with a 12-hour light/dark cycle (7am on, 7pm off) and provided *ad libitum* access to food (Teklad #7912) and water with weekly cage changes. All animals taking part in behavioral studies were permanently transferred to Sani-Chips bedding a minimum of one week before testing. Animals used in this study include wild type B6 mice (Jackson Laboratory #000664) and *Clic4*-floxed mice crossed to Plp-Cre-ER^T mice (described in Chapter 5). Between 8-11 weeks of age, oligodendrocyte-specific *Clic4* knockouts were induced in Plp-Cre-ER^T mice through 5 daily 75mg/kg i.p. injections of tamoxifen (Sigma-Aldrich #T5648) in a sunflower oil vehicle (Sigma-Aldrich #S5007). Tamoxifen was administered to both Cre⁺ and Cre⁻ animals.

CLIC4 Protein Localization Studies

Immunofluorescence – Wild type B6 mice were perfused with 1x PBS followed by 4% paraformaldehyde before brain extraction and 24-hour post-fixation. Cryoprotection performed in 30% sucrose and brains flash frozen then cut on a Leica 3050S cryostat at 20 μm per section, unless otherwise stated. Antigen retrieval performed for 15 minutes at 80°C in 10mM citrate buffer (pH6) before blocking with a 10% goat serum and 0.2% Triton X-100 solution for 30 minutes at room temperature. Free floating sections incubated overnight with primary antibodies at 4°C and secondary antibodies applied for 2 hours at room temperature. Mounting performed using VECTASHIELD Hardset with DAPI (#H-1500). Sample sizes include a minimum of 3 sections per animal and 3 animals per group.

Antibodies – Anti-CLIC4 (1:100; Cell Signaling Technology #D2A7D), anti-NEUN (1:500; Millipore #MAB377), anti-CAMKIIA (1:500; Cell Signaling Technology #50049), anti-NFH (1:1000; Abcam #ab4680), anti-CC1 (1:200; Millipore, OP80), anti-CNPase (1:400; Abcam #ab6319), anti-IBA1 (1:200; GeneTex #GT10312), anti-GLUL (1:200; Abcam #ab64613), AlexaFluor 488 anti-mouse (1:1000; ThermoFisher Scientific #A21121), AlexaFluor 488 anti-chicken (1:300; ThermoFisher Scientific

#A11039), and AlexaFluor 594 anti-rabbit (1:300; ThermoFisher Scientific #A11012).

Microscopy – Images taken on a Zeiss LSM700 with a 63x oil objective. Z-stacks sampled at Nyquist density with (43x43x130nm voxels) and a scan zoom set at either 1x or 4.6x (290x total). Deconvolution of 290x z-stacks performed with Scientific Volume Imaging Huygens Suite software v 19.04 using default settings and experimentally obtained point spread function files for each color channel generated using fluorescent beads. All additional image processing performed with FIJI distribution (Schindelin et al., 2012) of ImageJ (Rasband, 2015). Images analyzed in this study were taken from PFC brain regions including prelimbic, infralimbic, and anterior cingulate cortex (Chapter 2).

qRT-PCR Ethanol Gene Expression Studies

Acute ethanol exposure qRT-PCR study – Wild type adult male and female B6 mice were given i.p. injections of either normal saline, 0.5, 2.0, or 4.5 g/kg ethanol in normal saline (20% v/v). 4 hours after, animals were euthanized by cervical dislocation and decapitation and multiple brain regions including PFC were rapidly microdissected and flash frozen in liquid nitrogen. Further methodological details and data for gene targets not included in present study have been

previously published (van der Vaart, 2018). Sample sizes include 5-6 animals per group.

Chronic ethanol exposure qRT-PCR study – Wild type adult male and female B6 mice were single-housed and placed on a two-bottle choice paradigm with identical bottles containing water or 20% ethanol in water (v/v) provided for 24-hour periods, every other day, starting 2 hours before the dark cycle. Bottle position was rotated each drinking day and on non-drinking days ethanol bottles were replaced with a second water bottle. Drinking was continued for 5 weeks and animals were euthanized on week 6 by cervical dislocation and multiple brain regions including PFC were microdissected and flash frozen in liquid nitrogen as above. Further methodological details and data for gene targets not included in present study have been previously published (van der Vaart, 2018). Sample sizes include 5-6 animals per group.

qRT-PCR analysis – Total RNA was isolated from PFC by Qiagen RNeasy Mini Kit (#74104). RNA quality and concentration assessed by NanoDrop spectrophotometry and only samples with 260/280 ratios > 1.8 were analyzed further. cDNA was synthesized using the Bio-Rad iScript cDNA Synthesis Kit (#1708891). PCR performed with iQ SYBR Green Supermix (#1708880) and a Bio-

Rad CFX Connect thermocycler. Expression values calculated by delta-delta Ct method using the relatively ethanol-insensitive *Ublcp1* and *B2M* as reference genes. Statistical analysis was performed in R v3.6.2 (R Development Core Team & Team, 2016) using R Studio v 1.2.5033 (RStudio Team, 2016) and ggplot2 package for plotting (Wickham, 2016). Within-sex one-way ANOVAs and Tukey's HSD post-hoc testing was carried out for acute exposure data and unpaired Student's *t*-test for chronic ethanol exposure data.

Microarray Acute Ethanol Gene Expression Study

Acute ethanol exposure for microarray analysis – 5 weeks after tamoxifen, adult male and female *Clic4*-floxed Cre⁺ and Cre⁻ mice were given i.p. injections of either normal saline or 3.8 g/kg ethanol in normal saline (20% w/v). 4 hours after, animals were euthanized by cervical dislocation and decapitation and multiple brain regions including PFC were microdissected and flash frozen in liquid nitrogen as described above. Sample sizes were 5 animals per group (n=40 mice in total).

RNA extraction and microarray preparation – Total RNA was extracted from PFC tissue using Qiagen miRNeasy Mini Kits (#217004) and a BeadBug 6 homogenizer using stainless steel beads (#D1033-28). Only samples with Bioanalyzer RIN scores > 7 and NanoDrop spectrophotometer 260/280 ratios > 1.8 were used for

microarray preparation. Purified RNA was processed with Clariom S Mouse Assays kits (ThermoFisher Scientific #902930) per manufacturer protocol to produce fragmented and labeled ss-cDNA. Microarray hybridization, washing and scanning was performed by Tana Blevins within the VCUHS Tissue & Data Acquisition & Analysis Core. Hybridization was performed in an Affymetrix Genechip Hybridization Oven 645 for 16 hours at 45°C, 60 rpm. Washing and staining was performed with Genechip Fluidics Stations 450 and 450DX. An Affymetrix Genechip scanner 3000 7G was used for chip scanning and Affymetrix GeneChip Command Console software for scan analysis. Clariom S Mouse arrays provide coverage of over 20,000 well-annotated mouse genes.

Microarray analysis – Microarray data pre-processing and differential expression statistical analysis was performed with ThermoFisher Scientific Transcriptome Analysis Console Software (TAC) using default SST-RMA and Limma methodology. Default quality control metrics assessed by TAC include principal component analysis, analysis of hybridization and labeling controls, and area under the curve separation for positive and negative controls. Three female samples were dropped from further analysis due to one having a large air bubble on the scanned chip and two others being substantial outliers on PCA analysis. Due to minimal differential expression between males and females and males

having a larger sample size, analyses were largely focused on male mice. Separate TAC analyses were performed within male mice for the following contrasts: 1) Cre- mice treated with ethanol versus saline, 2) Ethanol-treated Cre+ versus Cre- mice, and 3) Saline-treated Cre+ versus Cre- mice. Differentially expressed genes from between-genotype contrasts 2 and 3 were filtered for unadjusted p-values < 0.05 and fold change values < -1.4 or > 1.4. For contrast 1, an FDR cutoff of 0.2 was applied with no fold change cutoff. Further analysis and visualization of differentially expressed genes was performed in R v3.6.2 (R Development Core Team & Team, 2016) using R Studio v 1.2.5033 (RStudio Team, 2016). Gene set overlaps were visualized with Venn diagrams produced by R package Vennerable (github.com/js229/Vennerable) and compared for degree of overlap using Fisher's exact tests.

Bioinformatics – Functional enrichment analysis of differentially expressed genes was performed using the web-based tool ToppGene (<https://toppgene.cchmc.org/>) (Chen et al., 2009). Databases queried included KEGG (Carbon et al., 2019; Kanehisa, 2000) and GO categories of Biological Processes, Cellular Components, and Molecular Functions. Database terms that included < 2 or > 1000 annotated genes were not considered. A p-value cutoff of 0.01 was applied to all terms and GO terms with > 90% redundancy were removed. Significantly enriched terms

were visually explored using the R package GOplot v.1.0.2 (Walter et al., 2015) to produce representative plots in **Figures 6.7-6.9**. The web-based tool GeneWeaver (<https://geneweaver.org/>) was used to perform an integrative genomic analysis across multiple published ethanol-responsive gene sets (Baker et al., 2012). Through GeneWeaver, two independent ethanol-exposure microarray studies were identified (GS128107 and GS354531) and assessed for gene set overlap using Fisher's exact tests.

6.3 Results

6.3.1 Expression Profile of CLIC4 in mPFC

CLIC4 protein expression in mPFC was characterized in oligodendrocytes, neurons, astrocytes, and microglia using immunofluorescent labeling techniques and confocal microscopy. CLIC4 was detected in virtually all observed CC1+ and CNP+ oligodendrocytes (**Figure 6.1a**). CC1 and CNP are both expressed in mature oligodendrocytes and while CC1 is cytosolic, CNP is membrane and myelin-associated (Snaidero et al., 2017). Dense punctate expression of CLIC4 was detected within cytosolic and nuclear compartments of oligodendrocytes as well as in punctate and linear patterns along CNP+ myelin (**Figure 6.1b**).

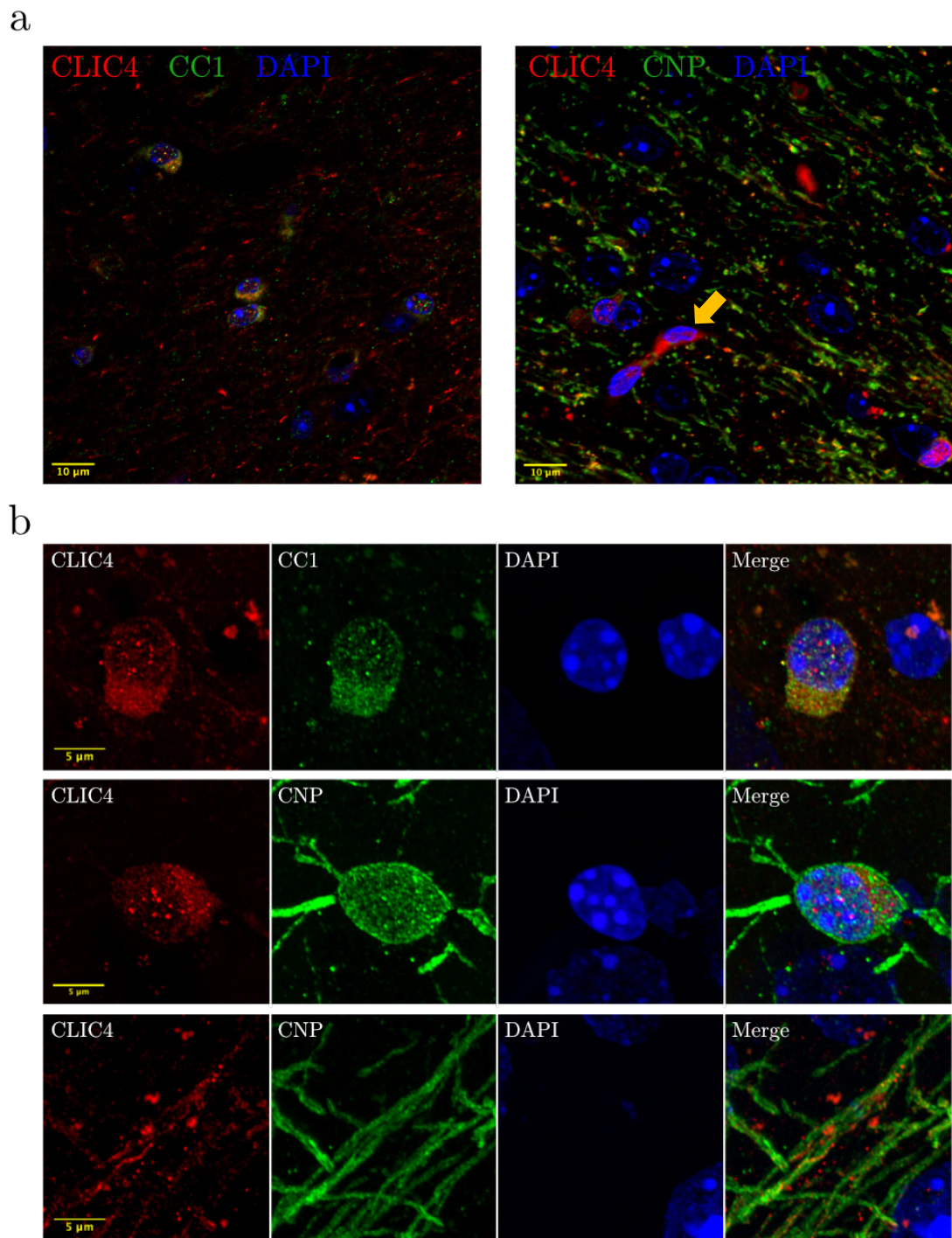


Figure 6.1. CLIC protein expression in oligodendrocytes. Confocal microscopy images depicting CLIC4 expression alongside oligodendrocyte markers CC1 and CNP in 63x slices (a) and 290x deconvolved z-stack maximum intensity projections (b). CNP+ myelin displayed in lower panel. Orange arrow indicates CLIC4+ endothelial cell.

CLIC4 expression was found to be sparse in NEUN⁺ and CAMKII α ⁺ neurons (**Figure 6.2a**) and largely restricted to cytosol (**Figure 6.2b**). In frontal cortex, NEUN has a pan-neuronal expression profile whereas CAMKII α is limited to glutamatergic cells. NFH was labeled in order to identify axons and CLIC4 was occasionally found to be expressed adjacently and in a linear pattern that generally matched the same trajectory (**Figure 6.2b**).

The majority of observed IBA1-labeled microglia displayed expression of CLIC4 protein (**Figure 6.3a**). Expression of CLIC4 in microglia tended to display a pattern of a single dense well-circumscribed region of cytoplasm (**Figure 6.3b**). In GFAP⁺ and GLUL⁺ astrocytes, CLIC4 was found to display a sparse punctate expression pattern (**Figure 6.4a**). While GFAP is a common marker for astrocytes, it labels only a small volume of the cell due its association with intermediate filaments of the cytoskeleton. The enzyme GLUL labels astrocytes more uniformly, having a diffuse cytosolic expression pattern. CLIC4 expression was not detected in all GFAP⁺ and GLUL⁺ cells, but was generally localized to the nucleus when observed (**Figure 6.4b**). Endothelial cells robustly expressed CLIC4 and were commonly detected and distinguished by morphology (**Figures 6.1a, 6.2a, 6.3b, 6.4a**).

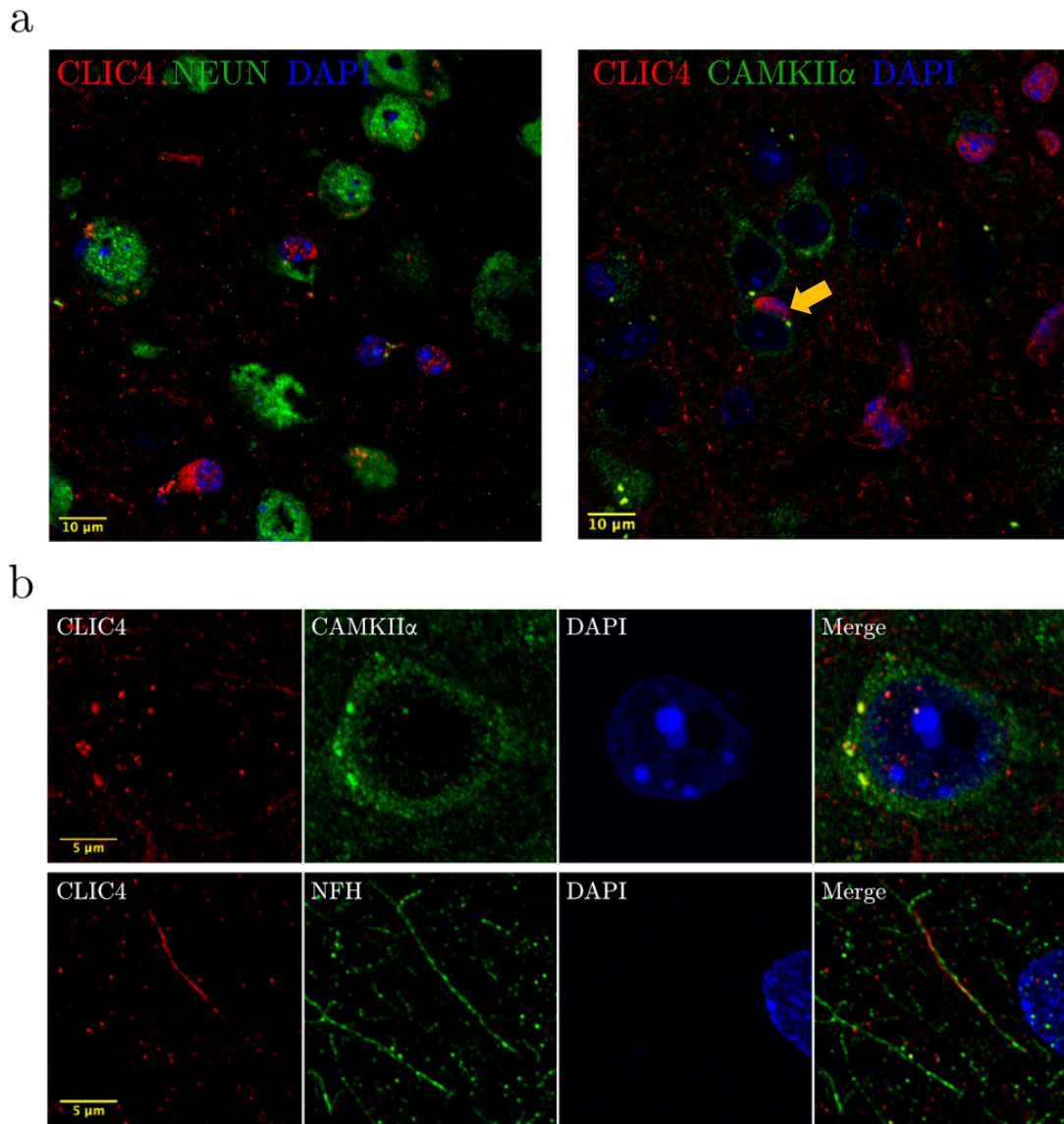
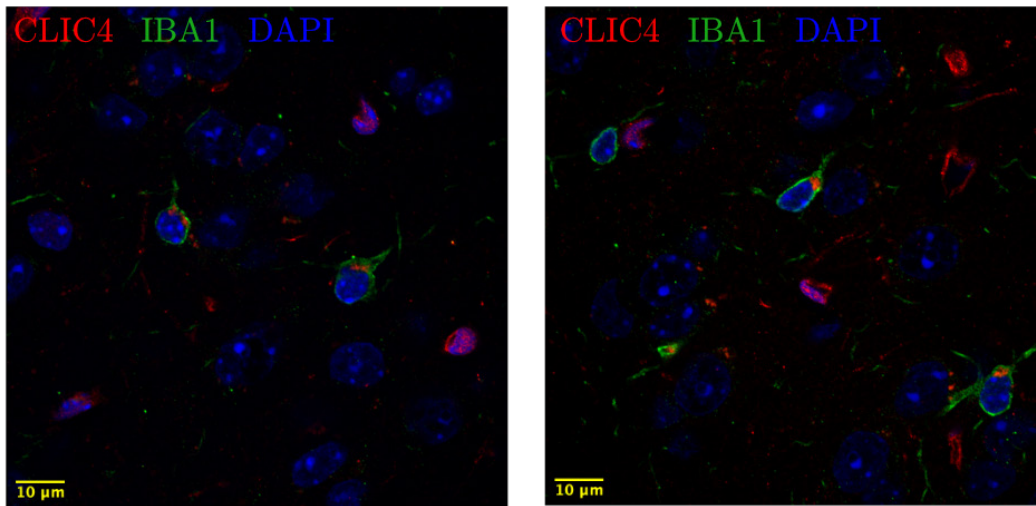


Figure 6.2. CLIC protein expression in neurons. Confocal microscopy images depicting CLIC4 expression alongside neuronal markers NEUN and CAMKII α in 63x slices (a) and CAMKII α and axonal marker NFH in 290x deconvolved z-stack maximum intensity projections (b). Orange arrow indicates CLIC4+ endothelial cell.

a



b

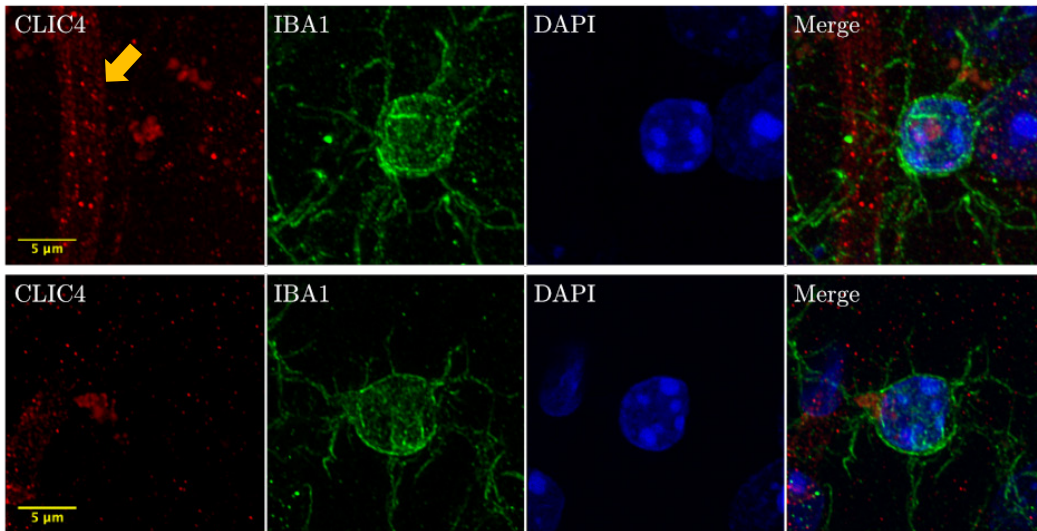


Figure 6.3. CLIC protein expression in microglia. Confocal microscopy images depicting CLIC4 expression alongside microglial marker IBA1 in 63x slices (a) and 290x deconvolved z-stack maximum intensity projections (b). Orange arrow indicates CLIC4+ blood vessel surrounded by microglial processes.

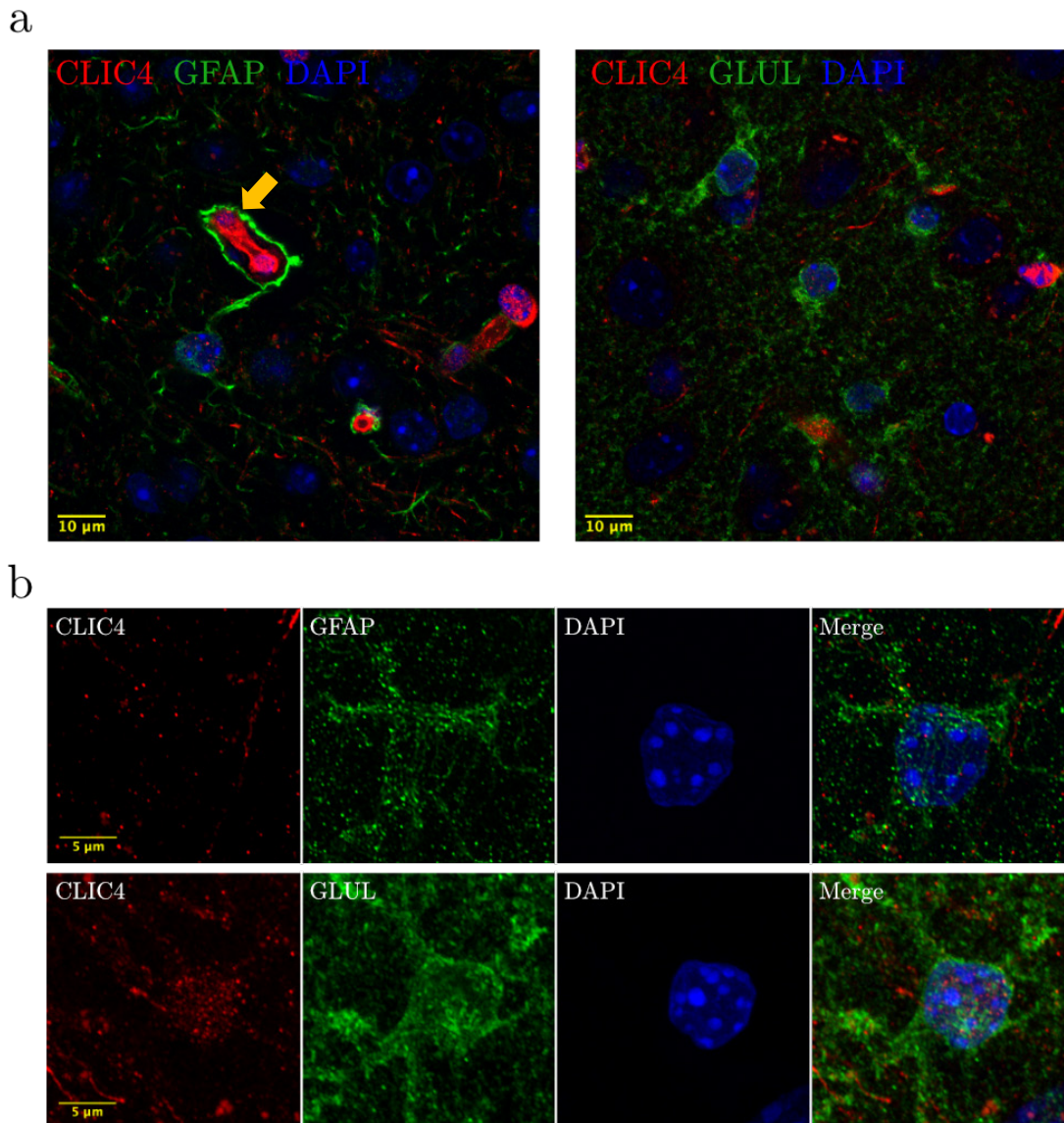


Figure 6.4. CLIC protein expression in astrocytes. Confocal microscopy images depicting CLIC4 expression alongside astrocyte markers GFAP and GLUL in 63x slices (a) and 290x deconvolved z-stack maximum intensity projections (b). Orange arrow indicates CLIC4⁺ endothelial cells encircled by astrocyte foot processes, displaying typical appearance of the blood-brain barrier.

6.3.2 PFC *Clic4* Expression Following Ethanol Exposure

Clic4 is known to be regulated by acute ethanol in D2 mouse PFC (Bhandari et al., 2012; Kerns et al., 2005), but this has not been thoroughly evaluated in B6 mice. To investigate this possibility, qRT-PCR was performed on PFC tissue isolated from wild type male and female B6 mice 4 hours after an i.p. injection of saline, 0.5g/kg, 2.0g/kg, or 4.0g/kg ethanol. A significant overall effect of treatment on *Clic4* expression was found in females (**Figure 6.5a**, $F(3,19) = 14.77$, $p < 0.001$) but not in males ($F(3,20) = 1.87$, $p = 0.17$). In females, Tukey's HSD post-hoc testing revealed an upregulation of *Clic4* in animals receiving a 4.0g/kg injection when compared to the 2.0g/kg ($p = 0.002$), 0.5g/kg ($p = 0.001$), and saline-treated ($p < 0.001$) groups.

Clic4 mRNA was also evaluated for altered expression in PFC following chronic ethanol exposure. Wild type male and female B6 mice were placed in a two-bottle choice intermittent ethanol access study for 5 weeks and paired with an equal number of control animals given access only to water. At the close of the study, neither male (**Figure 6.5b**, $t(8.74) = 1.19$, 0.27) or female ($t(9.21) = 0.38$, 0.71) chronic ethanol drinkers showed a difference in PFC *Clic4* mRNA expression when compared to water-only drinking controls.

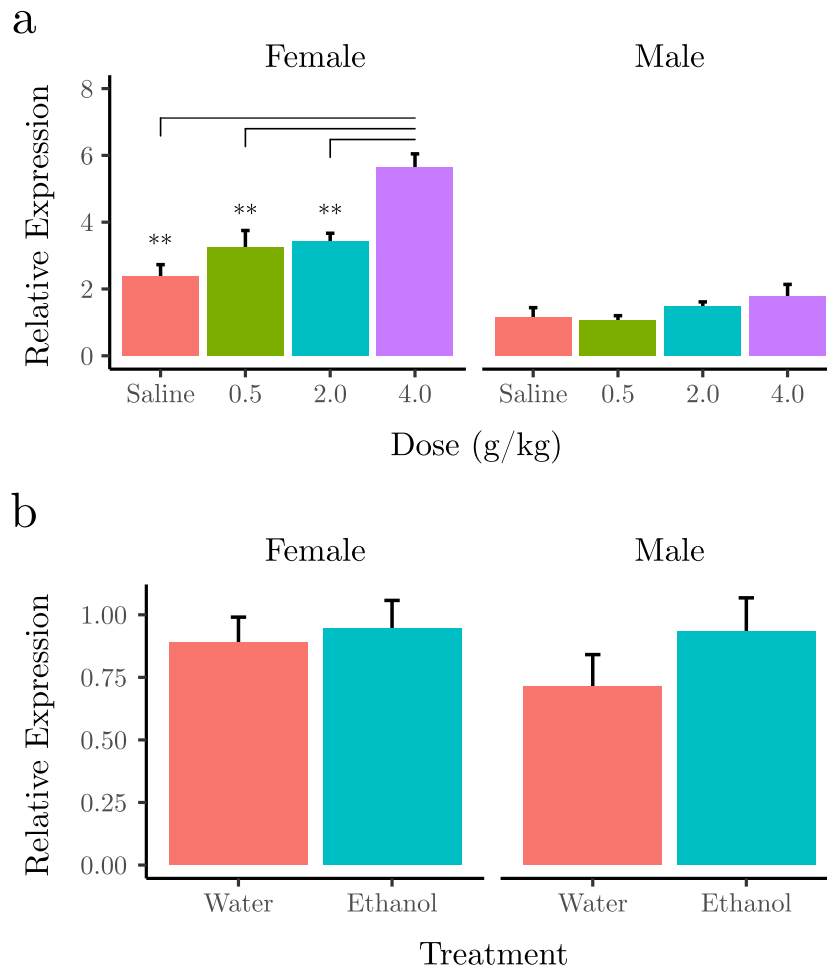


Figure 6.5. *Clic4* mRNA expression after ethanol exposure. (a) qRT-PCR analysis of *Clic4* mRNA in wild type B6 mouse PFC 4 hours after i.p. injection of saline or ethanol. (b) qRT-PCR analysis of *Clic4* mRNA in wild type B6 mouse PFC 1 week following a 5-week chronic intermittent voluntary ethanol drinking study. Groups correspond to water-only drinkers ethanol drinkers. Significance levels indicated by ** $p < 0.01$.

6.3.3 Transcriptomic Response to Acute Ethanol and *Clic4*

Deletion

In order to gain deeper insight into the biological functions of *Clic4* in brain, especially with regard to its role in the molecular response to ethanol, *Clic4* was deleted in oligodendrocytes of adult B6 mice and RNA microarrays were run on PFC tissue after acute exposure to high dose ethanol (4 g/kg x 4 hours). Transcriptomes of ethanol-treated Cre⁺ male and female mice were compared to control Cre⁻ and saline-treated mice. There were no significant differentially expressed genes resulting from the interaction of sex and ethanol treatment (**Table 6.1**). Nine genes did show differential expression between Cre⁻ ethanol-treated male and female mice, however, six of these were located on sex chromosomes (**Table 6.2**). The remaining three autosomal genes differentially regulated between sexes after ethanol treatment were *Fkbp5* (fold change = -2.1, FDR = 0.05), *Trp53inp1* (fold change = -1.9, FDR = 0.01), and *Tcam1* (fold change = 1.8, FDR = 0.07). Due to minimal sex-specific gene expression responses to ethanol and a lower relative sample size in females, additional analyses were directed towards males.

Three male-only contrasts were focused on for further differential expression and bioinformatic analysis, 1) Cre⁻ ethanol versus saline-treated mice, 2) Saline-treated Cre⁺ versus Saline-treated Cre⁻ mice, and 3) Ethanol-treated Cre⁺ versus Ethanol-treated Cre⁻ mice. While ethanol-treated Cre⁻ animals showed

robust gene expression changes when compared to saline-treated Cre- mice at an FDR cutoff of 0.20, differential expression across genotypes was more subtle. To improve detection power specifically in the two genotype contrasts, the alpha level was reduced to an unadjusted 0.05, but a fold change cutoff of < -1.4 or > 1.4 was implemented to maintain stringency. Utilizing these criteria, 544 genes were found to be differentially expressed due to genotype in saline-treated animals and 310 genes due to genotype in acute ethanol-treated animals (**Table 6.1, Table S6.1**). In both cases, *Clic4* deletion resulted in disproportionately more upregulated than downregulated genes. Applying an FDR cutoff 0.20, ethanol treatment was found to alter the expression of 593 genes in Cre- animals when compared to saline treatment, most of which were upregulated. *Clic4* was among the significantly upregulated genes in the Cre- male ethanol versus saline contrast (fold change = 2.9, FDR = 0.016). Significant overlap was noted between genes responding to ethanol in Cre- animals (**Figure 6.6**) and those responding to *Clic4* deletion in ethanol (OR = 2.6, $p = 2.3 \times 10^{-4}$) and saline-treated (OR = 4.7, $p < 2.2 \times 10^{-16}$) animals. To a lesser extent, this was also the case when comparing genes responsive to *Clic4* deletion in ethanol and saline-treated animals (OR = 1.9, $p = 0.023$).

To identify meaningful biological patterns within the large lists of differentially expressed genes, overrepresentation analysis was performed for GO

Genotype	Treatment	Sex	Contrast	Up	Down	Total
Cre-	Both	Both	Interaction	0	0	0
Cre-	Ethanol	Both	Sex	3	6	9
Cre-	Both	Male	Treatment	389	204	593*
Both	Saline	Male	Genotype	232	312	544*
Both	Ethanol	Male	Genotype	191	119	310*

Table 6.1. Summary of differential gene regulation.

Summary of contrast designs and differential gene expression results according to direction of regulation. Results are filtered by FDR < 0.2 in non-genotype contrasts and with p < 0.05 and fold change < -1.4 or > 1.4 for genotype contrasts. Gene sets indicated by an asterisk were the focus of further bioinformatic analysis.

Gene	Chr	FC	FDR	Description
<i>Trp53inp1</i>	chr4	-1.86	0.0964	transformation related protein 53 inducible nuclear protein 1
<i>Tcam1</i>	chr11	1.81	0.0748	testicular cell adhesion molecule 1
<i>Fkbp5</i>	chr17	-2.1	0.0536	FK506 binding protein 5
<i>Gm6121</i>	chrX	2.23	0.0279	predicted gene 6121
<i>Eif2s3x</i>	chrX	1.74	0.0279	eukaryotic translation initiation factor 2, subunit 3, structural gene X-linked
<i>Kdm5d</i>	chrY	-17.79	2.83e-10	lysine (K)-specific demethylase 5D
<i>Eif2s3y</i>	chrY	-98.65	3.12e-11	eukaryotic translation initiation factor 2, subunit 3, structural gene Y-linked
<i>Uty</i>	chrY	-57.73	1.87e-09	ubiquitously transcribed tetratricopeptide repeat gene, Y chromosome
<i>Ddx3y</i>	chrY	-118.42	7.64e-11	DEAD (Asp-Glu-Ala-Asp) box polypeptide 3, Y-linked

Table 6.2. Ethanol differentially regulated genes between sexes.

Summary of genes differentially expressed between sexes (FDR < 0.20) after ethanol treatment. Columns include gene symbol, chromosome (Chr), fold change (FC), false discovery rate adjusted p-value (FDR), and gene description.

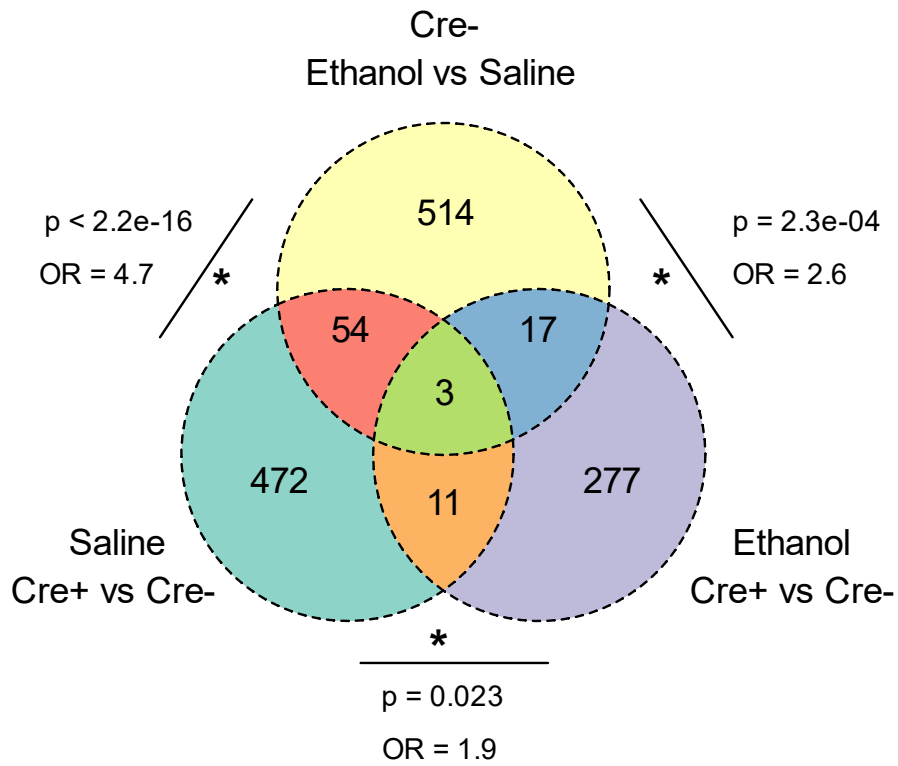
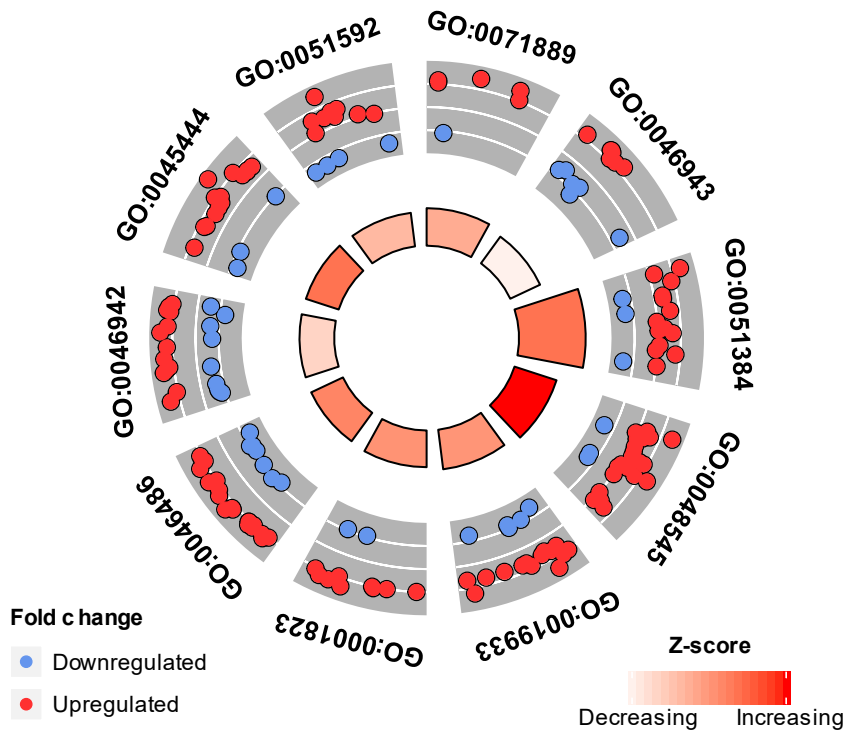


Figure 6.6. Summary of differential gene expression. Venn diagram depicting differentially expressed genes within each main contrast. Overlap between gene sets was evaluated by Fisher's exact tests providing odds ratios (OR) and p-values.

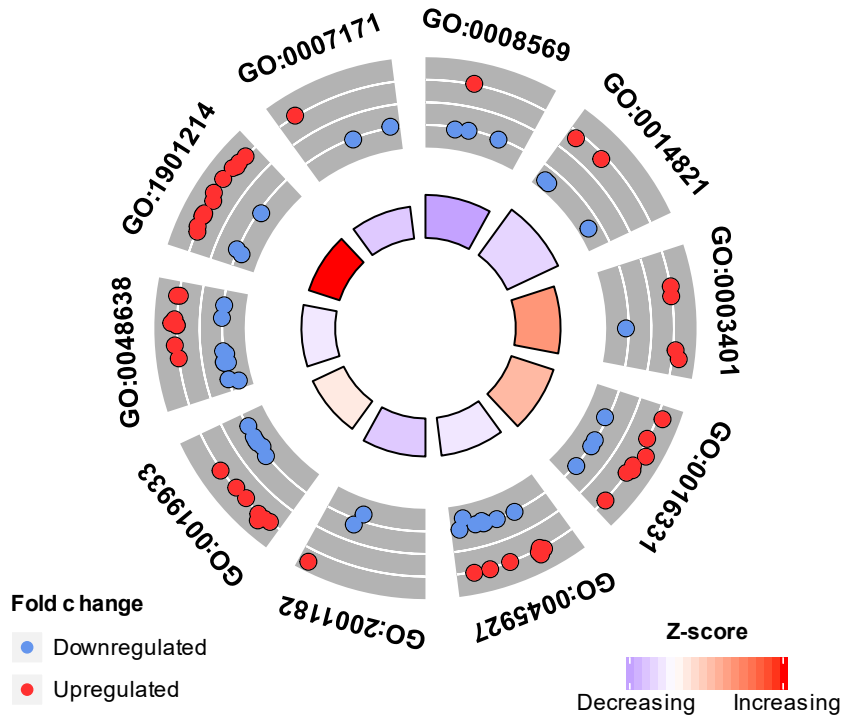
categories. The effect of ethanol treatment over saline in Cre- animals produced altered expression of genes related in a variety of biological functions glucocorticoid, steroid hormone, and cAMP signaling and carboxylic acid transport (**Figure 6.7, Table S6.2**). These GO terms were largely enriched by upregulated genes. In saline treated animals, *Clic4* deletion-responsive genes enriched processes related to cytoskeleton, cellular growth, and morphogenesis (**Figure 6.8**), including Axis Elongation (GO:0003401) and positive regulation growth (GO:0045927). These processes were mostly divided in gene regulation or downregulated with exception of Regulation of Neuron Death (GO:1901214), which showed marked overall upregulation. Genes responsive to *Clic4* deletion in the presence of acute high dose ethanol were overrepresented in immune and inflammatory processes (**Figure 6.9**) such as myeloid dendritic cell activation (GO:0002277). Redox-related processes were also enriched, including positive regulation of oxidoreductase activity (GO:0051353).

In an attempt to integrate our data with other published genomic studies of ethanol exposure, we compared our list of genes regulated by 4g/kg acute ethanol in Cre- mice with that of a 1.8g/kg low acute dose of ethanol study and also to a chronic ethanol drinking macaque study (**Figure 6.10, Table S6.3**). Significant overlap of ethanol-regulated genes was observed between all three gene sets, with the largest being between chronic drinking macaques and low dose treated mice.



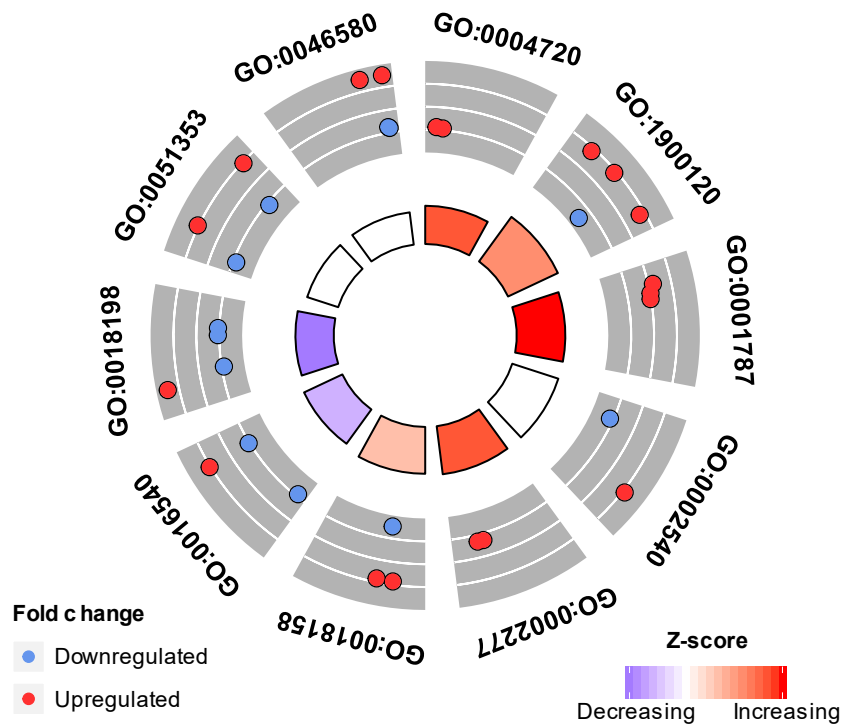
ID	Name	z-score	Hits	p-value
GO:0051384	response to glucocorticoid	2.7	17/163	9.03E-07
GO:0048545	response to steroid hormone	3.8	25/406	4.55E-05
GO:0019933	cAMP-mediated signaling	2.1	19/278	9.59E-05
GO:0071889	14-3-3 protein binding	1.6	6/31	1.44E-04
GO:0001823	mesonephros development	2.1	11/115	1.66E-04
GO:0046486	glycerolipid metabolic process	2.4	26/475	2.18E-04
GO:0046942	carboxylic acid transport	0.9	22/373	2.36E-04
GO:0045444	fat cell differentiation	2.7	17/251	2.45E-04
GO:0051592	response to calcium ion	1.4	13/163	2.74E-04
GO:0046943	carboxylic acid transmembrane transporter activity	0.3	13/158	3.19E-04

Figure 6.7. GO terms: Ethanol treatment in male mice. (a) Circle plot depicting differentially expressed genes (outer ring) overrepresented within top 10 GO terms by enrichment p-value. GO term enrichment p-value represented by inner circle bar size with fill color depicting z-score for overall direction of gene regulation. (b) Summary table for top 10 GO terms which includes gene hits out of total number of genes in terms.



ID	Name	z-score	Hits	p-value
GO:0014821	phasic smooth muscle contraction	-0.4	5/26	7.70E-05
GO:0003401	axis elongation	1.3	5/35	3.34E-04
GO:0016331	morphogenesis of embryonic epithelium	0.9	11/181	3.55E-04
GO:0008569	ATP-dependent microtubule motor activity, minus-end-directed	-1.0	4/20	4.19E-04
GO:0045927	positive regulation of growth	-0.3	15/331	7.71E-04
GO:2001182	regulation of interleukin-12 secretion	-0.6	3/11	7.86E-04
GO:0019933	cAMP-mediated signaling	0.3	13/278	1.28E-03
GO:0048638	regulation of developmental growth	-0.2	17/424	1.36E-03
GO:1901214	regulation of neuron death	2.5	16/394	1.64E-03
GO:0007171	activation of transmembrane receptor protein tyrosine kinase activity	-0.6	3/14	1.67E-03

Figure 6.8. GO terms: *Clic4* deletion in saline-treated male mice. (a) Circle plot depicting differentially expressed genes (outer ring) overrepresented within top 10 GO terms by enrichment p-value. GO term enrichment p-value represented by inner circle bar size with fill color depicting z-score for overall direction of gene regulation. (b) Summary table for top 10 GO terms which includes gene hits out of total number of genes in terms.



ID	Name	z-score	Hits	p-value
GO:1900120	regulation of receptor binding	1.0	4/28	9.78e-05
GO:0001787	natural killer cell proliferation	1.7	3/14	2.22e-04
GO:0002540	leukotriene production involved in inflammatory response	0.0	2/3	2.26e-04
GO:0002277	myeloid dendritic cell activation involved in immune response	1.4	2/3	2.26e-04
GO:0018158	protein oxidation	0.6	3/15	2.76e-04
GO:0016540	protein autoprocessing	-0.6	3/18	4.86e-04
GO:0018198	peptidyl-cysteine modification	-1.0	4/48	8.12e-04
GO:0004720	protein-lysine 6-oxidase activity	1.4	2/5	8.17e-04
GO:0051353	positive regulation of oxidoreductase activity	0.0	4/58	1.65e-03
GO:0046580	negative regulation of Ras protein signal transduction	0.0	4/58	1.65e-03

Figure 6.9. GO terms: *Clic4* deletion in ethanol-treated male mice. (a) Circle plot depicting differentially expressed genes (outer ring) overrepresented within top 10 GO terms by enrichment p-value. GO term enrichment p-value represented by inner circle bar size with fill color depicting z-score for overall direction of gene regulation. (b) Summary table for top 10 GO terms which includes gene hits out of total number of genes in terms.

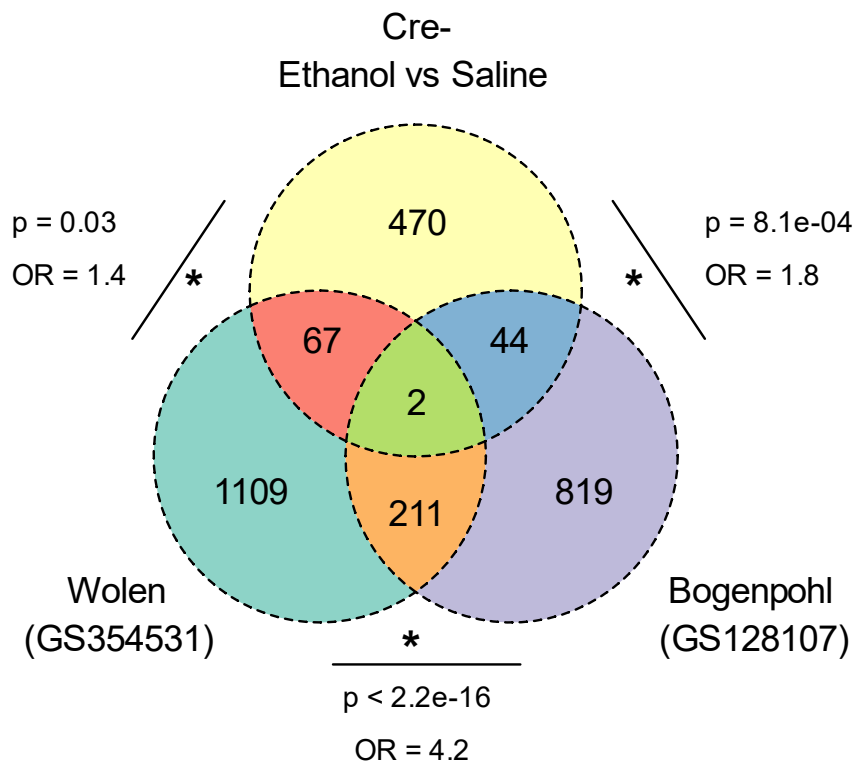


Figure 6.10. Overlap of ethanol-responsive gene sets. Venn diagram depicting overlap of ethanol-responsive genes in Cre- males and two independent published studies. These include ethanol-responsive genes from mouse PFC, VTA, and NAc following an acute dose of 1.8g/kg ethanol (GS354531) and macaque after 12 months of chronic voluntary ethanol drinking (GS128107). Overlap between gene sets was evaluated by Fisher's exact tests providing odds ratios (OR) and p-values.

(OR = 4.2, $p < 2.2 \times 10^{-16}$). Our high dose acute ethanol gene had 47 genes in common with the macaque study (OR = 1.8, $p = 8.1 \times 10^{-4}$) and 70 with the acute low dose treated mice (OR = 1.4, $p = 0.03$). Intriguingly, *Clic4* is one of only two genes regulated in all three of these diverse ethanol exposure studies, with the other being intermediate filament family orphan 2 (*Iffo2*).

6.4 Discussion

The overall goal of this study was to characterize expression patterns of *Clic4* RNA and protein in PFC, both basally and in response to ethanol exposure. This was the first study to examine CLIC4 protein expression by cell type and subcellular localization in brain and to show acute ethanol regulation of *Clic4* mRNA in B6 mouse PFC. Bioinformatic analysis of differentially expressed genes identified numerous biological processes associated with the molecular response to acute high dose ethanol and deletion of *Clic4*. Many of these process associations have been previously published but some are also novel. Taken together, the results from these studies provide a better foundation for interpreting the biological roles of *Clic4* and especially with regard to the molecular response to ethanol.

Confirming our initial hypothesis, CLIC4 was found to be highly expressed in CC1 and CNP+ myelinating oligodendrocytes in PFC. CLIC4 was also found to

be expressed on CNP⁺ myelin, suggesting it may have a role in myelin structure or function. Considering the lack of changes in MBP and PLP expression after *Clic4* knockout (Chapter 5), the latter is more likely. In neurons and astrocytes, CLIC4 was expressed in most but not all cells observed and in a sparse punctate pattern. CLIC4 was occasionally found to be expressed in a linear pattern adjacent to axonal cytoskeletal protein NFH, also potentially suggesting expression within myelin sheaths. Microglia showed distinct well-circumscribed regions of cytoplasm highly expressing CLIC4. This was detected in nearly all observed IBA1⁺ microglia. This expression pattern may represent phagocytic CLIC4-enriched oligodendrocyte debris or potentially functional expression of CLIC4 in microglial phagosomes. CLIC4 paralog CLIC1 has been observed in peripheral macrophages to associate with phagosomes where it promotes acidification (Jiang et al., 2012). Although not a direct aim of this study, CLIC4 was commonly detected in endothelial cells, which has been previously reported and CLIC4 has a known role in angiogenesis (Chalothorn et al., 2009; Ulmasov et al., 2009).

While *Clic4* mRNA has been shown to be ethanol-inducible in D2 mouse PFC, this has not been established in B6 mice. With qRT-PCR analysis, we identified significant upregulation of PFC *Clic4* following 4g/kg i.p. injection of ethanol in wild type B6 female mice but only a trend towards increased expression in males. However, our microarray analysis identified significant *Clic4*

upregulation in both male and female B6 Cre- mice following a 4g/kg i.p. injection of ethanol, confirming our initial hypothesis. Collectively, these results extend the current understanding of *Clic4*-regulation by acute ethanol in PFC to include B6 mice, which also exhibit *Clic4*-modulated drinking behavior (Chapter 5).

Clic4 has been associated with a myriad of diverse biological functions from ion channel (Littler et al., 2005) and enzymatic activity (Al Khamici et al., 2015) to membrane tracking (Chou et al., 2016) and apoptosis (Suh et al., 2004). However, the mechanisms and molecular partners through which *Clic4* carries out these functions are not well understood. Furthermore, the process by which *Clic4* modulates ethanol sedation sensitivity (Bhandari et al., 2012) and drinking behavior (Chapter 5) is also not known. Considering its rapid induction following acute ethanol, we speculated that *Clic4* plays an influential and unique role in the brain's molecular response to ethanol exposure. To gain insight into these processes, we performed microarray gene expression profiling of *Clic4* deletion in PFC both in the presence and absence of acute ethanol. Applying what we learned of CLIC4 expression characteristics in PFC, we specifically targeted oligodendrocytes for *Clic4* deletion. We identified a large set of ethanol-responsive genes in Cre- mice which was enriched for genes involved in glucocorticoid and steroid hormone signaling. This is an interesting finding considering the well-established associations between glucocorticoid signaling, HPA axis

dysregulation, and the risk for AUD development and relapse (Blaine & Sinha, 2017; Costin et al., 2013; Kerns et al., 2005). Further highlighting this connection, glucocorticoid receptor antagonist Mifepristone has shown promising effects in reducing alcohol consumption in animal models (Vendruscolo et al., 2015) and is currently undergoing clinical trials in humans (“Mifepristone for the Prevention of Relapses of Alcohol Drinking,” 2004). Integrative genomic analysis of this gene set with published gene sets representing regulation by low dose acute ethanol in mice and chronic ethanol drinking in macaques showed significant overlap. This not only replicates our findings, but also provides evidence that common sets of genes respond to differing ethanol exposures, even across species.

In saline-treated animals, *Clic4* deletion altered expression of genes overrepresented in cytoskeleton, morphogenesis, and growth-related processes. This is noteworthy considering known associations of *Clic4* with cytoskeleton (Elisabetta Argenzio et al., 2018; Ponsioen et al., 2009) and involvement in membrane reorganization and tubulogenesis (Chou et al., 2016; Ulmasov et al., 2009). *Clic4* deletion also led to a substantial upregulation of genes involved in regulating neuron cell death, a GO term that includes many genes related to apoptosis. This is noteworthy because *Cic4* is known to be involved in cell stress and apoptotic pathways (Fernandez-Salas et al., 2002; Suh et al., 2004; Xu et al., 2013).

Ethanol-treated animals displayed a unique set of differentially expressed genes responding to *Clic4* deletion that overlapped only minimally with those responding to deletion after saline-treatment. These genes were enriched for biological processes associated with inflammation and innate immunity as well as redox processes. Considering the former, *Clic4* has published roles in both, acting in an incompletely understood way to positively regulate inflammation (He et al., 2011; Tang et al., 2017). Enrichment of redox-related processes is also significant considering CLIC4 undergoes oxidation and reduction-triggered conformational changes (Littler et al., 2005) and acts as an oxidoreductase enzyme *in vitro* (Al Khamici et al., 2015). Another interesting connection, our microarray analysis of *Drosophila Clic* knockdown identified an enrichment of genes in the similar GO term, Oxidation-Reduction Processes (**Chapter 4**).

This study provides novel characterization of CLIC4 cellular and subcellular expression in PFC and evidence for acute ethanol-induced upregulation of *Clic4* in B6 mouse PFC. Bioinformatic analysis of oligodendrocyte-specific *Clic4* deletion identified many known biological processes previously associated with *Clic4* including redox activity, inflammation, cytoskeleton, and apoptosis. The novel pathways and genes identified here as regulated by *Clic4* deletion and ethanol exposure offer important new insight into the interactome surrounding *Clic4*. In summary, this study provides further evidence for an

involvement of *Clic4* in the brain's molecular response to ethanol and identifies several potential biological mechanisms through which it may be influencing ethanol-related behavior.

Supplemental Tables:

Table S6.1: Differentially Expressed Genes

Table S6.2: Enriched Gene Ontology Terms

Table S6.3: GeneWeaver Ethanol Gene Sets

Chapter 7

Conclusions, Discussion, and Future

Directions

7.1 Ethanol and the Synaptic Transcriptome

AUD is a complex neuropsychiatric disorder with a 48-58% genetic risk component (Prescott & Kendler, 1999). With a lifetime prevalence of 29% (Grant et al., 2015) and only moderately effective available treatments (Jonas et al., 2014), there is a strong interest in researching the molecular mechanisms underlying development of AUD. The hunt for an “alcoholism gene” has identified hundreds of genetic variants, each representing only a small portion of the disorder’s overall genetic risk (Deak et al., 2019; Tawa et al., 2016). This large list of candidate genes is lengthened further by thousands of ethanol-responsive genes identified in transcriptomic studies from human post-mortem tissue and animal models of AUD (Farris et al., 2010; Kerns et al., 2005; Liu et al., 2006; Wolen et al., 2012). With

an almost overwhelming number of potential gene targets to explore, a next major task for researchers is to distill them down to the most reproducible and biologically meaningful genes in context of our understanding of AUD pathophysiology. The most promising of these candidate genes can then be taken to animal models of AUD for evaluation of targeted pharmacotherapies or genetic manipulations.

This dissertation work began by taking a closer look at the synaptic transcriptome of frontal cortex neurons following acute and repeated intermittent ethanol exposures. Our goal was to identify differential gene expression and splicing events specifically associated with synaptic reorganization during ethanol-induced locomotor sensitization. Ethanol sensitization produced a more substantial differential gene expression response compared to acute ethanol and this was even more so the case with differential exon usage. Synaptic differential exon usage resulting from ethanol sensitization was enriched for RNA translation, RNA processing, and cellular energetics processes, which is consistent with sensitization-induced synaptic reorganization. As a possible mechanism for this shift in synaptic splice variants, we identified an enrichment of RNA binding protein targets and specific RNA-binding sequence motifs among our differential exon usage. From our findings, we hypothesize that repeated intermittent ethanol exposure, which induces locomotor sensitization, is mediating adaptive changes

in frontal cortex circuitry by way of specific synaptic reorganization events. An important follow up question this leaves is whether ethanol locomotor sensitization and associated synaptic remodeling can be blocked by temporary inhibition of specific molecular chaperones or RNA binding proteins identified in this study, such as FMRP.

7.2 *Clic4* in Ethanol and Anxiety-related Behavior

Bhandari et al. showed that expression modulation of *Clic4* and invertebrate orthologs alters sensitivity to ethanol sedation (Bhandari et al., 2012). However, the role of *Clic4* in ethanol consumption had not been evaluated prior to the current set of studies. Using a 3BC-IEA paradigm, we found that global oligodendrocyte-specific deletion of *Clic4* in B6 mice resulted in an increase in total ethanol and 15% ethanol intake in females and an increase in 15% choice over 30% ethanol in both sexes (**Table 7.1**). *Clic4* deletion also resulted in altered anxiety-like behavior, with males spending more time in the light in an untreated light/dark box task and females spending more time in the light after ethanol pretreatment in the light/dark box task.

The behavioral effects of global deletion of *Clic4* in oligodendrocytes were not reproduced by mPFC-specific *Clic4* deletion in oligodendrocytes. With this narrowing of regional specificity, anxiety-like behaviors were unaltered and

Behavior	Sex	AAV8-MBP-Cre	Plp-Cre-ER ^T
Drinking	Female	-	↑ total intake ↑ 15%/choice
Drinking	Male	↓ total intake ↓ 15%/choice	↑ 15% choice
Sensitivity	Female	-	-
Sensitivity	Male	-	-
Anxiety	Female	-	↓ anxiety (EIA)
Anxiety	Male	-	↓ anxiety (light/dark box)

Table 7.1: Summary of behavioral changes following *Clic4*-deletion. Overview of behavioral changes resulting from *Clic4* deletion in oligodendrocytes either broadly (Plp-Cre-ER^T) or specifically in mPFC (AAV8-MBP-Cre). Behaviors evaluated include chronic ethanol intake in a 3BC-IEA task (Drinking), sensitivity to ethanol sedation in a LORR task (Sensitivity), and anxiety-like behavior (Anxiety) in a light/dark box task or during ethanol-induced anxiolysis (EIA). Arrows indicate direction of behavioral effect when comparing *Clic4*-deleted animals to controls.

ethanol consumption behaviors were altered in a different manner, such that only males were affected and displayed lower ethanol consumption. This lack of concordance between the deletion approaches is highly suggestive of regional differences in function of *Clic4*. Considering the low overall expression of *Clic4* in brain with patterns of high regional expression (V. Padmakumar et al., 2014), the contributions of oligodendrocyte *Clic4* to ethanol drinking and anxiety-like behavior identified in the global deletions would appear to be mediated in regions other than mPFC. The mPFC was chosen as an initial region of interest due to the observed regulation of *Clic4* by acute ethanol in that brain region (Kerns 2005), and the altered ethanol sedation sensitivity of mPFC *Clic4* overexpressing D2 mice (Bhandari et al., 2012). However, ethanol consumption and anxiety-like behaviors are linked to a number of other brain regions including NAC, VTA, hippocampus, and amygdala (Chapter 2). Future studies directed at further characterizing the role of *Clic4* in ethanol-related behaviors might look in these brain areas, in particular the VTA where *Clic4* has shown ethanol-regulation in dopaminergic neurons (Marballi et al., 2016), or hippocampus where *Clic4* has been identified as part of an ethanol-responsive gene network (Farris et al., 2015). Another potentially interesting area to evaluate, the lateral septal complex shows high regional expression of *Clic4* on *in situ* hybridization (Lein et al., 2007; V. Padmakumar et al., 2014) and ethanol regulation of *Clic4* mRNA (Bogenpohl,

unpublished communication). The lateral septal complex is a component of the extended basal ganglia, is interconnected with the mesolimbic reward pathway, and has been reported to be involved in regulation of ethanol consumption (Ryabinin et al., 2008; Talishinsky & Rosen, 2012).

7.3 CLIC4 Protein Expression in PFC

Another major aim of this dissertation was to characterize the cellular expression profile of CLIC4 in mouse PFC, where it has previously been shown to be regulated by ethanol (Bhandari et al., 2012; Kerns et al., 2005) and to modulate ethanol sedation sensitivity (Bhandari et al., 2012). CLIC4 was observed incidentally but frequently in endothelial cells, which supports previous reports of its role in angiogenesis (Chalothorn et al., 2009; Ulmasov et al., 2009). CLIC4 was also robustly expressed in mature oligodendrocytes and along myelin (**Table 7.2**), which was previously suspected based on *in situ* hybridization data (V. Padmakumar et al., 2014). Microglia showed a unique pattern of expression localized to discrete cytoplasmic regions, possibly indicating phagosomes. In contrast, neurons and astrocytes displayed sparse punctate expression of CLIC4, which was not present in all cells observed. These co-localization studies of CLIC4 are the first to assess cell type expression within the brain. However, they are largely qualitative and future studies should seek to quantify the relative

Cell Type	Compartment	Markers	Expression
Neurons	Nucleus	NEUN, DAPI	No
Neurons	Cytosol	NEUN, CAMKII α	Yes
Neurons	Axon	NF-H	Yes
Oligodendrocytes	Nucleus	DAPI	Yes
Oligodendrocytes	Cytosol	CC1	Yes
Oligodendrocytes	Myelin	CNP	Yes
Oligodendrocytes	Plasma membrane	CNP	No
Astrocytes	Nucleus	DAPI	Yes
Astrocytes	Cytoskeleton	GFAP	No
Astrocytes	Cytosol	GLUL, GFAP	Yes
Microglia	Nucleus	DAPI	No
Microglia	Cytoplasm	IBA1 (interior to)	Yes
Microglia	Plasma membrane	IBA1	No

Table 7.2: Summary of CLIC4 protein expression in PFC. Expression characteristics of CLIC4 protein in wild type B6 mouse PFC identified through immunofluorescence and confocal microscopy techniques.

differences in CLIC4 expression between cell types using quantitative immunofluorescence or flow cytometry techniques. Considering not all neurons and astrocytes displayed CLIC4 expression, sub-classes of these cells, such as excitatory versus inhibitory neurons, may show differing expression patterns.

Co-localization of CLIC4 with CNP⁺ myelin and adjacent to NFH⁺ axons suggests CLIC4 may be expressed and therefore have a function in myelin. However, the two most abundant myelin proteins, MBP and PLP, were not found to be altered after *Clic4* deletion in oligodendrocytes, suggesting CLIC4 is not likely essential to overall myelin stability. However, this does not rule out ultrastructural changes which could affect myelin compactness, cytoplasmic channels, and axo-myelinic synapses. This possibility could be evaluated in future studies utilizing electron microscopy and specifically recent advances cryo-electron microscopy, which better preserve aqueous uncompact myelin domains (Snaidero et al., 2017).

If *Clic4* is altering ethanol-related behaviors through oligodendrocytes, but not by affecting abundance of myelin, it may instead be influencing oligodendrocyte trophic support of ensheathed axons. Considering the potentially large distances extending between axon segments and their respective neuronal cell bodies, distally projecting axons have an uphill battle in order to maintain their metabolic requirements (Nave, 2010). While previously viewed as a highly

compact and inert insulating structure, myelin is now considered to be structurally dynamic with uncompacted cytoplasmic channels connecting the axo-myelinic space in the inner tongue of the myelin sheath to the oligodendrocyte cell body (Michalski & Kothary, 2015; Snaidero et al., 2014, 2017). Oligodendrocytes have been reported to shuttle glycolytic metabolites, RNA, and proteins across the axo-myelinic space to support the metabolism and overall health of the underlying axon (Fünfschilling et al., 2012; Nave, 2010; Saab et al., 2016; Snaidero et al., 2017). The importance of this relationship is highlighted by the effects of disrupting myelin structure, which can directly lead to degeneration of axons (Griffiths et al., 1998).

Having observed that CLIC4 is expressed adjacent to NFH+ axons in CNP+ regions of myelin, it is possible that CLIC4 may be localized to uncompacted myelin supporting cytoskeletal dynamics or localizing to the axo-myelinic synapse itself. Potential evidence for the former hypothesis comes from published associations of *Clic4* with membrane dynamics and cytoskeleton remodeling (E. Argenzio et al., 2014; Ponsioen et al., 2009), which could be relevant to cytoplasmic channel patency, which is otherwise maintained under the antagonistic interplay of MBP and CNP (Snaidero et al., 2017). In terms of the latter hypothesis, *Clic4* has known roles in membrane trafficking of vesicles and receptors (Chou et al., 2016; Maeda et al., 2008), which may provide support for signaling and transport at the

axo-myelinic synapse. While these hypotheses are highly speculative at present, an examination of CLIC subcellular localization within myelin ultrastructure through electron microscopy could resolve these questions.

7.4 *Clic4*, Acute Ethanol, and the Transcriptome

Our transcriptomic analyses provide novel characterization of the molecular response to high dose acute ethanol in Cre⁺ and Cre⁻ *Clic4*-floxed mice. Our bioinformatic analyses identified several previously reported biological processes responding to ethanol treatment, including oxidation-reduction processes, inflammation and innate immunity, cytoskeletal processes, and apoptosis. These findings bring to light another possible mechanism by which *Clic4* may be modulating ethanol consumption and that is through its associated roles in oxidation-reduction processes. This connection was noted both in the *Drosophila Clic* knockdown (Chapter 4) and the ethanol-treated mouse *Clic4* knockdown microarray (Chapter 6) analyses. Currently not well understood, *Clic4* has been reported in a number of oxidation-reduction related processes including oxidoreductase activity (Al Khamici et al., 2015). It is possible that *Clic4* has an important role in buffering the response of either myelin or oligodendrocyte cell bodies to ROS damage, and modulation of its expression either experimentally or through human genetic variation, alters ROS vulnerability. This vulnerability may

not be outright lethal to oligodendrocytes, as suggested by our Western blot data showing consistent MBP and PLP expression for 5 months following *Clic4* deletion, but it may be sufficient to increase cellular stress and reduce effectivity of oligodendrocyte trophic support to myelin and underlying axons. This hypothesis is supported by our *Clic* knockdown *Drosophila* experiments, which under hyperoxic conditions, showed increased sensitivity to ethanol sedation. A potentially useful follow-up experiment would be to provide oligodendrocyte-specific *Clic4* knockout mice an oxidative stressor, such as paraquat, and evaluate their ethanol consumption.

7.5 Concluding Remarks

The studies presented in this dissertation attempt to shed light on the molecular responses and adaptations that follow acute ethanol exposure in brain, and particularly how these processes are influenced by *Clic4*. It is clear from our findings that oligodendrocyte *Clic4* is an important modulator of ethanol consumption and anxiety-like behavior, although the exact brain regions where these effects are mediated remain to be determined. Our findings suggest oxidation-reduction related processes may be mechanistic, but future studies we will be needed for confirmation. As an acute ethanol-regulated gene and modulator of ethanol consumption and sedation sensitivity, *Clic4* represents an

important candidate gene for investigating the biological mechanisms underlying the transition from casual ethanol consumption to AUD. Collectively, this dissertation has provided behavioral and gene expression characterization of acute and repeated ethanol exposures while also deepening our understanding of the candidate gene *Clic4*.

References

- Aggleton, J. P., Burton, M. J., & Passingham, R. E. (1980). Cortical and subcortical afferents to the amygdala of the rhesus monkey (*Macaca mulatta*). *Brain Research*, 190(2), 347–368. [https://doi.org/10.1016/0006-8993\(80\)90279-6](https://doi.org/10.1016/0006-8993(80)90279-6)
- Al Khamici, H., Brown, L. J., Hossain, K. R., Hudson, A. L., Sinclair-Burton, A. A., Ng, J. P. M., Daniel, E. L., Hare, J. E., Cornell, B. A., Curmi, P. M. G., Davey, M. W., & Valenzuela, S. M. (2015). Members of the Chloride Intracellular Ion Channel Protein Family Demonstrate Glutaredoxin-Like Enzymatic Activity. *PLoS ONE*, 10(1), e115699. <https://doi.org/10.1371/journal.pone.0115699>
- American Psychiatric Association. (2013). Diagnostic and Statistical Manual of Mental Disorders: DSM-V. In *American Psychiatric Association*. <https://doi.org/10.1176/appi.books.9780890425596.744053>
- An, X., Bandler, R., Ongür, D., & Price, J. L. (1998). Prefrontal cortical projections to longitudinal columns in the midbrain periaqueductal gray in macaque monkeys. *The Journal of Comparative Neurology*, 401(4), 455–479. [https://doi.org/10.1002/\(SICI\)1096-9861\(19981130\)401:4<455::AID-CNE3>3.0.CO;2-6](https://doi.org/10.1002/(SICI)1096-9861(19981130)401:4<455::AID-CNE3>3.0.CO;2-6)
- Anders, S., Reyes, A., & Huber, W. (2012). Detecting differential usage of exons from RNA-seq data. *Genome Research*, 22(10), 2008–2017. <https://doi.org/10.1101/gr.133744.111>
- Anton, R. F., O'Malley, S. S., Ciraulo, D. A., Cisler, R. A., Couper, D., Donovan, D. M., Gastfriend, D. R., Hosking, J. D., Johnson, B. A., LoCastro, J. S., Longabaugh, R., Mason, B. J., Mattson, M. E., Miller, W. R., Pettinati, H. M., Randall, C. L., Swift, R., Weiss, R. D., Williams, L. D., ... COMBINE Study Research Group, for the. (2006). Combined Pharmacotherapies and Behavioral Interventions for Alcohol Dependence. *Jama*, 295(17), 2003. <https://doi.org/10.1001/jama.295.17.2003>
- Argenzio, E., Margadant, C., Leyton-Puig, D., Janssen, H., Jalink, K., Sonnenberg, A., & Moolenaar, W. H. (2014). CLIC4 regulates cell adhesion and α 1 integrin trafficking. *Journal of Cell Science*, 127(24), 5189–5203.

<https://doi.org/10.1242/jcs.150623>

- Argenzio, Elisabetta, Klarenbeek, J., Kedziora, K. M., Nahidiazar, L., Isogai, T., Perrakis, A., Jalink, K., Moolenaar, W. H., & Innocenti, M. (2018). Profilin 1 binding couples chloride intracellular channel protein CLIC4 to RhoA–mDia2 signaling and filopodium formation. In *Journal of Biological Chemistry*. <https://doi.org/10.1074/jbc.RA118.002779>
- Bailey, T. L., Boden, M., Buske, F. A., Frith, M., Grant, C. E., Clementi, L., Ren, J., Li, W. W., & Noble, W. S. (2009). MEME Suite: Tools for motif discovery and searching. *Nucleic Acids Research*, 37(SUPPL. 2). <https://doi.org/10.1093/nar/gkp335>
- Baker, E. J., Jay, J. J., Bubier, J. A., Langston, M. A., & Chesler, E. J. (2012). GeneWeaver: A web-based system for integrative functional genomics. *Nucleic Acids Research*. <https://doi.org/10.1093/nar/gkr968>
- Ballenger, J. C., & Post, R. M. (1978). Kindling as a model for alcohol withdrawal syndromes. *British Journal of Psychiatry*, 133(7), 1–14. <https://doi.org/10.1192/bjp.133.1.1>
- Barbas, H., & de Olmos, J. (1990). Projections from the amygdala to basoventral and mediodorsal prefrontal regions in the rhesus monkey. *Journal of Comparative Neurology*, 300(4), 549–571. <https://doi.org/10.1002/cne.903000409>
- Barco, A., Alarcon, J. M., & Kandel, E. R. (2002). Expression of constitutively active CREB protein facilitates the late phase of long-term potentiation by enhancing synaptic capture. *Cell*, 108(5), 689–703. <https://doi.org/S0092867402006578> [pii]
- Bechara, A. (2005). Decision making, impulse control and loss of willpower to resist drugs: a neurocognitive perspective. *Nature Neuroscience*, 8(11), 1458–1463. <https://doi.org/10.1038/nn1584>
- Bechara, A., Damasio, A. R., Damasio, H., & Anderson, S. W. (1994). Insensitivity to future consequences following damage to human prefrontal cortex. *Cognition*, 50(1–3), 7–15. [https://doi.org/10.1016/0010-0277\(94\)90018-3](https://doi.org/10.1016/0010-0277(94)90018-3)
- Becker, H. C., & Ron, D. (2014). Animal models of excessive alcohol consumption:

- Recent advances and future challenges. *Alcohol*, 48(3), 205–208. <https://doi.org/10.1016/j.alcohol.2014.04.001>
- Becker, J. B., & Koob, G. F. (2016). Sex Differences in Animal Models: Focus on Addiction. *Pharmacological Reviews*, 68(2), 242–263. <https://doi.org/10.1124/pr.115.011163>
- Beier, K. T., Steinberg, E. E., Deloach, K. E., Xie, S., Miyamichi, K., Schwarz, L., Gao, X. J., Kremer, E. J., Malenka, R. C., & Luo, L. (2015). Circuit Architecture of VTA Dopamine Neurons Revealed by Systematic Input-Output Mapping. *Cell*, 162(3), 622–634. <https://doi.org/10.1016/j.cell.2015.07.015>
- Belknap, J. K., Crabbe, J. C., & Young, E. R. (1993). Voluntary consumption of ethanol in 15 inbred mouse strains. *Psychopharmacology*. <https://doi.org/10.1007/BF02244901>
- Bengtsson, S. L., Nagy, Z., Skare, S., Forsman, L., Forsberg, H., & Ullén, F. (2005). Extensive piano practicing has regionally specific effects on white matter development. *Nature Neuroscience*, 8(9), 1148–1150. <https://doi.org/10.1038/nn1516>
- Benjamini, Y., & Hochberg, Y. (1995). Controlling the False Discovery Rate: A Practical and Powerful Approach to Multiple Testing. *Journal of the Royal Statistical Society: Series B (Methodological)*. <https://doi.org/10.1111/j.2517-6161.1995.tb02031.x>
- Bergman, H., Engelbrektson, K., Fransson, A., Herlitz, K., Hindmarsh, T., & Neiman, J. (1998). Alcohol-induced cognitive impairment is reversible. Neuropsychological tests but not MRT show improvement after abstinence. *Lakartidningen*, 95(39), 4228,4231-4236. <http://www.ncbi.nlm.nih.gov/pubmed/9785771>
- Berry, K. L., Bülow, H. E., Hall, D. H., & Hobert, O. (2003). A *C. elegans* CLIC-like Protein Required for Intracellular Tube Formation and Maintenance. *Science*, 302(5653), 2134–2137. <https://doi.org/10.1126/science.1087667>
- Berryman, M. A., & Goldenring, J. R. (2003). CLIC4 Is Enriched at Cell-Cell Junctions and Colocalizes With AKAP350 at the Centrosome and Midbody of Cultured Mammalian Cells. *Cell Motility and the Cytoskeleton*.

<https://doi.org/10.1002/cm.10141>

- Bhandari, P., Hill, J. S., Farris, S. P., Costin, B., Martin, I., Chan, C.-L., Alaimo, J. T., Bettinger, J. C., Davies, A. G., Miles, M. F., & Grotewiel, M. (2012). Chloride intracellular channels modulate acute ethanol behaviors in *Drosophila*, *Caenorhabditis elegans* and mice. *Genes, Brain and Behavior*, *11*(4), 387–397. <https://doi.org/10.1111/j.1601-183X.2012.00765.x>
- Bickel, W. K., Jarmolowicz, D. P., Mueller, E. T., Gatchalian, K. M., & McClure, S. M. (2012). Are executive function and impulsivity antipodes? A conceptual reconstruction with special reference to addiction. In *Psychopharmacology* (Vol. 221, Issue 3, pp. 361–387). <https://doi.org/10.1007/s00213-012-2689-x>
- Blaine, S. K., & Sinha, R. (2017). Alcohol, stress, and glucocorticoids: From risk to dependence and relapse in alcohol use disorders. In *Neuropharmacology*. <https://doi.org/10.1016/j.neuropharm.2017.01.037>
- Board, P. G., Coggan, M., Chelvanayagam, G., Easteal, S., Jermiin, L. S., Schulte, G. K., Danley, D. E., Hoth, L. R., Griffor, M. C., Kamath, A. V, Rosner, M. H., Chrnyk, B. A., Perregaux, D. E., Gabel, C. A., Geoghegan, K. F., & Pandit, J. (2000). Identification, characterization, and crystal structure of the omega class glutathione transferases. *Journal of Biological Chemistry*, *275*(32), 24798–24806. <https://doi.org/10.1074/jbc.M001706200>
- Bohman, S., Matsumoto, T., Suh, K., Dimberg, A., Jakobsson, L., Yuspa, S., & Claesson-Welsh, L. (2005). Proteomic analysis of vascular endothelial growth factor-induced endothelial cell differentiation reveals a role for chloride intracellular channel 4 (CLIC4) in tubular morphogenesis. *Journal of Biological Chemistry*, *280*(51), 42397–42404. <https://doi.org/10.1074/jbc.M506724200>
- Bramham, C. R., & Wells, D. G. (2007). Dendritic mRNA: transport, translation and function. *Nat Rev Neurosci*, *8*(10), 776–789. <https://doi.org/nrn2150> [pii]10.1038/nrn2150
- Brenhouse, H. C., Sonntag, K. C., & Andersen, S. L. (2008). Transient D1 dopamine receptor expression on prefrontal cortex projection neurons: relationship to enhanced motivational salience of drug cues in adolescence. *J Neurosci*, *28*(10), 2375–2382. <https://doi.org/10.1523/JNEUROSCI.5064-07.2008>

- Brodmann, K. (1910). Vergleichende Lokalisationslehre der Grosshirnrinde. *The Journal of Nervous and Mental Disease*, 37(12), 783–784. <https://doi.org/10.1097/00005053-191012000-00013>
- Brog, J. S., Salyapongse, A., Deutch, A. Y., & Zahm, D. S. (1993). The patterns of afferent innervation of the core and shell in the “Accumbens” part of the rat ventral striatum: Immunohistochemical detection of retrogradely transported fluoro-gold. *Journal of Comparative Neurology*, 338(2), 255–278. <https://doi.org/10.1002/cne.903380209>
- Burgin, K. E., Waxham, M. N., Rickling, S., Westgate, S. A., Mobley, W. C., & Kelly, P. T. (1990). In situ hybridization histochemistry of Ca²⁺/calmodulin-dependent protein kinase in developing rat brain. *J Neurosci*, 10(6), 1788–1798. <http://www.ncbi.nlm.nih.gov/pubmed/2162385>
- Cajigas, I. J., Tushev, G., Will, T. J., tom Dieck, S., Fuerst, N., & Schuman, E. M. (2012). The local transcriptome in the synaptic neuropil revealed by deep sequencing and high-resolution imaging. *Neuron*, 74(3), 453–466. <https://doi.org/10.1016/j.neuron.2012.02.036>S0896-6273(12)00286-3 [pii]
- Camarini, R., & Hodge, C. W. (2004). Ethanol preexposure increases ethanol self-administration in C57BL/6J and DBA/2J mice. *Pharmacol Biochem Behav*, 79(4), 623–632. [https://doi.org/S0091-3057\(04\)00302-8](https://doi.org/S0091-3057(04)00302-8) [pii]10.1016/j.pbb.2004.09.012
- Carbon, S., Douglass, E., Dunn, N., Good, B., Harris, N. L., Lewis, S. E., Mungall, C. J., Basu, S., Chisholm, R. L., Dodson, R. J., Hartline, E., Fey, P., Thomas, P. D., Albou, L. P., Ebert, D., Kesling, M. J., Mi, H., Muruganujan, A., Huang, X., ... Westerfield, M. (2019). The Gene Ontology Resource: 20 years and still GOing strong. *Nucleic Acids Research*. <https://doi.org/10.1093/nar/gky1055>
- Carlezon, W. A., & Thomas, M. J. (2009). Biological substrates of reward and aversion: A nucleus accumbens activity hypothesis. *Neuropharmacology*, 56(SUPPL. 1), 122–132. <https://doi.org/10.1016/j.neuropharm.2008.06.075>
- Carlsen, J. (1988). Immunocytochemical localization of glutamate decarboxylase in the rat basolateral amygdaloid nucleus, with special reference to GABAergic innervation of amygdalostriatal projection neurons. *Journal of Comparative Neurology*, 273(4), 513–526. <https://doi.org/10.1002/cne.902730407>

- Carmichael, S. T., & Price, J. L. (1995). Limbic connections of the orbital and medial prefrontal cortex in macaque monkeys. *The Journal of Comparative Neurology*, 363(4), 615–641. <https://doi.org/10.1002/cne.903630408>
- Carpenter-Hyland, E. P., & Chandler, L. J. (2006). Homeostatic plasticity during alcohol exposure promotes enlargement of dendritic spines. *Eur J Neurosci*, 24(12), 3496–3506. <https://doi.org/EJN5247> [pii]10.1111/j.1460-9568.2006.05247.x
- Carvalho, B. S., & Irizarry, R. A. (2010). A framework for oligonucleotide microarray preprocessing. *Bioinformatics*. <https://doi.org/10.1093/bioinformatics/btq431>
- Casadio, A., Martin, K. C., Giustetto, M., Zhu, H., Chen, M., Bartsch, D., Bailey, C. H., & Kandel, E. R. (1999). A transient, neuron-wide form of CREB-mediated long-term facilitation can be stabilized at specific synapses by local protein synthesis. *Cell*, 99(2), 221–237. [https://doi.org/S0092-8674\(00\)81653-0](https://doi.org/S0092-8674(00)81653-0) [pii]
- Chalothorn, D., Zhang, H., Smith, J. E., Edwards, J. C., & Faber, J. E. (2009). Chloride Intracellular Channel-4 Is a Determinant of Native Collateral Formation in Skeletal Muscle and Brain. *Circulation Research*, 105(1), 89–98. <https://doi.org/10.1161/CIRCRESAHA.109.197145>
- Chan, R. F., Lewellyn, L., Deloyht, J. M., Sennett, K., Coffman, S., Hewitt, M., Bettinger, J. C., Warrick, J. M., & Grotewiel, M. (2014). Contrasting influences of Drosophila white/mini-white on ethanol sensitivity in two different behavioral assays. *Alcoholism: Clinical and Experimental Research*, 38(6), 1582–1593. <https://doi.org/10.1111/acer.12421>
- Chanraud, S., Martelli, C., Delain, F., Kostogianni, N., Douaud, G., Aubin, H.-J., Reynaud, M., & Martinot, J.-L. (2007). Brain Morphometry and Cognitive Performance in Detoxified Alcohol-Dependents with Preserved Psychosocial Functioning. *Neuropsychopharmacology*, 32(2), 429–438. <https://doi.org/10.1038/sj.npp.1301219>
- Chanraud, S., Pitel, A. L., Rohlfing, T., Pfefferbaum, A., & Sullivan, E. V. (2010). Dual tasking and working memory in alcoholism: relation to frontocerebellar circuitry. *Neuropsychopharmacology: Official Publication of the American College of Neuropsychopharmacology*, 35(9), 1868–1878.

<https://doi.org/10.1038/npp.2010.56>

- Chavkin, C., James, I. F., & Goldstein, A. (1982). Dynorphin is a specific endogenous ligand of the κ opioid receptor. *Pain*, 14(2), 201. [https://doi.org/10.1016/0304-3959\(82\)90120-8](https://doi.org/10.1016/0304-3959(82)90120-8)
- Chen, J., Bardes, E. E., Aronow, B. J., & Jegga, A. G. (2009). ToppGene Suite for gene list enrichment analysis and candidate gene prioritization. *Nucleic Acids Research*, 37(SUPPL. 2). <https://doi.org/10.1093/nar/gkp427>
- Chicurel, M. E., Terrian, D. M., & Potter, H. (1993). mRNA at the synapse: analysis of a synaptosomal preparation enriched in hippocampal dendritic spines. *J Neurosci*, 13(9), 4054–4063. <http://www.ncbi.nlm.nih.gov/pubmed/8396172>
- Chou, S., Hsu, K., Otsu, W., Hsu, Y., Luo, Y., Yeh, C., Shehab, S. S., Chen, J., Shieh, V., He, G., Marean, M. B., Felsen, D., Ding, A., & Poppas, D. P. (2016). CLIC4 regulates apical exocytosis and renal tube luminogenesis through retromer- and actin-mediated endocytic trafficking. *Nature Communications*, 7, 1–14. <https://doi.org/10.1038/ncomms10412>
- Ciccocioppo, R., Angeletti, S., & Weiss, F. (2001). Long-lasting resistance to extinction of response reinstatement induced by ethanol-related stimuli: role of genetic ethanol preference. *Alcoholism, Clinical and Experimental Research*, 25(10), 1414–1419. <https://doi.org/10.1111/j.1530-0277.2001.tb02141.x>
- Clarke, T. K., Adams, M. J., Davies, G., Howard, D. M., Hall, L. S., Padmanabhan, S., Murray, A. D., Smith, B. H., Campbell, A., Hayward, C., Porteous, D. J., Deary, I. J., & McIntosh, A. M. (2017). Genome-wide association study of alcohol consumption and genetic overlap with other health-related traits in UK biobank (N=112117). *Molecular Psychiatry*. <https://doi.org/10.1038/mp.2017.153>
- Cook, K. B., Kazan, H., Zuberi, K., Morris, Q., & Hughes, T. R. (2011). RBPDB: A database of RNA-binding specificities. *Nucleic Acids Research*, 39(SUPPL. 1). <https://doi.org/10.1093/nar/gkq1069>
- Costin, B. N., Dever, S. M., & Miles, M. F. (2013). Ethanol regulation of serum glucocorticoid kinase 1 expression in DBA2/J mouse prefrontal cortex. *PLoS One*, 8(8), e72979. <https://doi.org/10.1371/journal.pone.0072979>

- Crews, F. T., & Boettiger, C. A. (2009). Impulsivity, frontal lobes and risk for addiction. *Pharmacology Biochemistry and Behavior*, 93(3), 237–247. <https://doi.org/10.1016/j.pbb.2009.04.018>
- Cruz-Martin, A., Crespo, M., & Portera-Cailliau, C. (2012). Glutamate induces the elongation of early dendritic protrusions via mGluRs in wild type mice, but not in fragile X mice. *PLoS One*, 7(2), e32446. <https://doi.org/10.1371/journal.pone.0032446>
- D'Souza, M. S., Ikegami, A., Olsen, C. M., & Duvauchelle, C. L. (2003). Chronic D1 agonist and ethanol coadministration facilitate ethanol-mediated behaviors. *Pharmacology Biochemistry and Behavior*, 76(2), 335–342. <https://doi.org/10.1016/j.pbb.2003.08.004>
- Darnell, J. C., Van Driesche, S. J., Zhang, C., Hung, K. Y. S., Mele, A., Fraser, C. E., Stone, E. F., Chen, C., Fak, J. J., Chi, S. W., Licatalosi, D. D., Richter, J. D., & Darnell, R. B. (2011). FMRP stalls ribosomal translocation on mRNAs linked to synaptic function and autism. *Cell*, 146(2), 247–261. <https://doi.org/10.1016/j.cell.2011.06.013>
- Deak, J. D., Miller, A. P., & Gizer, I. R. (2019). Genetics of alcohol use disorder: a review. In *Current Opinion in Psychology*. <https://doi.org/10.1016/j.copsyc.2018.07.012>
- Demirakca, T., Ende, G., Kämmerer, N., Welzel-Marquez, H., Hermann, D., Heinz, A., & Mann, K. (2011). Effects of alcoholism and continued abstinence on brain volumes in both genders. *Alcoholism: Clinical and Experimental Research*, 35(9), 1678–1685. <https://doi.org/10.1111/j.1530-0277.2011.01514.x>
- Depaulis, A., Keay, K. A., & Bandler, R. (1992). Longitudinal neuronal organization of defensive reactions in the midbrain periaqueductal gray region of the rat. *Experimental Brain Research*, 90(2), 307–318. <https://doi.org/10.1007/BF00227243>
- Diana, M., Pistis, M., Carboni, S., Gessa, G. L., & Rossetti, Z. L. (1993). Profound decrement of mesolimbic dopaminergic neuronal activity during ethanol withdrawal syndrome in rats: electrophysiological and biochemical evidence. *Proceedings of the National Academy of Sciences of the United States of America*, 90(17), 7966–7969. <https://doi.org/10.1073/pnas.90.17.7966>

- Doyle, M., & Kiebler, M. A. (2011). Mechanisms of dendritic mRNA transport and its role in synaptic tagging. In *EMBO Journal* (Vol. 30, Issue 17, pp. 3540–3552). Nature Publishing Group. <https://doi.org/10.1038/emboj.2011.278>
- Dulhunty, A., Gage, P., Curtis, S., Chelvanayagam, G., & Board, P. (2001). The Glutathione Transferase Structural Family Includes a Nuclear Chloride Channel and a Ryanodine Receptor Calcium Release Channel Modulator. *Journal of Biological Chemistry*. <https://doi.org/10.1074/jbc.M007874200>
- Durinck, S., Spellman, P. T., Birney, E., & Huber, W. (2009). Mapping identifiers for the integration of genomic datasets with the R/ Bioconductor package biomaRt. *Nature Protocols*, 4(8), 1184–1191. <https://doi.org/10.1038/nprot.2009.97>
- Fallon, J. H., & Leslie, F. M. (1986). Distribution of dynorphin and enkephalin peptides in the rat brain. *Journal of Comparative Neurology*, 249(3), 293–336. <https://doi.org/10.1002/cne.902490302>
- Farris, S. P., Harris, R. a., & Ponomarev, I. (2015). Epigenetic modulation of brain gene networks for cocaine and alcohol abuse. *Frontiers in Neuroscience*, 9(May), 1–10. <https://doi.org/10.3389/fnins.2015.00176>
- Farris, S. P., & Miles, M. F. (2013). Fyn-Dependent Gene Networks in Acute Ethanol Sensitivity. *PLoS ONE*, 8(11), e82435. <https://doi.org/10.1371/journal.pone.0082435>
- Farris, S. P., Wolen, A. R., & Miles, M. F. (2010). Using expression genetics to study the neurobiology of ethanol and alcoholism. *International Review of Neurobiology*, 91(10), 95–128. [https://doi.org/10.1016/S0074-7742\(10\)91004-0](https://doi.org/10.1016/S0074-7742(10)91004-0)
- Fein, G., Di Sclafani, V., Cardenas, V. A., Goldmann, H., Tolou-Shams, M., & Meyerhoff, D. J. (2002). Cortical gray matter loss in treatment-naïve alcohol dependent individuals. *Alcoholism, Clinical and Experimental Research*, 26(4), 558–564. <https://doi.org/10.1016/j.micinf.2011.07.011>.Innate
- Fernández-Salas, E., Sagar, M., Cheng, C., Yuspa, S. H., & Weinberg, W. C. (1999). p53 and tumor necrosis factor α regulate the expression of a mitochondrial chloride channel protein. *Journal of Biological Chemistry*. <https://doi.org/10.1074/jbc.274.51.36488>

- Fernandez-Salas, E., Suh, K. S., Speransky, V. V., Bowers, W. L., Levy, J. M., Adams, T., Pathak, K. R., Edwards, L. E., Hayes, D. D., Cheng, C., Steven, A. C., Weinberg, W. C., & Yuspa, S. H. (2002). mtCLIC/CLIC4, an Organellar Chloride Channel Protein, Is Increased by DNA Damage and Participates in the Apoptotic Response to p53. *Molecular and Cellular Biology*. <https://doi.org/10.1128/mcb.22.11.3610-3620.2002>
- Field, M., & Duka, T. (2002). Cues paired with a low dose of alcohol acquire conditioned incentive properties in social drinkers. *Psychopharmacology*, *159*(3), 325–334. <https://doi.org/10.1007/s00213-001-0923-z>
- Fields, R. D. (2005). Myelination: An Overlooked Mechanism of Synaptic Plasticity? *The Neuroscientist*, *11*(6), 528–531. <https://doi.org/10.1177/1073858405282304>
- Fields, R. D. (2010). Neuroscience. Change in the brain's white matter. *Science (New York, N.Y.)*, *330*(6005), 768–769. <https://doi.org/10.1126/science.1199139>
- Fields, R. D. (2015). A new mechanism of nervous system plasticity: activity-dependent myelination. *Nature Reviews Neuroscience*, *16*(12), 756–767. <https://doi.org/10.1038/nrn4023>
- Filbey, F. M., Claus, E., Audette, A. R., Niculescu, M., Banich, M. T., Tanabe, J., Du, Y. P., & Hutchison, K. E. (2008). Exposure to the Taste of Alcohol Elicits Activation of the Mesocorticolimbic Neurocircuitry. *Neuropsychopharmacology*, *33*(6), 1391–1401. <https://doi.org/10.1038/sj.npp.1301513>
- Floresco, S. B., & Magyar, O. (2006). Mesocortical dopamine modulation of executive functions: Beyond working memory. In *Psychopharmacology* (Vol. 188, Issue 4, pp. 567–585). <https://doi.org/10.1007/s00213-006-0404-5>
- Fox, J., & Weisberg, S. (2019). *An R Companion to Applied Regression* (Third). Sage. <https://socialsciences.mcmaster.ca/jfox/Books/Companion/>
- Frey, U., & Morris, R. G. (1997). Synaptic tagging and long-term potentiation. *Nature*, *385*(6616), 533–536. <https://doi.org/10.1038/385533a0>
- Fünfschilling, U., Supplie, L. M., Mahad, D., Boretius, S., Saab, A. S., Edgar, J.,

- Brinkmann, B. G., Kassmann, C. M., Tzvetanova, I. D., Möbius, W., Diaz, F., Meijer, D., Suter, U., Hamprecht, B., Sereda, M. W., Moraes, C. T., Frahm, J., Goebbels, S., & Nave, K. A. (2012). Glycolytic oligodendrocytes maintain myelin and long-term axonal integrity. *Nature*, *485*(7399), 517–521. <https://doi.org/10.1038/nature11007>
- Funk, C. K., Zorrilla, E. P., Lee, M. J., Rice, K. C., & Koob, G. F. (2007). Corticotropin-Releasing Factor 1 Antagonists Selectively Reduce Ethanol Self-Administration in Ethanol-Dependent Rats. *Biological Psychiatry*, *61*(1), 78–86. <https://doi.org/10.1016/j.biopsych.2006.03.063>
- Gallaher, E. J., Jones, G. E., Belknap, J. K., & Crabbe, J. C. (1996). Identification of genetic markers for initial sensitivity and rapid tolerance to ethanol-induced ataxia using quantitative trait locus analysis in BXD recombinant inbred mice. *The Journal of Pharmacology and Experimental Therapeutics*, *277*(2), 604–612. <http://www.ncbi.nlm.nih.gov/pubmed/8627537>
- George, O., Sanders, C., Freiling, J., Grigoryan, E., Vu, S., Allen, C. D., Crawford, E., Mandyam, C. D., & Koob, G. F. (2012). Recruitment of medial prefrontal cortex neurons during alcohol withdrawal predicts cognitive impairment and excessive alcohol drinking. *Proceedings of the National Academy of Sciences*, *109*(44), 18156–18161. <https://doi.org/10.1073/pnas.1116523109>
- Giudice, G., Sánchez-Cabo, F., Torroja, C., & Lara-Pezzi, E. (2016). ATtRACT-a database of RNA-binding proteins and associated motifs. *Database*, *2016*. <https://doi.org/10.1093/database/baw035>
- Goldstein, R. Z., & Volkow, N. D. (2011). Dysfunction of the prefrontal cortex in addiction: neuroimaging findings and clinical implications. *Nature Reviews Neuroscience*, *12*(11), 652–669. <https://doi.org/10.1038/nrn3119>
- Gonzales, R. A., Job, M. O., & Doyon, W. M. (2004). The role of mesolimbic dopamine in the development and maintenance of ethanol reinforcement. *Pharmacology and Therapeutics*, *103*(2), 121–146. <https://doi.org/10.1016/j.pharmthera.2004.06.002>
- Goodchild, S. C., Curmi, P. M. G., & Brown, L. J. (2011). Structural gymnastics of multifunctional metamorphic proteins. *Biophysical Reviews*, *3*(3), 143–153. <https://doi.org/10.1007/s12551-011-0053-8>

- Grahame, N. J., & Cunningham, C. L. (1997). Intravenous ethanol self-administration in C57BL/6J and DBA/2J mice. *Alcoholism: Clinical and Experimental Research*. <https://doi.org/10.1111/j.1530-0277.1997.tb03728.x>
- Grant, B. F., Goldstein, R. B., Saha, T. D., Chou, S. P., Jung, J., Zhang, H., Pickering, R. P., Ruan, W. J., Smith, S. M., Huang, B., & Hasin, D. S. (2015). Epidemiology of DSM-5 Alcohol Use Disorder. *JAMA Psychiatry*, *72*(8), 757. <https://doi.org/10.1001/jamapsychiatry.2015.0584>
- Griffiths, I., Klugmann, M., Anderson, T., Yool, D., Thomson, C., Schwab, M. H., Schneider, A., Zimmermann, F., McCulloch, M., Nadon, N., & Nave, K. A. (1998). Axonal swellings and degeneration in mice lacking the major proteolipid of myelin. *Science*. <https://doi.org/10.1126/science.280.5369.1610>
- Grooms, S. Y., Noh, K. M., Regis, R., Bassell, G. J., Bryan, M. K., Carroll, R. C., & Zukin, R. S. (2006). Activity bidirectionally regulates AMPA receptor mRNA abundance in dendrites of hippocampal neurons. *J Neurosci*, *26*(32), 8339–8351. <https://doi.org/10.1523/JNEUROSCI.0472-06.2006>
- Grotewiel, M., & Bettinger, J. C. (2015). *Drosophila* and *Caenorhabditis elegans* as Discovery Platforms for Genes Involved in Human Alcohol Use Disorder. In *Alcoholism: Clinical and Experimental Research*. <https://doi.org/10.1111/acer.12785>
- Grüsser, S. M., Wrase, J., Klein, S., Hermann, D., Smolka, M. N., Ruf, M., Weber-Fahr, W., Herta, F., Mann, K., Braus, D. F., & Heinz, A. (2004). Cue-induced activation of the striatum and medial prefrontal cortex is associated with subsequent relapse in abstinent alcoholics. *Psychopharmacology*, *175*(3), 296–302. <https://doi.org/10.1007/s00213-004-1828-4>
- Gupta, S., Stamatoyannopoulos, J. A., Bailey, T. L., & Noble, W. S. (2007). Quantifying similarity between motifs. *Genome Biology*, *8*(2). <https://doi.org/10.1186/gb-2007-8-2-r24>
- Haber, S. N., Kunishio, K., Mizobuchi, M., & Lynd-Balta, E. (1995). The orbital and medial prefrontal circuit through the primate basal ganglia. *The Journal of Neuroscience: The Official Journal of the Society for Neuroscience*, *15*(7 Pt 1), 4851–4867.

- Hardy, S. G. P., & Holmes, D. E. (1988). Prefrontal stimulus-produced hypotension in rat. *Experimental Brain Research*, 73(2), 249–255. <https://doi.org/10.1007/BF00248217>
- Harrop, S. J., DeMaere, M. Z., Fairlie, W. D., Reztsova, T., Valenzuela, S. M., Mazzanti, M., Tonini, R., Qiu, M. R., Jankova, L., Warton, K., Bauskin, A. R., Wu, W. M., Pankhurst, S., Campbell, T. J., Breit, S. N., & Curmi, P. M. G. (2001). Crystal Structure of a Soluble Form of the Intracellular Chloride Ion Channel CLIC1 (NCC27) at 1.4-Å Resolution. *Journal of Biological Chemistry*, 276(48), 44993–45000. <https://doi.org/10.1074/jbc.M107804200>
- He, G., Ma, Y., Chou, S. Y., Li, H., Yang, C., Chuang, J. Z., Sung, C. H., & Ding, A. (2011). Role of CLIC4 in the host innate responses to bacterial lipopolysaccharide. *European Journal of Immunology*. <https://doi.org/10.1002/eji.201041266>
- Heinrichs, S. C., MENZAGHI, F., SCHULTEIS, G., G. F., K. O. O. B., Stinus, L., Koob, G. F., & Stinus, L. (1995). Suppression of Corticotropin-releasing Factor in the Amygdala Attenuates Aversive Consequences of Morphine-withdrawal. *Behavioural Pharmacology*, 6(1), 74–80. <https://www.scopus.com/inward/record.uri?eid=2-s2.0-0028860024&partnerID=40&md5=ac1bb43f5536ede424bbb3e7e43d0c1a>
- Heinz, A., Wrase, J., Kahnt, T., Beck, A., Bromand, Z., Grüsser, S. M., Kienast, T., Smolka, M. N., Flor, H., & Mann, K. (2007). Brain activation elicited by affectively positive stimuli is associated with a lower risk of relapse in detoxified alcoholic subjects. *Alcoholism: Clinical and Experimental Research*, 31(7), 1138–1147. <https://doi.org/10.1111/j.1530-0277.2007.00406.x>
- Hirabayashi, M., & Alam, M. R. (1981). Enhancing effect of methamphetamine on ambulatory activity produced by repeated administration in mice. *Pharmacol Biochem Behav*, 15(6), 925–932. <http://www.ncbi.nlm.nih.gov/pubmed/7323118>
- Hodgson, R. J. (1980). The Course of Alcoholism: Four Years After Treatment: Editorial Note. *British Journal of Addiction*, 75(4), 343–343. <https://doi.org/10.1111/j.1360-0443.1980.tb01393.x>
- Holmes, A., Fitzgerald, P. J., MacPherson, K. P., DeBrouse, L., Colacicco, G., Flynn, S. M., Masneuf, S., Pleil, K. E., Li, C., Marcinkiewicz, C. A., Kash, T. L.,

- Gunduz-Cinar, O., & Camp, M. (2012). Chronic alcohol remodels prefrontal neurons and disrupts NMDAR-mediated fear extinction encoding. *Nature Neuroscience*, 15(10), 1359–1361. <https://doi.org/10.1038/nn.3204>
- Horger, B. A., Shelton, K., & Schenk, S. (1990). Preexposure sensitizes rats to the rewarding effects of cocaine. *Pharmacol Biochem Behav*, 37(4), 707–711. <http://www.ncbi.nlm.nih.gov/pubmed/2093176>
- Howell, S., Duncan, R. R., & Ashley, R. H. (1996). Identification and characterisation of a homologue of p64 in rat tissues. *FEBS Letters*, 390(2), 207–210. [https://doi.org/10.1016/0014-5793\(96\)00676-X](https://doi.org/10.1016/0014-5793(96)00676-X)
- Hu, Y., Flockhart, I., Vinayagam, A., Bergwitz, C., Berger, B., Perrimon, N., & Mohr, S. E. (2011). An integrative approach to ortholog prediction for disease-focused and other functional studies. *BMC Bioinformatics*. <https://doi.org/10.1186/1471-2105-12-357>
- Huang, D. W., Sherman, B. T., & Lempicki, R. A. (2009). Systematic and integrative analysis of large gene lists using DAVID bioinformatics resources. *Nature Protocols*. <https://doi.org/10.1038/nprot.2008.211>
- Hurley, K. M., Herbert, H., Moga, M. M., & Saper, C. B. (1991). Efferent projections of the infralimbic cortex of the rat. *Journal of Comparative Neurology*, 308(2), 249–276. <https://doi.org/10.1002/cne.903080210>
- Jassal, B., Matthews, L., Viteri, G., Gong, C., Lorente, P., Fabregat, A., Sidiropoulos, K., Cook, J., Gillespie, M., Haw, R., Loney, F., May, B., Milacic, M., Rothfels, K., Sevilla, C., Shamovsky, V., Shorsler, S., Varusai, T., Weiser, J., ... D'Eustachio, P. (2020). The reactome pathway knowledgebase. *Nucleic Acids Research*. <https://doi.org/10.1093/nar/gkz1031>
- Jiang, L., Salao, K., Li, H., Rybicka, J. M., Yates, R. M., Luo, X. W., Shi, X. X., Kuffner, T., Tsai, V. W. W., Husaini, Y., Wu, L., Brown, D. A., Grewal, T., Brown, L. J., Curmi, P. M. G., & Breit, S. N. (2012). Intracellular chloride channel protein CLIC1 regulates macrophage function through modulation of phagosomal acidification. *Journal of Cell Science*. <https://doi.org/10.1242/jcs.110072>
- Johnson, D. R., Lee, P. K., Holmes, V. F., & Alvarez-Cohen, L. (2005). An internal

- reference technique for accurately quantifying specific mRNAs by real-time PCR with application to the *tceA* reductive dehalogenase gene. *Appl Environ Microbiol*, 71(7), 3866–3871. <https://doi.org/71/7/3866> [pii]10.1128/AEM.71.7.3866-3871.2005
- Jonas, D. E., Amick, H. R., Feltner, C., Bobashev, G., Thomas, K., Wines, R., Kim, M. M., Shanahan, E., Gass, C. E., Rowe, C. J., & Garbutt, J. C. (2014). Pharmacotherapy for Adults With Alcohol Use Disorders in Outpatient Settings. *Jama*, 311(18), 1889. <https://doi.org/10.1001/jama.2014.3628>
- Jones, M. A., Amr, S., Ferebee, A., Huynh, P., Rosenfeld, J. A., Miles, M. F., Davies, A. G., Korey, C. A., Warrick, J. M., Shiang, R., Elsea, S. H., Girirajan, S., & Grotewiel, M. (2014). Genetic studies in *Drosophila* and humans support a model for the concerted function of *CISD2*, *PPT1* and *CLN3* in disease. *Biology Open*. <https://doi.org/10.1242/bio.20147559>
- Kalivas, P. W., & Stewart, J. (1991). Dopamine transmission in the initiation and expression of drug- and stress-induced sensitization of motor activity. *Brain Res Brain Res Rev*, 16(3), 223–244. <http://www.ncbi.nlm.nih.gov/pubmed/1665095>
- Kalivas, P. W., Volkow, N., & Seamans, J. (2005). Unmanageable motivation in addiction: A pathology in prefrontal-accumbens glutamate transmission. In *Neuron* (Vol. 45, Issue 5, pp. 647–650). <https://doi.org/10.1016/j.neuron.2005.02.005>
- Kandel, E. R., Schwartz, J. H., & Jessell, T. M. (2012). Principles of Neural Science. In *Neurology* (Vol. 5). <https://doi.org/10.1036/0838577016>
- Kanehisa, M. (2000). KEGG: Kyoto Encyclopedia of Genes and Genomes. *Nucleic Acids Research*. <https://doi.org/10.1093/nar/28.1.27>
- Kang, H., & Schuman, E. M. (1996). A requirement for local protein synthesis in neurotrophin-induced hippocampal synaptic plasticity. *Science*, 273(5280), 1402–1406. <http://www.ncbi.nlm.nih.gov/pubmed/8703078>
- Karolchik, D. (2004). The UCSC Table Browser data retrieval tool. *Nucleic Acids Research*, 32(90001), 493D – 496. <https://doi.org/10.1093/nar/gkh103>

- Keistler, C. R., Hammarlund, E., Barker, J. M., Bond, C. W., DiLeone, R. J., Pittenger, C., & Taylor, J. R. (2017). Regulation of Alcohol Extinction and Cue-Induced Reinstatement by Specific Projections among Medial Prefrontal Cortex, Nucleus Accumbens, and Basolateral Amygdala. *The Journal of Neuroscience*, 37(17), 4462–4471. <https://doi.org/10.1523/JNEUROSCI.3383-16.2017>
- Kelleher, R. J., Govindarajan, A., & Tonegawa, S. (2004). Translational Regulatory Mechanisms in Persistent Forms of Synaptic Plasticity. *Neuron*, 44(1), 59–73. <https://doi.org/10.1016/j.neuron.2004.09.013>
- Kerns, R. T., Ravindranathan, A., Hassan, S., Cage, M. P., York, T., Sikela, J. M., Williams, R. W., & Miles, M. F. (2005). Ethanol-responsive brain region expression networks: implications for behavioral responses to acute ethanol in DBA/2J versus C57BL/6J mice. *The Journal of Neuroscience: The Official Journal of the Society for Neuroscience*, 25(9), 2255–2266. <https://doi.org/10.1523/JNEUROSCI.4372-04.2005>
- Kim, A., Zamora-Martinez, E. R., Edwards, S., & Mandyam, C. D. (2015). Structural reorganization of pyramidal neurons in the medial prefrontal cortex of alcohol dependent rats is associated with altered glial plasticity. *Brain Structure and Function*, 220(3), 1705–1720. <https://doi.org/10.1007/s00429-014-0755-3>
- Kim, D., Perte, G., Trapnell, C., Pimentel, H., Kelley, R., & Salzberg, S. L. (2013). TopHat2: Accurate alignment of transcriptomes in the presence of insertions, deletions and gene fusions. *Genome Biology*, 14(4). <https://doi.org/10.1186/gb-2013-14-4-r36>
- Kim, M. J., Loucks, R. A., Palmer, A. L., Brown, A. C., Solomon, K. M., Marchante, A. N., & Whalen, P. J. (2011). The structural and functional connectivity of the amygdala: From normal emotion to pathological anxiety. *Behavioural Brain Research*, 223(2), 403–410. <https://doi.org/10.1016/j.bbr.2011.04.025>
- Klenowski, P. M. (2018). Emerging role for the medial prefrontal cortex in alcohol-seeking behaviors. *Addictive Behaviors*, 77(1873-6327 (Electronic)), 102–106. <https://doi.org/10.1016/j.addbeh.2017.09.024>
- Klenowski, P. M., Fogarty, M. J., Shariff, M., Belmer, A., Bellingham, M. C., &

- Bartlett, S. E. (2016). Increased Synaptic Excitation and Abnormal Dendritic Structure of Prefrontal Cortex Layer V Pyramidal Neurons following Prolonged Binge-Like Consumption of Ethanol. *Eneuro*, 3(6), ENEURO.0248-16.2016. <https://doi.org/10.1523/ENEURO.0248-16.2016>
- Kong, E. C., Woo, K., Li, H., Lebestky, T., Mayer, N., Sniffen, M. R., Heberlein, U., Bainton, R. J., Hirsh, J., & Wolf, F. W. (2010). A pair of dopamine neurons target the D1-like dopamine receptor dopr in the central complex to promote ethanol-stimulated locomotion in drosophila. *PLoS ONE*. <https://doi.org/10.1371/journal.pone.0009954>
- Koob, G F. (2008). A role for brain stress systems in addiction. *Neuron*, 59(1), 11–34. <https://doi.org/10.1016/j.neuron.2008.06.012>
- Koob, George F. (2013). Addiction is a Reward Deficit and Stress Surfeit Disorder. *Frontiers in Psychiatry*, 4(August), 72. <https://doi.org/10.3389/fpsy.2013.00072>
- Koob, George F., Everitt, B. J., & Robbins, T. W. (2012). Reward, Motivation, and Addiction. *Fundamental Neuroscience: Fourth Edition*, 871–898. <https://doi.org/10.1016/B978-0-12-385870-2.00041-X>
- Kroener, S., Mulholland, P. J., New, N. N., Gass, J. T., Becker, H. C., & Chandler, L. J. (2012). Chronic alcohol exposure alters behavioral and synaptic plasticity of the rodent prefrontal cortex. *PLoS ONE*, 7(5). <https://doi.org/10.1371/journal.pone.0037541>
- Lappe-Siefke, C., Goebbels, S., Gravel, M., Nicksch, E., Lee, J., Braun, P. E., Griffiths, I. R., & Navel, K. A. (2003). Disruption of Cnp1 uncouples oligodendroglial functions in axonal support and myelination. *Nature Genetics*. <https://doi.org/10.1038/ng1095>
- Lê, A. D., & Shaham, Y. (2002). Neurobiology of relapse to alcohol in rats. In *Pharmacology and Therapeutics* (Vol. 94, Issues 1–2, pp. 137–156). [https://doi.org/10.1016/S0163-7258\(02\)00200-0](https://doi.org/10.1016/S0163-7258(02)00200-0)
- Lee, S., Kim, S.-J., Kwon, O.-B., Lee, J. H., & Kim, J.-H. (2013). Inhibitory networks of the amygdala for emotional memory. *Frontiers in Neural Circuits*, 7(August), 1–10. <https://doi.org/10.3389/fncir.2013.00129>

- Lein, E. S., Hawrylycz, M. J., Ao, N., Ayres, M., Bensinger, A., Bernard, A., Boe, A. F., Boguski, M. S., Brockway, K. S., Byrnes, E. J., Chen, L., Chen, L., Chen, T.-M. M., Chin, M. C., Chong, J., Crook, B. E., Czaplinska, A., Dang, C. N., Datta, S., ... Jones, A. R. (2007). Genome-wide atlas of gene expression in the adult mouse brain. *Nature*, *445*(7124), 168–176. <https://doi.org/10.1038/nature05453>
- Lessov, C. N., Palmer, A. A., Quick, E. A., & Phillips, T. J. (2001). Voluntary ethanol drinking in C57BL/6J and DBA/2J mice before and after sensitization to the locomotor stimulant effects of ethanol. *Psychopharmacology (Berl)*, *155*(1), 91–99. <http://www.ncbi.nlm.nih.gov/pubmed/11374341>
- Lewohl, J. M., Wixey, J., Harper, C. G., & Dodd, P. R. (2005). Expression of MBP, PLP, MAG, CNP, and GFAP in the Human Alcoholic Brain. *Alcohol Clin.Exp.Res.*, *29*(9), 1698–1705. <https://doi.org/10.1097/01.alc.0000179406.98868.59>
- Li, H., Handsaker, B., Wysoker, A., Fennell, T., Ruan, J., Homer, N., Marth, G., Abecasis, G., Durbin, R., Data, G. P., Sam, T., & Subgroup, 1000 Genome Project Data Processing. (2009). The Sequence Alignment / Map format and SAMtools. *Bioinformatics*, *25*(16), 2078–2079. <https://doi.org/10.1093/bioinformatics/btp352>
- Lindholm, S., Ploj, K., Franck, J., & Nylander, I. (2000). Repeated ethanol administration induces short- and long-term changes in enkephalin and dynorphin tissue concentrations in rat brain. *Alcohol*, *22*(3), 165–171. [https://doi.org/10.1016/S0741-8329\(00\)00118-X](https://doi.org/10.1016/S0741-8329(00)00118-X)
- Link, W., Konietzko, U., Kauselmann, G., Krug, M., Schwanke, B., Frey, U., & Kuhl, D. (1995). Somatodendritic expression of an immediate early gene is regulated by synaptic activity. *Proc Natl Acad Sci U S A*, *92*(12), 5734–5738. <http://www.ncbi.nlm.nih.gov/pubmed/7777577>
- Linsenbardt, D. N., Moore, E. M., Gross, C. D., Goldfarb, K. J., Blackman, L. C., & Boehm, S. L. (2009). Sensitivity and tolerance to the hypnotic and ataxic effects of ethanol in adolescent and adult C57BL/6J and DBA/2J mice. *Alcoholism: Clinical and Experimental Research*. <https://doi.org/10.1111/j.1530-0277.2008.00857.x>
- Lister, R. G. (1987). The effects of ethanol on exploration in DBA/2 and C57B1/6

mice. *Alcohol*. [https://doi.org/10.1016/0741-8329\(87\)90054-1](https://doi.org/10.1016/0741-8329(87)90054-1)

- Litman, P., Barg, J., & Ginzburg, I. (1994). Microtubules are involved in the localization of tau mRNA in primary neuronal cell cultures. *Neuron*, 13(6), 1463–1474. [https://doi.org/0896-6273\(94\)90432-4](https://doi.org/0896-6273(94)90432-4) [pii]
- Littler, D. R., Assaad, N. N., Harrop, S. J., Brown, L. J., Pankhurst, G. J., Luciani, P., Aguilar, M. I., Mazzanti, M., Berryman, M. A., Breit, S. N., & Curmi, P. M. G. (2005). Crystal structure of the soluble form of the redox-regulated chloride ion channel protein CLIC4. *FEBS Journal*, 272(19), 4996–5007. <https://doi.org/10.1111/j.1742-4658.2005.04909.x>
- Littler, D. R., Harrop, S. J., Brown, L. J., Pankhurst, G. J., Mynott, A. V., Luciani, P., Mandyam, R. A., Mazzanti, M., Tanda, S., Berryman, M. A., Breit, S. N., & Curmi, P. M. G. (2008). Comparison of vertebrate and invertebrate CLIC proteins: The crystal structures of *Caenorhabditis elegans* EXC-4 and *Drosophila melanogaster* DmCLIC. *Proteins: Structure, Function and Genetics*, 71(1), 364–378. <https://doi.org/10.1002/prot.21704>
- Littler, D. R., Harrop, S. J., Fairlie, W. D., Brown, L. J., Pankhurst, G. J., Pankhurst, S., DeMaere, M. Z., Campbell, T. J., Bauskin, A. R., Tonini, R., Mazzanti, M., Breit, S. N., & Curmi, P. M. G. G. (2004). The Intracellular Chloride Ion Channel Protein CLIC1 Undergoes a Redox-controlled Structural Transition. *Journal of Biological Chemistry*, 279(10), 9298–9305. <https://doi.org/10.1074/jbc.M308444200>
- Littler, D. R., Harrop, S. J., Goodchild, S. C., Phang, J. M., Mynott, A. V., Jiang, L., Valenzuela, S. M., Mazzanti, M., Brown, L. J., Breit, S. N., & Curmi, P. M. G. (2010). The enigma of the CLIC proteins: Ion channels, redox proteins, enzymes, scaffolding proteins? *FEBS Letters*, 584(10), 2093–2101. <https://doi.org/10.1016/j.febslet.2010.01.027>
- Liu, J., Lewohl, J. M., Harris, R. A., Iyer, V. R., Dodd, P. R., Randall, P. K., & Mayfield, R. D. (2006). *Patterns of Gene Expression in the Frontal Cortex Discriminate Alcoholic from Nonalcoholic Individuals*. 1574–1582. <https://doi.org/10.1038/sj.npp.1300947>
- Lyford, G. L., Yamagata, K., Kaufmann, W. E., Barnes, C. A., Sanders, L. K., Copeland, N. G., Gilbert, D. J., Jenkins, N. A., Lanahan, A. A., & Worley, P. F.

- (1995). Arc, a growth factor and activity-regulated gene, encodes a novel cytoskeleton-associated protein that is enriched in neuronal dendrites. *Neuron*, 14(2), 433–445. [https://doi.org/0896-6273\(95\)90299-6](https://doi.org/0896-6273(95)90299-6) [pii]
- Maeda, K., Haraguchi, M., Kuramasu, A., Sato, T., Ariake, K., Sakagami, H., Kondo, H., Yanai, K., Fukunaga, K., Yanagisawa, T., & Sukegawa, J. (2008). CLIC4 interacts with histamine H3 receptor and enhances the receptor cell surface expression. *Biochemical and Biophysical Research Communications*, 369(2), 603–608. <https://doi.org/10.1016/j.bbrc.2008.02.071>
- Malik, M., Shukla, A., Amin, P., Niedelman, W., Lee, J., Jividen, K., Phang, J. M., Ding, J., Suh, K. S., Curmi, P. M. G., & Yuspa, S. H. (2010). S-Nitrosylation Regulates Nuclear Translocation of Chloride Intracellular Channel Protein CLIC4. *Journal of Biological Chemistry*, 285(31), 23818–23828. <https://doi.org/10.1074/jbc.M109.091611>
- Marballi, K., Genabai, N. K., Blednov, Y. A., Harris, R. A., & Ponomarev, I. (2016). Alcohol consumption induces global gene expression changes in VTA dopaminergic neurons. *Genes, Brain and Behavior*, 15(3), 318–326. <https://doi.org/10.1111/gbb.12266>
- Margolis, E. B., Lock, H., Chefer, V. I., Shippenberg, T. S., Hjelmstad, G. O., & Fields, H. L. (2006). Kappa opioids selectively control dopaminergic neurons projecting to the prefrontal cortex. *Proc. Natl. Acad. Sci. U. S. A.*, 103(8), 2938–2942. <https://doi.org/10.1073/pnas.0511159103>
- Marques, S., Zeisel, A., Codeluppi, S., van Bruggen, D., Mendanha Falcao, A., Xiao, L., Li, H., Haring, M., Hochgerner, H., Romanov, R. A., Gyllborg, D., Munoz-Manchado, A. B., La Manno, G., Lonnerberg, P., Floriddia, E. M., Rezayee, F., Ernfors, P., Arenas, E., Hjerling-Leffler, J., ... Castelo-Branco, G. (2016). Oligodendrocyte heterogeneity in the mouse juvenile and adult central nervous system. *Science*, 352(6291), 1326–1329. <https://doi.org/10.1126/science.aaf6463>
- Martin, K. C., & Kosik, K. S. (2002). Synaptic tagging -- who's it? *Nat Rev Neurosci*, 3(10), 813–820. <https://doi.org/10.1038/nrn942nrn942> [pii]
- Masur, J., Oliveira de Souza, M. L., & Zwicker, A. P. (1986). The excitatory effect of ethanol: absence in rats, no tolerance and increased sensitivity in mice.

Pharmacol Biochem Behav, 24(5), 1225–1228.
<http://www.ncbi.nlm.nih.gov/pubmed/3725828>

- Matsumoto, M., Setou, M., & Inokuchi, K. (2007). Transcriptome analysis reveals the population of dendritic RNAs and their redistribution by neural activity. *Neurosci Res*, 57(3), 411–423. [https://doi.org/S0168-0102\(06\)00325-7](https://doi.org/S0168-0102(06)00325-7) [pii]10.1016/j.neures.2006.11.015
- McCarthy, D. J., Chen, Y., & Smyth, G. K. (2012). Differential expression analysis of multifactor RNA-Seq experiments with respect to biological variation. *Nucleic Acids Research*, 40(10), 4288–4297. <https://doi.org/10.1093/nar/gks042>
- McDonald, A. J. (1982). Cytoarchitecture of the central amygdaloid nucleus of the rat. *Journal of Comparative Neurology*, 208(4), 401–418. <https://doi.org/10.1002/cne.902080409>
- McFarland, K., Lapish, C. C., & Kalivas, P. W. (2003). Prefrontal glutamate release into the core of the nucleus accumbens mediates cocaine-induced reinstatement of drug-seeking behavior. *The Journal of Neuroscience: The Official Journal of the Society for Neuroscience*, 23(8), 3531–3537. <https://doi.org/23/8/3531> [pii]
- McTigue, D. M., & Tripathi, R. B. (2008). The life, death, and replacement of oligodendrocytes in the adult CNS. *Journal of Neurochemistry*, 107(1), 1–19. <https://doi.org/10.1111/j.1471-4159.2008.05570.x>
- Melendez, R. I., Middaugh, L. D., & Kalivas, P. W. (2006). Development of an alcohol deprivation and escalation effect in C57BL/6J mice. *Alcoholism: Clinical and Experimental Research*. <https://doi.org/10.1111/j.1530-0277.2006.00248.x>
- Metten, P., Phillips, T. J., Crabbe, J. C., Tarantino, L. M., McClearn, G. E., Plomin, R., Erwin, V. G., & Belknap, J. K. (1998). High genetic susceptibility to ethanol withdrawal predicts low ethanol consumption. *Mammalian Genome*, 9(12), 983–990. <https://doi.org/10.1007/s003359900911>
- Michaelsen-Preusse, K., Feuge, J., & Korte, M. (2018). Imbalance of synaptic actin dynamics as a key to fragile X syndrome? *J Physiol*. <https://doi.org/10.1113/JP275571>

- Michalski, J.-P., & Kothary, R. (2015). Oligodendrocytes in a Nutshell. *Frontiers in Cellular Neuroscience*, 9(September), 1–11. <https://doi.org/10.3389/fncel.2015.00340>
- Micu, I., Plemel, J. R., Caprariello, A. V., Nave, K. A., & Stys, P. K. (2018). Axo-myelinic neurotransmission: A novel mode of cell signalling in the central nervous system. *Nature Reviews Neuroscience*, 19(1), 49–57. <https://doi.org/10.1038/nrn.2017.128>
- Mifepristone for the Prevention of Relapses of Alcohol Drinking. (2004). NCT02243709. <https://clinicaltrials.gov/ct2/show/NCT02243709>
- Miles, M. F., Diaz, J. E., & DeGuzman, V. S. (1991). Mechanisms of neuronal adaptation to ethanol. Ethanol induces Hsc70 gene transcription in NG108-15 neuroblastoma x glioma cells. *J Biol Chem*, 266(4), 2409–2414. <http://www.ncbi.nlm.nih.gov/pubmed/1989992>
- Miles, M. F., Wilke, N., Elliot, M., Tanner, W., & Shah, S. (1994). Ethanol-responsive genes in neural cells include the 78-kilodalton glucose-regulated protein (GRP78) and 94-kilodalton glucose-regulated protein (GRP94) molecular chaperones. *Mol Pharmacol*, 46(5), 873–879. <http://www.ncbi.nlm.nih.gov/pubmed/7969074>
- Mokdad, A. H. (2004). Actual Causes of Death in the United States, 2000. *JAMA*, 291(10), 1238. <https://doi.org/10.1001/jama.291.10.1238>
- Morozova, T. V., Anholt, R. H., & Mackay, T. F. C. (2006). Transcriptional response to alcohol exposure in *Drosophila melanogaster*. *Genome Biology*. <https://doi.org/10.1186/gb-2006-7-10-r95>
- Morozova, T. V., Anholt, R. R. H., & Mackay, T. F. C. (2007). Phenotypic and transcriptional response to selection for alcohol sensitivity in *Drosophila melanogaster*. *Genome Biology*. <https://doi.org/10.1186/gb-2007-8-10-r231>
- Morris, E. P., Stewart, S. H., & Ham, L. S. (2005). The relationship between social anxiety disorder and alcohol use disorders: A critical review. *Clinical Psychology Review*, 25(6), 734–760. <https://doi.org/10.1016/j.cpr.2005.05.004>
- Most, D., Ferguson, L., Blednov, Y., Mayfield, R. D., & Harris, R. A. (2015). The

- synaptoneurosome transcriptome: a model for profiling the molecular effects of alcohol. *Pharmacogenomics J*, 15(2), 177–188. <https://doi.org/10.1038/tpj.2014.43>
- Mulligan, M. K., Ponomarev, I., Hitzemann, R. J., Belknap, J. K., Tabakoff, B., Harris, R. A., Crabbe, J. C., Blednov, Y. A., Grahame, N. J., Phillips, T. J., Finn, D. A., Hoffman, P. L., Iyer, V. R., Koob, G. F., & Bergeson, S. E. (2006). Toward understanding the genetics of alcohol drinking through transcriptome meta-analysis. *Proceedings of the National Academy of Sciences*, 103(16), 6368–6373. <https://doi.org/10.1073/pnas.0510188103>
- Nakamura, K., & Kubota, K. (1996). The primate temporal pole: Its putative role in object recognition and memory. In *Behavioural Brain Research* (Vol. 77, Issues 1–2, pp. 53–77). [https://doi.org/10.1016/0166-4328\(95\)00227-8](https://doi.org/10.1016/0166-4328(95)00227-8)
- Nakamura, Kazuhiro, Xiu, Y., Ohtsuji, M., Sugita, G., Abe, M., Ohtsuji, N., Hamano, Y., Jiang, Y., Takahashi, N., Shirai, T., Nishimura, H., & Hirose, S. (2003). Genetic dissection of anxiety in autoimmune disease. *Human Molecular Genetics*, 12(10), 1079–1086. <https://doi.org/10.1093/hmg/ddg128>
- Narendran, R., Mason, N. S., Paris, J., Himes, M. L., Douaihy, A. B., & Frankle, W. G. (2014). Decreased prefrontal cortical dopamine transmission in alcoholism. *American Journal of Psychiatry*, 171(8), 881–888. <https://doi.org/10.1176/appi.ajp.2014.13121581>
- Navarro, A. I., & Mandyam, C. D. (2015). Protracted abstinence from chronic ethanol exposure alters the structure of neurons and expression of oligodendrocytes and myelin in the medial prefrontal cortex. *Neuroscience*, 293, 35–44. <https://doi.org/10.1016/j.neuroscience.2015.02.043>
- Nave, K. A. (2010). Myelination and support of axonal integrity by glia. *Nature*, 468(7321), 244–252. <https://doi.org/10.1038/nature09614>
- Nestler, E. J. (2001). Molecular neurobiology of addiction. *Am J Addict*, 10(3), 201–217. <http://www.ncbi.nlm.nih.gov/pubmed/11579619>
- Nestler, E. J., Hope, B. T., & Widnell, K. L. (1993). Drug addiction: a model for the molecular basis of neural plasticity. *Neuron*, 11(6), 995–1006. [https://doi.org/0896-6273\(93\)90213-B](https://doi.org/0896-6273(93)90213-B) [pii]

- O'Brien, M. A., Weston, R. M., Sheth, N. U., Bradley, S., Bigbee, J., Pandey, A., Williams, R. W., Wolstenholme, J. T., Miles, M. F., O'Brien, M. A., Weston, R. M., Sheth, N. U., Bradley, S., Bigbee, J., Pandey, A., Williams, R. W., Wolstenholme, J. T., & Miles, M. F. (2018). Ethanol-Induced Behavioral Sensitization Alters the Synaptic Transcriptome and Exon Utilization in DBA/2J Mice. *Frontiers in Genetics*, 9(September), 402. <https://doi.org/10.3389/fgene.2018.00402>
- O'Leary, M. R., Radford, L. M., Chaney, E. F., & Schau, E. J. (1977). Assessment of cognitive recovery in alcoholics by use of the trail-making test. *Journal of Clinical Psychology*, 33(2), 579–582. [https://doi.org/10.1002/1097-4679\(197704\)33:2<579::AID-JCLP2270330254>3.0.CO;2-R](https://doi.org/10.1002/1097-4679(197704)33:2<579::AID-JCLP2270330254>3.0.CO;2-R)
- Olson, I. R., Plotzker, A., & Ezzyat, Y. (2007). The Enigmatic temporal pole: A review of findings on social and emotional processing. In *Brain* (Vol. 130, Issue 7, pp. 1718–1731). <https://doi.org/10.1093/brain/awm052>
- Ongür, D., An, X., & Price, J. L. (1998). Prefrontal cortical projections to the hypothalamus in macaque monkeys. *The Journal of Comparative Neurology*, 401(4), 480–505. [https://doi.org/10.1002/\(SICI\)1096-9861\(19981130\)401:4<480::AID-CNE4>3.0.CO;2-F](https://doi.org/10.1002/(SICI)1096-9861(19981130)401:4<480::AID-CNE4>3.0.CO;2-F)
- Ongür, D., & Price, J. L. (2000). The organization of networks within the orbital and medial prefrontal cortex of rats, monkeys and humans. *Cerebral Cortex*, 10(3), 206–219. <https://doi.org/10.1093/cercor/10.3.206>
- Overstreet, D. H., Knapp, D. J., & Breese, G. R. (2004). Modulation of multiple ethanol withdrawal-induced anxiety-like behavior by CRF and CRF1receptors. *Pharmacology Biochemistry and Behavior*, 77(2), 405–413. <https://doi.org/10.1016/j.pbb.2003.11.010>
- Padmakumar, V. C., Speer, K., Pal-Ghosh, S., Masiuk, K. E., Ryscavage, A., Dengler, S. L., Hwang, S., Edwards, J. C., Coppola, V., Tessarollo, L., Stepp, M. A., & Yuspa, S. H. (2012). Spontaneous skin erosions and reduced skin and corneal wound healing characterize CLIC4 NULL mice. *American Journal of Pathology*, 181(1), 74–84. <https://doi.org/10.1016/j.ajpath.2012.03.025>
- Padmakumar, V., Masiuk, K. E., Luger, D., Lee, C., Coppola, V., Tessarollo, L., Hoover, S. B., Karavanova, I., Buonanno, A., Simpson, R., & Yuspa, S. H.

- (2014). Detection of differential fetal and adult expression of chloride intracellular channel 4 (CLIC4) protein by analysis of a green fluorescent protein knock-in mouse line. *BMC Developmental Biology*, 14(1), 24. <https://doi.org/10.1186/1471-213X-14-24>
- Peters, A., & Jones, E. G. (1984). Cellular components of the cerebral cortex. In *Cerebral Cortex, Vol. 1: Cellular Components of the Cerebral Cortex* (pp. 107–121).
- Peters, J., Kalivas, P. W., & Quirk, G. J. (2009). Extinction circuits for fear and addiction overlap in prefrontal cortex. *Learning & Memory*, 16(5), 279–288. <https://doi.org/10.1101/lm.1041309>
- Peters, J., LaLumiere, R. T., & Kalivas, P. W. (2008). Infralimbic Prefrontal Cortex Is Responsible for Inhibiting Cocaine Seeking in Extinguished Rats. *Journal of Neuroscience*, 28(23), 6046–6053. <https://doi.org/10.1523/JNEUROSCI.1045-08.2008>
- Petrides, M., & Pandya, D. N. (1994). Comparative architectonic analysis of the human and the macaque frontal cortex. In *Handbook of neuropsychology* (Vol. 9, pp. 17–58).
- Pfarr, S., Meinhardt, M. W., Klee, M. L., Hansson, A. C., Vengeliene, V., Schonig, K., Bartsch, D., Hope, B. T., Spanagel, R., & Sommer, W. H. (2015). Losing Control: Excessive Alcohol Seeking after Selective Inactivation of Cue-Responsive Neurons in the Infralimbic Cortex. *Journal of Neuroscience*, 35(30), 10750–10761. <https://doi.org/10.1523/JNEUROSCI.0684-15.2015>
- Pfefferbaum, A., & Sullivan, E. V. (2005). Disruption of brain white matter microstructure by excessive intracellular and extracellular fluid in alcoholism: evidence from diffusion tensor imaging. *Neuropsychopharmacology: Official Publication of the American College of Neuropsychopharmacology*, 30(2), 423–432. <https://doi.org/10.1038/sj.npp.1300623>
- Phillips, T. J., Dickinson, S., & Burkhart-Kasch, S. (1994). Behavioral sensitization to drug stimulant effects in C57BL/6J and DBA/2J inbred mice. *Behavioral Neuroscience*. <https://doi.org/10.1037/0735-7044.108.4.789>
- Phillips, Tamara J., Belknap, J. K., Buck, K. J., & Cunningham, C. L. (1998). Genes on mouse chromosomes 2 and 9 determine variation in ethanol consumption.

Mammalian Genome, 9(12), 936–941. <https://doi.org/10.1007/s003359900903>

Phillips, Tamara J., Crabbe, J. C., Metten, P., & Belknap, J. K. (1994). Localization of Genes Affecting Alcohol Drinking in Mice. *Alcoholism: Clinical and Experimental Research*, 18(4), 931–941. <https://doi.org/10.1111/j.1530-0277.1994.tb00062.x>

Piazza, P. V, Deminiere, J. M., le Moal, M., & Simon, H. (1990). Stress- and pharmacologically-induced behavioral sensitization increases vulnerability to acquisition of amphetamine self-administration. *Brain Res*, 514(1), 22–26. [https://doi.org/0006-8993\(90\)90431-A](https://doi.org/0006-8993(90)90431-A) [pii]

Pinheiro, J., Bates, D., DebRoy, S., & Sarkar, D. (2020). *nlme: Linear and Nonlinear Mixed Effects Models*. <https://cran.r-project.org/package=nlme>

Poirier, L., Shane, A., Zheng, J., & Seroude, L. (2008). Characterization of the Drosophila Gene-Switch system in aging studies: A cautionary tale. *Aging Cell*. <https://doi.org/10.1111/j.1474-9726.2008.00421.x>

Ponsioen, B., van Zeijl, L., Langeslag, M., Berryman, M., Littler, D., Jalink, K., & Moolenaar, W. H. (2009). Spatiotemporal regulation of chloride intracellular channel protein CLIC4 by RhoA. *Molecular Biology of the Cell*, 20(22), 4664–4672. <https://doi.org/10.1091/mbc.e09-06-0529>

Poon, M. M., Choi, S. H., Jamieson, C. A., Geschwind, D. H., & Martin, K. C. (2006). Identification of process-localized mRNAs from cultured rodent hippocampal neurons. *J Neurosci*, 26(51), 13390–13399. <https://doi.org/26/51/13390> [pii]10.1523/JNEUROSCI.3432-06.2006

Prescott, C. A., & Kendler, K. S. (1999). Genetic and environmental contributions to alcohol abuse and dependence in a population-based sample of male twins. *The American Journal of Psychiatry*, 156(1), 34–40. <https://doi.org/10.1176/ajp.156.1.34>

Proutski, I., Karoulias, N., & Ashley, R. H. (2002). Overexpressed chloride intracellular channel protein CLIC4 (p64H1) is an essential component of novel plasma membrane anion channels. *Biochemical and Biophysical Research Communications*, 297(2), 317–322. [https://doi.org/10.1016/S0006-291X\(02\)02199-X](https://doi.org/10.1016/S0006-291X(02)02199-X)

- Qiang, M., Denny, A. D., & Ticku, M. K. (2007). Chronic intermittent ethanol treatment selectively alters N-methyl-D-aspartate receptor subunit surface expression in cultured cortical neurons. *Mol Pharmacol*, 72(1), 95–102. <https://doi.org/mol.106.033043> [pii]10.1124/mol.106.033043
- Quinlan, A. R., & Hall, I. M. (2010). BEDTools: A flexible suite of utilities for comparing genomic features. *Bioinformatics*, 26(6), 841–842. <https://doi.org/10.1093/bioinformatics/btq033>
- R Development Core Team, & Team, R. D. C. (2016). R: A Language and Environment for Statistical Computing. *R Foundation for Statistical Computing Vienna Austria, 0*, {ISBN} 3-900051-07-0. <https://doi.org/10.1038/sj.hdy.6800737>
- Rao, A., & Steward, O. (1993). Evaluation of RNAs present in synaptodendrosomes: dendritic, glial, and neuronal cell body contribution. *J Neurochem*, 61(3), 835–844. <http://www.ncbi.nlm.nih.gov/pubmed/7689643>
- Rasband, W. (2015). ImageJ [Software]. *U. S. National Institutes of Health, Bethesda, Maryland, USA*.
- Ray, J. P., & Price, J. L. (1993). The organization of projections from the mediodorsal nucleus of the thalamus to orbital and medial prefrontal cortex in macaque monkeys. *Journal of Comparative Neurology*, 337(1), 1–31. <https://doi.org/10.1002/cne.903370102>
- Resstel, L. B. M., & Corrêa, F. M. A. (2006). Involvement of the medial prefrontal cortex in central cardiovascular modulation in the rat. In *Autonomic Neuroscience: Basic and Clinical* (Vols. 126–127, pp. 130–138). <https://doi.org/10.1016/j.autneu.2006.02.022>
- Ridge, J. P., Ho, A. M.-C., Innes, D. J., & Dodd, P. R. (2008). The expression of NMDA receptor subunit mRNA in human chronic alcoholics. *Annals of the New York Academy of Sciences*, 1139, 10–19. <https://doi.org/10.1196/annals.1432.053>
- Ritchie, M. E., Phipson, B., Wu, D., Hu, Y., Law, C. W., Shi, W., & Smyth, G. K. (2015). Limma powers differential expression analyses for RNA-sequencing and microarray studies. *Nucleic Acids Research*. <https://doi.org/10.1093/nar/gkv007>

- Rivers, L. E., Young, K. M., Rizzi, M., Jamen, F., Psachoulia, K., Wade, A., Kessar, N., & Richardson, W. D. (2008). PDGFRA/NG2 glia generate myelinating oligodendrocytes and piriform projection neurons in adult mice. *Nature Neuroscience*, *11*(12), 1392–1401. <https://doi.org/10.1038/nn.2220>
- Robinson, M. D., McCarthy, D. J., & Smyth, G. K. (2010). edgeR: a Bioconductor package for differential expression analysis of digital gene expression data. *Bioinformatics*, *26*(1), 139–140. <https://doi.org/10.1093/bioinformatics/btp616>
- Robinson, T. E., & Berridge, K. C. (1993). The neural basis of drug craving: an incentive-sensitization theory of addiction. *Brain Res Brain Res Rev*, *18*(3), 247–291. <http://www.ncbi.nlm.nih.gov/pubmed/8401595>
- Rønnov-Jessen, L., Villadsen, R., Edwards, J. C., & Petersen, O. W. (2002). Differential expression of a chloride intracellular channel gene, CLIC4, in transforming growth factor-beta1-mediated conversion of fibroblasts to myofibroblasts. *The American Journal of Pathology*, *161*(2), 471–480. [https://doi.org/10.1016/S0002-9440\(10\)64203-4](https://doi.org/10.1016/S0002-9440(10)64203-4)
- Rosene, D., & Van Hoesen, G. (1977). Hippocampal efferents reach widespread areas of cerebral cortex and amygdala in the rhesus monkey. *Science*, *198*(4314), 315–317. <https://doi.org/10.1126/science.410102>
- RStudio Team. (2016). *RStudio server: Integrated Development for R*. RStudio, Inc., Boston, MA.
- Ryabinin, A. E., Yoneyama, N., Tanchuck, M. A., Mark, G. P., & Finn, D. A. (2008). Urocortin 1 microinjection into the mouse lateral septum regulates the acquisition and expression of alcohol consumption. *Neuroscience*, *151*(3), 780–790. <https://doi.org/10.1016/j.neuroscience.2007.11.014>
- Ryan, C., & Butters, N. (1980). Learning and Memory Impairments in Young and Old Alcoholics: Evidence for the Premature-Aging Hypothesis. *Alcoholism: Clinical and Experimental Research*, *4*(3), 288–293. <https://doi.org/10.1111/j.1530-0277.1980.tb04816.x>
- Saab, A. S., Tzvetavona, I. D., Trevisiol, A., Baltan, S., Dibaj, P., Kusch, K., Möbius, W., Goetze, B., Jahn, H. M., Huang, W., Steffens, H., Schomburg, E. D., Pérez-Samartín, A., Pérez-Cerdá, F., Bakhtiari, D., Matute, C., Löwel, S., Griesinger,

- C., Hirrlinger, J., ... Nave, K. A. (2016). Oligodendroglial NMDA Receptors Regulate Glucose Import and Axonal Energy Metabolism. *Neuron*. <https://doi.org/10.1016/j.neuron.2016.05.016>
- Sacks, J. J., Gonzales, K. R., Bouchery, E. E., Tomedi, L. E., & Brewer, R. D. (2015). 2010 National and State Costs of Excessive Alcohol Consumption. *American Journal of Preventive Medicine*, 49(5), e73–e79. <https://doi.org/10.1016/j.amepre.2015.05.031>
- Schier, C. J., Dilly, G. A., & Gonzales, R. A. (2013). Intravenous Ethanol Increases Extracellular Dopamine in the Medial Prefrontal Cortex of the Long-Evans Rat. *Alcoholism: Clinical and Experimental Research*, 37(5), 740–747. <https://doi.org/10.1111/acer.12042>
- Schindelin, J., Arganda-Carreras, I., Frise, E., Kaynig, V., Longair, M., Pietzsch, T., Preibisch, S., Rueden, C., Saalfeld, S., Schmid, B., Tinevez, J. Y., White, D. J., Hartenstein, V., Eliceiri, K., Tomancak, P., & Cardona, A. (2012). Fiji: An open-source platform for biological-image analysis. In *Nature Methods*. <https://doi.org/10.1038/nmeth.2019>
- Scholz, J., Klein, M. C., Behrens, T. E. J., & Johansen-Berg, H. (2009). Training induces changes in white-matter architecture. *Nature Neuroscience*, 12(11), 1370–1371. <https://doi.org/10.1038/nn.2412>
- Schuckit, M. A. (1994). Low level of response to alcohol as a predictor of future alcoholism. *American Journal of Psychiatry*, 151(2), 184–189. <https://doi.org/10.1176/ajp.151.2.184>
- Schuckit, M. A., & Smith, T. L. (1996). An 8-year follow-up of 450 sons of alcoholic and control subjects. *Archives of General Psychiatry*, 53(3), 202–210. <https://doi.org/10.1001/archpsyc.1996.01830030020005>
- Schultz, W., Dayan, P., & Montague, P. R. (1997). A Neural Substrate of Prediction and Reward. *Science*, 275(5306), 1593–1599. <https://doi.org/10.1126/science.275.5306.1593>
- Schultz, Wolfram. (2002). Getting Formal with Dopamine and Reward. *Neuron*, 36(2), 241–263. [https://doi.org/10.1016/S0896-6273\(02\)00967-4](https://doi.org/10.1016/S0896-6273(02)00967-4)

- Schultz, Wolfram, Apicella, P., Scarnati, E., & Ljungberg, T. (1992). Neuronal activity in monkey ventral striatum related to the expectation of reward. *The Journal of Neuroscience : The Official Journal of the Society for Neuroscience*, 12(12), 4595–4610. <https://doi.org/1432059>
- Schultz, Wolfram, Tremblay, L., & Hollerman, J. R. (1998). Reward prediction in primate basal ganglia and frontal cortex. *Neuropharmacology*, 37(4–5), 421–429. [https://doi.org/10.1016/S0028-3908\(98\)00071-9](https://doi.org/10.1016/S0028-3908(98)00071-9)
- Shen, L. (2013). GeneOverlap: An R package to test and visualize gene overlaps. *R Package Version 1.22.0*. <http://shenlab-sinai.github.io/shenlab-sinai/>
- Shippenberg, T. S., Zapata, A., & Chefer, V. I. (2007). Dynorphin and the pathophysiology of drug addiction. In *Pharmacology and Therapeutics* (Vol. 116, Issue 2, pp. 306–321). <https://doi.org/10.1016/j.pharmthera.2007.06.011>
- Shukla, A., Malik, M., Cataisson, C., Ho, Y., Friesen, T., Suh, K. S., & Yuspa, S. H. (2009). TGF-beta signalling is regulated by Schnurri-2-dependent nuclear translocation of CLIC4 and consequent stabilization of phospho-Smad2 and 3. *Nature Cell Biology*, 11(6), 777–784. <https://doi.org/10.1038/ncb1885>
- Shuster, L., Webster, G. W., & Yu, G. (1975). Increased running response to morphine in morphine-pretreated mice. *J Pharmacol Exp Ther*, 192(1), 64–67. <http://www.ncbi.nlm.nih.gov/pubmed/235638>
- Singh, H., & Ashley, R. H. (2007). CLIC4 (p64H1) and its putative transmembrane domain form poorly selective, redox-regulated ion channels. *Molecular Membrane Biology*, 24(1), 41–52. <https://doi.org/10.1080/09687860600927907>
- Sinha, R., & Li, C. S. R. (2007). Imaging stress- and cue-induced drug and alcohol craving: Association with relapse and clinical implications. In *Drug and Alcohol Review* (Vol. 26, Issue 1, pp. 25–31). <https://doi.org/10.1080/09595230601036960>
- Snaidero, N., Möbius, W., Czopka, T., Hekking, L. H. P., Mathisen, C., Verkleij, D., Goebbels, S., Edgar, J., Merkler, D., Lyons, D. A., Nave, K. A., & Simons, M. (2014). Myelin membrane wrapping of CNS axons by PI(3,4,5)P3-dependent polarized growth at the inner tongue. *Cell*. <https://doi.org/10.1016/j.cell.2013.11.044>

- Snaidero, N., Velte, C., Myllykoski, M., Raasakka, A., Ignatev, A., Werner, H. B., Erwig, M. S., Möbius, W., Kursula, P., Nave, K. A., & Simons, M. (2017). Antagonistic Functions of MBP and CNP Establish Cytosolic Channels in CNS Myelin. *Cell Reports*, 18(2), 314–323. <https://doi.org/10.1016/j.celrep.2016.12.053>
- Spencer, K. B., Mulholland, P. J., & Chandler, L. J. (2016). FMRP Mediates Chronic Ethanol-Induced Changes in NMDA, Kv4.2, and KChIP3 Expression in the Hippocampus. *Alcohol Clin Exp Res*, 40(6), 1251–1261. <https://doi.org/10.1111/acer.13060>
- Steward, O., & Banker, G. A. (1992). Getting the message from the gene to the synapse: sorting and intracellular transport of RNA in neurons. *Trends Neurosci*, 15(5), 180–186. <http://www.ncbi.nlm.nih.gov/pubmed/1377425>
- Steward, O., & Levy, W. B. (1982). Preferential localization of polyribosomes under the base of dendritic spines in granule cells of the dentate gyrus. *J Neurosci*, 2(3), 284–291. <http://www.ncbi.nlm.nih.gov/pubmed/7062109>
- Steward, O., & Reeves, T. M. (1988). Protein-synthetic machinery beneath postsynaptic sites on CNS neurons: association between polyribosomes and other organelles at the synaptic site. *J Neurosci*, 8(1), 176–184. <http://www.ncbi.nlm.nih.gov/pubmed/3339407>
- Steward, O., & Schuman, E. M. (2001). Protein synthesis at synaptic sites on dendrites. *Annu Rev Neurosci*, 24, 299–325. <https://doi.org/10.1146/annurev.neuro.24.1.299> [pii]
- Steward, O., Wallace, C. S., Lyford, G. L., & Worley, P. F. (1998). Synaptic activation causes the mRNA for the IEG Arc to localize selectively near activated postsynaptic sites on dendrites. *Neuron*, 21(4), 741–751. [https://doi.org/S0896-6273\(00\)80591-7](https://doi.org/S0896-6273(00)80591-7) [pii]
- Steward, O., & Worley, P. F. (2001). Selective targeting of newly synthesized Arc mRNA to active synapses requires NMDA receptor activation. *Neuron*, 30(1), 227–240. [https://doi.org/S0896-6273\(01\)00275-6](https://doi.org/S0896-6273(01)00275-6) [pii]
- Subramanian, A., Narayan, R., Corsello, S. M., Peck, D. D., Natoli, T. E., Lu, X., Gould, J., Davis, J. F., Tubelli, A. A., Asiedu, J. K., Lahr, D. L., Hirschman, J.

- E., Liu, Z., Donahue, M., Julian, B., Khan, M., Wadden, D., Smith, I. C., Lam, D., ... Golub, T. R. (2017). A Next Generation Connectivity Map: L1000 Platform and the First 1,000,000 Profiles. *Cell*, 171(6), 1437-1452.e17. <https://doi.org/10.1016/j.cell.2017.10.049>
- Suh, K. S., Mutoh, M., Nagashima, K., Fernandez-Salas, E., Edwards, L. E., Hayes, D. D., Crutchley, J. M., Marin, K. G., Dumont, R. A., Levy, J. M., Cheng, C., Garfield, S., & Yuspa, S. H. (2004). The Organelle Chloride Channel Protein CLIC4/mtCLIC Translocates to the Nucleus in Response to Cellular Stress and Accelerates Apoptosis. *Journal of Biological Chemistry*, 279(6), 4632-4641. <https://doi.org/10.1074/jbc.M311632200>
- Supek, F., Bošnjak, M., Škunca, N., & Šmuc, T. (2011). Revigo summarizes and visualizes long lists of gene ontology terms. *PLoS ONE*, 6(7). <https://doi.org/10.1371/journal.pone.0021800>
- Swanson, L. W., Sawchenko, P. E., Rivier, J., & Vale, W. W. (1983). Organization of ovine corticotropin-releasing factor immunoreactive cells and fibers in the rat brain: An immunohistochemical study. *Neuroendocrinology*, 36(3), 156-186. <https://doi.org/10.1159/000123454>
- Talishinsky, A., & Rosen, G. D. (2012). Systems Genetics of the Lateral Septal Nucleus in Mouse: Heritability, Genetic Control, and Covariation with Behavioral and Morphological Traits. *PLoS ONE*, 7(8), e44236. <https://doi.org/10.1371/journal.pone.0044236>
- Tang, T., Lang, X., Xu, C., Wang, X., Gong, T., Yang, Y., Cui, J., Bai, L., Wang, J., Jiang, W., & Zhou, R. (2017). CLICs-dependent chloride efflux is an essential and proximal upstream event for NLRP3 inflammasome activation. *Nature Communications*, 8(1). <https://doi.org/10.1038/s41467-017-00227-x>
- Tarantino, L. M., McClearn, G. E., Rodriguez, L. A., & Plomin, R. (1998). Confirmation of quantitative trait loci for alcohol preference in mice. *Alcoholism: Clinical and Experimental Research*, 22(5), 1099-1105. <https://doi.org/10.1111/j.1530-0277.1998.tb03707.x>
- Tawa, E. A., Hall, S. D., & Lohoff, F. W. (2016). Overview of the genetics of alcohol use disorder. *Alcohol and Alcoholism*, 51(5), 507-514. <https://doi.org/10.1093/alcalc/agw046>

- Temkin, P., Morishita, W., Goswami, D., Arendt, K., Chen, L., & Malenka, R. (2017). The Retromer Supports AMPA Receptor Trafficking During LTP. *Neuron*, *94*(1), 74-82.e5. <https://doi.org/10.1016/j.neuron.2017.03.020>
- Thifault, S., Ondřej, Š. Š., Sun, Y., Fortin, A., Skamene, E., Lalonde, R., Tremblay, J., & Hamet, P. (2008). Genetic determinants of emotionality and stress response in AcB/BcA recombinant congenic mice and in silico evidence of convergence with cardiovascular candidate genes. *Human Molecular Genetics*, *17*(3), 331–344. <https://doi.org/10.1093/hmg/ddm277>
- Todtenkopf, M. S., Marcus, J. F., Portoghese, P. S., & Carlezon, W. A. (2004). Effects of κ -opioid receptor ligands on intracranial self-stimulation in rats. *Psychopharmacology*, *172*(4), 463–470. <https://doi.org/10.1007/s00213-003-1680-y>
- Tongiorgi, E., Righi, M., & Cattaneo, A. (1997). Activity-dependent dendritic targeting of BDNF and TrkB mRNAs in hippocampal neurons. *J Neurosci*, *17*(24), 9492–9505. <http://www.ncbi.nlm.nih.gov/pubmed/9391005>
- Trantham-Davidson, H., Burnett, E. J., Gass, J. T., Lopez, M. F., Mulholland, P. J., Centanni, S. W., Floresco, S. B., & Chandler, L. J. (2014). Chronic alcohol disrupts dopamine receptor activity and the cognitive function of the medial prefrontal cortex. *J Neurosci*, *34*(10), 3706–3718. <https://doi.org/10.1523/JNEUROSCI.0623-13.2014>
- Tsai, G., & Coyle, J. T. (1998). The role of glutamatergic neurotransmission in the pathophysiology of alcoholism. *Annu Rev Med*, *49*, 173–184. <https://doi.org/10.1146/annurev.med.49.1.173>
- Tulk, B. M., Schlesinger, P. H., Kapadia, S. A., & Edwards, J. C. (2000). CLIC-1 functions as a chloride channel when expressed and purified from bacteria. *Journal of Biological Chemistry*, *275*(35), 26986–26993. <https://doi.org/10.1074/jbc.M004301200>
- Ulmasov, B., Bruno, J., Gordon, N., Hartnett, M. E., & Edwards, J. C. (2009). Chloride intracellular channel protein-4 functions in angiogenesis by supporting acidification of vacuoles along the intracellular tubulogenic pathway. *American Journal of Pathology*, *174*(3), 1084–1096. <https://doi.org/10.2353/ajpath.2009.080625>

- Urizar, N. L., Yang, Z., Edenberg, H. J., & Davis, R. L. (2007). *Drosophila homer* is required in a small set of neurons including the ellipsoid body for normal ethanol sensitivity and tolerance. *Journal of Neuroscience*. <https://doi.org/10.1523/JNEUROSCI.0305-07.2007>
- van der Vaart, A. (2018). *Molecular Brain Adaptations to Ethanol: Role of Glycogen Synthase Kinase-3 Beta in the Transition to Excessive Consumption*. Virginia Commonwealth University.
- Vanderschuren, L. J., & Kalivas, P. W. (2000). Alterations in dopaminergic and glutamatergic transmission in the induction and expression of behavioral sensitization: a critical review of preclinical studies. *Psychopharmacology (Berl)*, *151*(2–3), 99–120. <http://www.ncbi.nlm.nih.gov/pubmed/10972458>
- Vendruscolo, L. F., Estey, D., Goodell, V., Macshane, L. G., Logrip, M. L., Schlosburg, J. E., McGinn, M. A., Zamora-Martinez, E. R., Belanoff, J. K., Hunt, H. J., Sanna, P. P., George, O., Koob, G. F., Edwards, S., & Mason, B. J. (2015). Glucocorticoid receptor antagonism decreases alcohol seeking in alcohol-dependent individuals. *Journal of Clinical Investigation*. <https://doi.org/10.1172/JCI79828>
- Vogt, B. A., & Pandya, D. N. (1987). Cingulate cortex of the rhesus monkey: II. Cortical afferents. *J Comp Neurol*, *262*(2), 271–289. <https://doi.org/10.1002/cne.902620208>
- Volkow, N. D., & Fowler, J. S. (2000). Addiction, a disease of compulsion and drive: involvement of the orbitofrontal cortex. *Cerebral Cortex (New York, N.Y. : 1991)*, *10*(3), 318–325. <https://doi.org/10.1093/cercor/10.3.318>
- Volkow, N. D., Wang, G.-J., Telang, F., Fowler, J. S., Logan, J., Jayne, M., Ma, Y., Pradhan, K., & Wong, C. (2007). Profound Decreases in Dopamine Release in Striatum in Detoxified Alcoholics: Possible Orbitofrontal Involvement. *Journal of Neuroscience*, *27*(46), 12700–12706. <https://doi.org/10.1523/JNEUROSCI.3371-07.2007>
- Vu, V. Q. (2011). *ggbiplot: A ggplot2 based biplot. R package version 0.55*. Vu, Vincent Q.
- Walker, B. M., & Koob, G. F. (2008). Pharmacological Evidence for a Motivational

- Role of κ -Opioid Systems in Ethanol Dependence. *Neuropsychopharmacology*, 33(3), 643–652. <https://doi.org/10.1038/sj.npp.1301438>
- Walker, B. M., Zorrilla, E. P., & Koob, G. F. (2011). Systemic κ -opioid receptor antagonism by nor-binaltorphimine reduces dependence-induced excessive alcohol self-administration in rats. *Addiction Biology*, 16(1), 116–119. <https://doi.org/10.1111/j.1369-1600.2010.00226.x>
- Wallace, C. S., Lyford, G. L., Worley, P. F., & Steward, O. (1998). Differential intracellular sorting of immediate early gene mRNAs depends on signals in the mRNA sequence. *J Neurosci*, 18(1), 26–35. <http://www.ncbi.nlm.nih.gov/pubmed/9412483>
- Walter, W., Sánchez-Cabo, F., & Ricote, M. (2015). GOplot: An R package for visually combining expression data with functional analysis. *Bioinformatics*. <https://doi.org/10.1093/bioinformatics/btv300>
- Wang, X., Pandey, A. K., Mulligan, M. K., Williams, E. G., Mozhui, K., Li, Z., Jovaisaite, V., Quarles, L. D., Xiao, Z., Huang, J., Capra, J. A., Chen, Z., Taylor, W. L., Bastarache, L., Niu, X., Pollard, K. S., Ciobanu, D. C., Reznik, A. O., Tishkov, A. V, ... Williams, R. W. (2016). Joint mouse-human phenome-wide association to test gene function and disease risk. *Nat Commun*, 7, 10464. <https://doi.org/10.1038/ncomms10464>
- Watabe-Uchida, M., Zhu, L., Ogawa, S. K., Vamanrao, A., & Uchida, N. (2012). Whole-Brain Mapping of Direct Inputs to Midbrain Dopamine Neurons. *Neuron*, 74(5), 858–873. <https://doi.org/10.1016/j.neuron.2012.03.017>
- Watson, S. J., Khachaturian, H., Akil, H., Coy, D. H., & Goldstein, A. (1982). Comparison of the distribution of dynorphin systems and enkephalin systems in brain. *Science (New York, N.Y.)*, 218(4577), 1134–1136.
- Wee, S., & Koob, G. F. (2010). The role of the dynorphin- κ opioid system in the reinforcing effects of drugs of abuse. In *Psychopharmacology* (Vol. 209, Issue 2, pp. 121–135). <https://doi.org/10.1007/s00213-010-1825-8>
- Weiss, F., Lorang, M. T., Bloom, F. E., & Koob, G. F. (1993). Oral alcohol self-administration stimulates dopamine release in the rat nucleus accumbens: genetic and motivational determinants. *J Pharmacol Exp Ther*, 267(1), 250–258.

<https://doi.org/10.1207/s15327752jpa8502>

- Weiss, F., Parsons, L. H., Schulteis, G., Hyytiä, P., Lorang, M. T., Bloom, F. E., & Koob, G. F. (1996). Ethanol self-administration restores withdrawal-associated deficiencies in accumbal dopamine and 5-hydroxytryptamine release in dependent rats. *The Journal of Neuroscience: The Official Journal of the Society for Neuroscience*, *16*(10), 3474–3485. <https://doi.org/10.1111/acer.12056>
- Weitlauf, C., & Woodward, J. J. (2008). Ethanol selectively attenuates nmdar-mediated synaptic transmission in the prefrontal cortex. *Alcoholism: Clinical and Experimental Research*, *32*(4), 690–698. <https://doi.org/10.1111/j.1530-0277.2008.00625.x>
- Weng, J., Symons, M. N., & Singh, S. M. (2009). Studies on syntaxin 12 and alcohol preference involving C57BL/6J and DBA/2J strains of mice. *Behavior Genetics*, *39*(2), 183–191. <https://doi.org/10.1007/s10519-008-9249-5>
- White, F. J., & Kalivas, P. W. (1998). Neuroadaptations involved in amphetamine and cocaine addiction. *Drug Alcohol Depend*, *51*(1–2), 141–153. [https://doi.org/S0376-8716\(98\)00072-6](https://doi.org/S0376-8716(98)00072-6) [pii]
- Wickham, H. (2016). *ggplot2: Elegant Graphics for Data Analysis*. Springer-Verlag New York.
- Williams, C., Mehrian Shai, R., Wu, Y., Hsu, Y. H., Sitzer, T., Spann, B., McCleary, C., Mo, Y., & Miller, C. A. (2009). Transcriptome analysis of synaptoneuroosomes identifies neuroplasticity genes overexpressed in incipient Alzheimer's disease. *PLoS One*, *4*(3), e4936. <https://doi.org/10.1371/journal.pone.0004936>
- Wobrock, T., Falkai, P., Schneider-Axmann, T., Frommann, N., Wölwer, W., & Gaebel, W. (2009). Effects of abstinence on brain morphology in alcoholism: AAA MRI study. *European Archives of Psychiatry and Clinical Neuroscience*, *259*(3), 143–150. <https://doi.org/10.1007/s00406-008-0846-3>
- Wolen, A. R., Phillips, C. a, Langston, M. a, Putman, A. H., Vorster, P. J., Bruce, N. a, York, T. P., Williams, R. W., & Miles, M. F. (2012). Genetic Dissection of Acute Ethanol Responsive Gene Networks in Prefrontal Cortex: Functional and Mechanistic Implications. *PLoS ONE*, *7*(4), e33575.

<https://doi.org/10.1371/journal.pone.0033575>

- Wolfe, S. A., Farris, S. P., Mayfield, J. E., Heaney, C. F., Erickson, E. K., Harris, R. A., Mayfield, R. D., & Raab-Graham, K. F. (2019). Ethanol and a rapid-acting antidepressant produce overlapping changes in exon expression in the synaptic transcriptome. *Neuropharmacology*. <https://doi.org/10.1016/j.neuropharm.2018.11.007>
- Wolfe, S. A., Workman, E. R., Heaney, C. F., Niere, F., Namjoshi, S., Cacheaux, L. P., Farris, S. P., Drew, M. R., Zemelman, B. V., Harris, R. A., & Raab-Graham, K. F. (2016). FMRP regulates an ethanol-dependent shift in GABABR function and expression with rapid antidepressant properties. *Nature Communications*, 7, 12867. <https://doi.org/10.1038/ncomms12867>
- Xu, Y., Kang, J., Yuan, Z., Li, H., Su, J., Li, Y., Kong, X., Zhang, H., Wang, W., & Sun, L. (2013). Suppression of CLIC4/mtCLIC enhances hydrogen peroxide-induced apoptosis in C6 glioma cells. *Oncology Reports*. <https://doi.org/10.3892/or.2013.2265>
- Zbukvic, I. C., Ganella, D. E., Perry, C. J., Madsen, H. B., Bye, C. R., Lawrence, A. J., & Kim, J. H. (2016). Role of Dopamine 2 Receptor in Impaired Drug-Cue Extinction in Adolescent Rats. *Cerebral Cortex*, 26(6), 2895–2904. <https://doi.org/10.1093/cercor/bhw051>
- Zeisel, A., Muñoz Manchado, A. B., Codeluppi, S., Lönnerberg, P., La Manno, G., Juréus, A., Marques, S., Munguba, H., He, L., Betsholtz, C., Rolny, C., Castelo-Branco, G., Hjerling-Lefler, J., & Linnarson, S. (2015). Cell types in the mouse cortex and hippocampus revealed by RNA-Seq. *Science (New York, N.Y.)*, 347(February), 1138–1142.
- Zhang, Y., Chen, K., Sloan, S. A., Bennett, M. L., Scholze, A. R., O’Keefe, S., Phatnani, H. P., Guarnieri, P., Caneda, C., Ruderisch, N., Deng, S., Liddelow, S. A., Zhang, C., Daneman, R., Maniatis, T., Barres, B. A., & Wu, J. Q. (2014). An RNA-sequencing transcriptome and splicing database of glia, neurons, and vascular cells of the cerebral cortex. *Journal of Neuroscience*. <https://doi.org/10.1523/JNEUROSCI.1860-14.2014>
- Zhong, Y., Dong, G., Luo, H., Cao, J., Wang, C., Wu, J., Feng, Y. Q., & Yue, J. (2012). Induction of brain CYP2E1 by chronic ethanol treatment and related oxidative

stress in hippocampus, cerebellum, and brainstem. *Toxicology*.
<https://doi.org/10.1016/j.tox.2012.08.009>

Zhou, F. C., Anthony, B., Dunn, K. W., Lindquist, W. B., Xu, Z. C., & Deng, P. (2007). Chronic alcohol drinking alters neuronal dendritic spines in the brain reward center nucleus accumbens. *Brain Res*, 1134(1), 148–161.
[https://doi.org/S0006-8993\(06\)03263-X](https://doi.org/S0006-8993(06)03263-X) [pii]10.1016/j.brainres.2006.11.046

Zorrilla, E. P., Logrip, M. L., & Koob, G. F. (2014). Corticotropin releasing factor: A key role in the neurobiology of addiction. *Frontiers in Neuroendocrinology*, 35(2), 234–244. <https://doi.org/10.1016/j.yfrne.2014.01.001>

